Matter bounce cosmology with dark energy

Anna Paula Ramos Bacalhau

Centro Brasileiro de Pesquisas Físicas

COSMO - Coordenação de Cosmologia, Astrofísica e Interações Fundamentais

Dissertation presented to the Brazilian Center for Research in Physics in partial fulfillment of the requirements for the degree of Doctor of Philosophy

Matter bounce cosmology with dark energy

Anna Paula Ramos Bacalhau

Supervisor Nelson Pinto-Neto
Second supervisor Sandro Dias Pinto Vitenti

2017

Anna Paula Ramos Bacalhau

Matter bounce cosmology with dark energy

Dissertation presented to the Brazilian Center for Research in Physics in partial fulfillment of the requirements for the degree of Doctor of Philosophy, 2017

Supervisors: Nelson Pinto-Neto and Sandro Dias Pinto Vitenti

Centro Brasileiro de Pesquisas Físicas

COSMO - Coordenação de Cosmologia, Astrofísica e Interações Fundamentais

Xavier Sigaud, 150.

29999-000 and Rio de Janeiro

To my grandfather João Bastista Bacalhau, whose library nourrished my curiosity and whose life inspired my path.

Abstract

A single field matter bounce with an exponential potential is numerically studied. The quantum bounce prescribed when the kinetic term dominates the evolution of the background was already demonstrated in the literature. To form a complete background, the quantum bounce is matched with the classical exponential-potential-driven evolution, which presents a past matter repeller. This configuration allows two possible mutually excluding scenarios: case **A**, in which a Dark Energy (DE) epoch is present in the contraction phase and case **B**, in which DE is present in the expansion phase. The latter is used as the background to study cosmological perturbations. The evolution of the primordial scalar and tensor modes from vacuum initial conditions shows a consistent power spectra with the right amplitudes, tensor-to-scalar ratio and spectral index.

Since bounce cosmologies may suffer from the growth of anisotropies during the contracting phase, a matter bounce driven by a Galileon scalar field with an ekpyrotic potential is studied. Previous studies with this model claims that the final background dynamics suppresses the anisotropy growth. In the last part of this work, numerical solutions are obtained and they reveal a richer dynamics for the background, which contains one, two or even three bounces depending on the initial conditions and in the amount of anisotropy.
Keywords: bounce, matter bounce, dark energy, primordial perturbations, quantum gravity, quantum bounce.

Resumo

No presente trabalho são abordados dois problemas ligados a cosmologia de ricochete: as perturbações primordiais em modelos contendo uma fase de energia escura e o crescimento instável de anisotropias na fase de contração.

Na primeira parte é estudado numericamente um modelo de ricochete constituído de um campo escalar com potencial exponencial. O ricochete é produzido por correções quânticas quando o termo cinético domina a dinâmica do campo. Essa configuração permite dois cenário mutuamente excludentes: no primeiro, a energia escura está presente na contração, e no segundo, a energia escura está presente na expansão. O último caso constitui o fundo usado para se estudar as perturbações cosmológicas primordiais, cujo espectro obtido numericamente é coerente com os limites observacionais no que diz respeito à amplitude, razão tensor-escalar e índice espectral.

No entanto, modelos de ricochete podem apresentar crescimento instável de anisotropia. Na segunda parte do trabalho são estudados modelos de fundo contendo um, dois ou mais ricochetes no contexto dos chamados “New Ekpyrotic scenarios”, todos contendo inicialmente uma anitropia não nula, porém convergindo em uma fase de expansão final isotrópica. Esses cenários ainda não vistos na literatura ajudam a vincular o espaço de parâmetros do modelo, e são cruciais para um estudo futuro das perturbações cosmologicas.
Palavras-chave: ricochete, ricochete de matéria, energia escura, perturbações primordiais, gravidade quântica, ricochete quântico.

Acknowledgement

I acknowledge CNPq/MCTIIC and the program “Ciência sem fronteiras” for the financial support.

The present work would never be possible without the support and care of very special people.

The generous share of knowledge of Nelson Pinto-Neto, Sandro Dias Vitenti and Patrick Peter.

The students from the Centro Brasileiro de Pesquisas Físicas, who leave their homes, families, even countries to pursue their dreams.

My friends who have shared home with me in Rio de Janeiro: Jaime, Lupita, Cenê, Bita, Mário, Marc and my friends from Maison du Brèsil in Paris.

My family, Anna Claudia, Marcus e João Marcus Bacalhau for their love, care, support and understanding.

My partner, Julien, for his unbreakable optimism.

My friends Ana Bárbara, Arthur S. , Arthur R., Bita, Cláudia, Cynthia, Emanuel, Fabrício, Grazi, Jaime, Josephine, Leo, Lídia, Marina, Mário, Nathalia, Raíra, Vanessa.

For you all my eternal gratitude.

Contents

1 Introduction

Non-singular bounce models have been extensively studied as an alternative to the Big Bang paradigm, since they avoid the initial singularity and address other puzzles of ever-expanding cosmologies, which are approached by the inflationary epoch in the standard cosmological model. A typical bouncing Universe is characterized by one or many contraction/expansion sequences connected by the bounce period that is trigged by corrections of gravity at high energy scales or non-canonical scalar fields [1, 2, 3, 4].

Despite the fact that inflation has not yet a fundamental physics behind it, a simple slow-roll prescription for the "inflaton" scalar field is enough to amplify the quantum vacuum fluctuations after the Big Bang, thus giving rise to an almost scale invariant adiabatic power spectrum in high agreement with the CMB [5]. It is a challenge for bounce cosmologies to reproduce such results, and many models have been scrutinized over the years in order to provide a competitive scenario to be confronted with observations, thereby discarding or constraining bouncing cosmologies.

That goal has not been accomplished so far, and many questions remain to be answered in order to have a realistic model. The present work addresses two key aspects for a viable scenario: the primordial power spectrum in a matter bounce model containing a DE epoch at late times, and the claimed solution of the anisotropy problem by means of an ekpyrotic contraction, aspects whose motivations will be clarified in the next lines. The results presented here were published under Refs. [6] and [7], which will be the guide lines for the further developments.

The expansion history probed by current observations presents an accelerated expansion credited to the existence of a DE component, only relevant when the scale factor has increased about 7 e-folds from the last scattering surface. Whether

DE is a cosmological constant or a quintessence field, it should be present during the contraction phase in a bouncing Universe, in which it would be also relevant at a certain energy scale maybe impacting in the final power spectra. The role of DE in the contraction phase has previously been discussed in Refs. [8, 9, 10, 11, 12, 13].

In particular, the scalar and tensor perturbations were analyzed in Ref. [11] for the case of a cosmological constant and a non-negligible dependence of the scalar spectral index with the wave-number was observed. However, the cosmological constant spoils the past Minkowski vacuum. In the Ref. [11], the initial condition are set in a transient matter domination epoch, which is not a robust solution.

The aforementioned result motivates the search for a DE model with a transient equation of state. This is the case, for instance, when the exponential potential is prescribed for a canonical scalar field. The final phase space in spatially flat, homogeneous and isotropic Universe contains critical points, that can be set to produce a matter epoch in the far past of the contraction phase, and also presents a transient DE epoch [14, 15, 16, 17]. This is the starting point for the background model studied in Ref. [7] and discussed in the Chapters 2 and 3.

The past matter dominated epoch, which provides the necessary Minkowsky vacuum fluctuations as the origin of the primordial perturbation, also produces scale invariant perturbations if the modes enter the Hubble radius during the matter domination epoch [18, 19, 20, 21].

Bounce models with an epoch of matter domination during the contraction phase are often called "*matter bounce*" models [22, 23, 3], and they have been extensively studied in the literature in the past 15 years as a promising alternative to the Big Bang/Inflation scenario, as they provide scale-invariant spectrum of cosmological perturbations. However, it was claimed that they may present a "non-go" theorem in what concerns primordial perturbations: small non-Gaussianities and a small scalar-to-tensor ratio are incompatible features if GR is valid during the bounce [24, 25, 26].

In Chapter 4, the dependencies of the primordial power spectra will be carefully studied in the context of a matter bounce driven by a canonical scalar field with an exponential potential, which contains a transient DE epoch. The calculations will be performed without any approximations, since the single scalar field model can drive the bounce if quantum corrections of gravity are considered. Therefore, the main difference with respect to the previous approaches is the quantum bounce.

Known cosmological solutions obtained with the use of the De Broglie-Bohm formulation of quantum mechanics [27] can be applied to the studied system, since the classical contraction and expansion phases happens when the kinetic term dominates the scalar field dynamics. Those results are valid for scales above 10^2 - 10^3 Planck lengths, for which the canonical quantization of GR may be an effective limit of more fundamental theories of quantum gravity.

Due to the quantum bounce, two scenarios come up when using the exponential potential: in one, the DE epoch happens during the contraction phase, in the other, the DE epoch happens during the expansion phase. Since they are mutually excluding scenarios, only the last one is a viable model. Therefore, the final scenario is a matter bounce with a future DE epoch and the results obtained in Chapter 4 are even more general than initially expected.

The rigorous numerical calculations performed showed that the quantum bounce boosts the scalar modes, hence providing a tensor-to-scalar ration within the observational limit, which is a scenario not yet envisaged in the literature for a bounce model containing a DE epoch. Also, the strong influence of the matter epoch duration in the amplitudes had not yet been explored numerically, as performed in Chapter 4. Those are new findings and correspond to the main contribution of the present work.

Even though they provide a tempting scenario for the growth of the primordial perturbation, small anisotropy fluctuations may tend to grow and even dominate over the other regular matter components, leading to the so-called Belinsky, Khalatnikov and Lifshitz (BKL) instability [28, 29, 30, 31].

The current mechanism studied in the literature to suppress the growth of anisotropies is inspired in the Ekpyrotic model, which is an effective 4 dimensional model from multi-dimensional brane theory of gravity [32]. The induced 4 dimensional dynamics is consistent with the domination of a scalar field with a negative potential, which dynamically overcomes the anisotropy contribution, avoiding the instability [33, 3].

In Chapter 5 the model proposed in [33] is studied. The proposed scenario consists of a matter field with a non-canonical scalar field, which possess an ekpyrotic potential and a Galileon coupling with gravity. In that so-called "New ekpyrotic" model the possible outcomes from a variety of initial conditions are found numerically and present still unforeseen multiple bounce solutions [6]. The high non-linearity of the equations together with the presence of a small amount of initial anisotropy allows for rich dynamics and for all cases the final ever expanding isotropic phase may be indistinguishable. Those findings are crucial to discuss the viability of the ekpyrotic mechanism in suppressing the anisotropic stress.

In the following developments $\hbar = c = 1$, the reduced Planck mass $M_{\rm Pl} \equiv 1/\kappa \equiv 1/\sqrt{8\pi G}$ and the metric with signature is $(+,-,-,-)$.

2 Standard cosmology and bounce models

In the year of 2015, Einstein's theory of gravity, General Relativity (GR), completed 100 years. One year later, LIGO and VIRGO collaborations made history when they finally detected GR's ultimate prediction: the gravitational waves [34]. The many successes of GR in the face of observations makes it the ground of Cosmology allowing scientists to build models that describe the Universe and to confront those models with the available cosmic data.

Observables of large scale distances, such as supernovae type Ia (SNIa) [35, 36], baryon acoustic oscillations (BAO) [37], and the background cosmic microwave radiation (CMB) [38, 39] point to a Universe highly homogeneous and isotropic. Particularly, SNIa data shows a recent accelerated expansion that cosmologist attribute to the existence of an exotic energy component, named Dark Energy (DE). The DE is responsible for approximately 70% of the nowadays energy density and it has an equation of state estimated to be around -1. The standard cosmological model assumes that DE is the cosmological constant, named Λ, a constant term up to which GR's equations remain intact.

Observables as galaxies distributions [40], gravitational lensing [41, 42], dispersion velocities in clusters, rotation velocity of galaxies [43, 44] and, again, the CMB point to another important discovery from the modern cosmology, the Dark Matter (DM). It seems that DM only interacts gravitationally, or very weakly with other particles, and it is the key ingredient for the structure formation of the Universe, contributing up to 25% to the total energy density. The DM indirectly detected in gravitational systems presents low velocities compared to the speed of light, hence they are named Cold Dark Matter (CDM).

The aforementioned discoveries compose the standard model of Cosmology known as ΛCDM. As we will see in the next section, GR applied to Cosmology leads to equations that describe the space-time dynamics at each epoch of the expanding Universe: radiation epoch, matter epoch and the current dark energy epoch.

Moving backwards in the expansion history, classical GR predicts an initial singularity, the Big Bang, assumed as the origin of space-time in the standard cosmological model. However, the Big Bang scenario demands space-time to have a period of exponential growth in order to accommodate the current observations without extreme fine tuning on initial conditions. That period is called Inflation.

Alternatively, space-time could be eternal. Two categories of models provide eternal Universes: the pre-Big Bang models and the bouncing models. The last one is the subject of the present work, and in the last decades have been shown to be a viable alternative to the Big Bang paradigm [3, 45, 22, 31, 29] . Many issues regarding the initial singularity are addressed by bouncing models, hence an inflationary epoch is no longer needed[1].

The most common bouncing models consist of a huge and rarefied Universe that contracts from the infinite far past until the scale factor reaches a minimum value. Then, some new physics takes place and drives the Universe through a bounce ans a subsequent expanding phase. In some cyclic models, the Universe undergoes infinite expansions and contractions.

The basics of the standard cosmological model with the Big Bang conundrums and how inflation addresses them are discussed in Sec. 2.1. Section 2.2 is dedicated to bouncing models: how can they provide an alternative to the Big Bang scenario, its current limitations and challenges.

[1] Some bouncing models with an inflationary period can be found in the literature, but they motivation lies beyond the scope of the present work.

2.1 Standard cosmology

The core of GR are the Einstein's field equations (EFE)

$$R^{\mu}_{\nu} - \frac{1}{2}\delta^{\mu}_{\nu}R = 8\pi G T^{\mu}_{\nu} \tag{2.1}$$

which relates the geometry of space-time to the energy-momentum tensor, $T_{\mu\nu}$. The geometry is described by the Ricci tensor, R^{μ}_{ν}, and the Ricci scalar, R, both containing the metric and its derivatives. The cosmological principle states that space-time is homogeneous and isotropic. However, the cosmological principle is more than just a simplifying assumption, it is also in high agreement with large scales observations, which also indicates a flat Universe. The metric satisfying those requirements is the Friedmann-Lemaître-Robertson-Walker (FLRW) metric for null spatial curvature, namely

$$\mathrm{d}s^2 = \mathrm{d}t^2 - a(t)\mathrm{d}x^i\mathrm{d}x_i, \tag{2.2}$$

where t is the cosmic time. Because of its diagonal symmetry, the FLRW metric results in a Ricci tensor for which the only non vanishing components are the diagonal terms.

The energy-momentum tensor should also satisfy the cosmological principle and the non-vanishing components are $T_{00} = \rho(t)$ and $T_{ii} = p(t)$, the energy density and the pressure, respectively. In the case of a canonical scalar field with potential $V(\phi)$, the Lagrangian density reads

$$\mathcal{L} = \frac{\dot{\phi}^2}{2} - V(\phi)$$

and from the variational principle we can associate to the scalar field an effective energy density and pressure, which read:

$$\rho = \frac{\dot{\phi}^2}{2} + V(\phi),, \tag{2.3}$$

$$p = \frac{\dot{\phi}^2}{2} - V(\phi), \tag{2.4}$$

where $\dot{} = \frac{\mathrm{d}}{\mathrm{d}t}$ is the derivative with respect to the cosmic time.

Replacing the metric (2.2), in EFE, Eq. (2.1), the $^0_0$ component and the trace component read

$$H^2 = \frac{\kappa^2}{3}\rho, \tag{2.5}$$

$$\dot{H} = -\frac{\kappa^2}{2}(p+\rho), \tag{2.6}$$

where $H \equiv \frac{\dot{a}}{a}$ is the Hubble function. Eq. (2.5) is known as Friedmann equation and combined with Eq. (2.6) gives the continuity equation[2]

$$\dot{\rho} + 3H(p+\rho) = 0. \tag{2.7}$$

The continuity equation together with Eq. (2.6) gives the background evolution, whose solutions are constrained by Eq. (2.5). Equation (2.5) allows for solutions with $H > 0$, space-time expansion, and $H < 0$, space-time contraction.

For a perfect fluid with equation of state (EoS) $p = w\rho$, Eq. (2.7) gives $\rho \propto a^{-3(1+w)}$. Different EoS will implicate in different rates of decaying and growing. For instance, the energy density of radiation ($w = 1/3$) goes with a^{-4}, dust ($w = 0$) with a^{-3} and the cosmological constant ($w = -1$) , as the name suggests, have a constant energy density.

During a expanding phase, while the scale factor is small, radiation dominates and we have the aforementioned radiation epoch. Because radiation decays faster then

[2]The deduction can also be made by evaluating $T^{0\mu}_{;\mu} = 0$, where ; is the covariant derivative.

dust, a matter epoch emerge. Finally matter decays until it becomes negligible with respect to the DE, and the dark energy epoch begins.

Singularity problem

Classical GR when applied to expanding models such as ΛCDM implies in the existence of a primordial singularity from which space-time would inexplicably emerges in what's called the Big Bang [46]. Based on the singularity theorems of Hawking and Penrose [47], such models are past-incomplete and an important scientific question, which is "what trigged the Big Bang?" can not be addressed.

One way to get rid of this "singularity problem", as often named in the literature, is to suppose that at high energies GR may not be the correct theory when the Universe reaches a high-energy regime, since quantum mechanics corrections should start to be relevant.

Horizon problem

An issue when adopting the Big Bang paradigm is the so called "horizon problem". There are many "horizons" in cosmology and it is worth to clarify their meanings [48].

A very useful time parameter in cosmology is the conformal time $\eta(t)$ defined as

$$\mathrm{d}\eta \equiv \frac{1}{a}\mathrm{d}t, \tag{2.8}$$

in which the metric (2.2) reads

$$\mathrm{d}s^2 = a^2(\eta)(\mathrm{d}\eta^2 - \delta_{ij}\mathrm{d}x^i\mathrm{d}x^j). \tag{2.9}$$

The conformal time is the comoving distance traveled by light from the Big Bang to a time t. No information could have propagate further then η in the interval between the Big Bang and t, so the distance limited by η is usually referred as

"conformal horizon". Setting $t_0 = \eta_0 = 0$ the initial time at the Big Bang, Eq. (2.8) reads

$$\eta = \int_0^t \frac{1}{a(\bar{t})} \mathrm{d}\bar{t}. \tag{2.10}$$

A particle is causally connected to regions within the radius

$$d_{\mathrm{H}}(t) \equiv a\eta(t), \tag{2.11}$$

which is called the *particle horizon*. If Eq. (2.10) converges, then the particle horizon is limited and there are regions in the Universe that have never been in contact. There is no *a priori* reason why regions outside the particle horizon would share any physical resemblance with regions within it. This is the case with the CMB.

The CMB is black body radiation, which means that the photons emitted by the last scattering surface (LSS) were in thermal equilibrium. This would only be possible if they were in causal contact in the past.

At the LSS the particle horizon is roughly [49]

$$d_{\mathrm{H}} \approx \frac{1}{(1+z_{LSS})^{\frac{3}{2}}}, \tag{2.12}$$

where z_{LSS} is the redshift at which radiation decouples from matter. (As usual the redshift is defined by the relation $a = \frac{1}{1+z}$.) To estimate what this distance means we can compare to the angular diameter distance from the LSS to us, which reads [49, 29]

$$d_{\mathrm{A}} \approx \frac{1}{1+z_{LSS}} \tag{2.13}$$

in radians. The LSS happen with $z = 1100$ and

$$\frac{d_{\mathrm{H}}}{d_{\mathrm{A}}} \approx 1.6. \tag{2.14}$$

This estimate means that the CMB signals received from regions separated by more then 1.6 radians were not in causal contact and there is no explanation why they

were in thermal equilibrium. This is the horizon problem. In other words, the horizon size by the time of the LSS in the Big Bang model is not enough to explain the CMB thermalization.

In order to address this inconsistency, the standard model assumes that after the Big Bang an epoch of fast accelerated expansion took place, inflation. During inflation H is nearly constant, and the scale factor goes with $a \propto \mathrm{e}^{Ht}$ implicating in a particle horizon that grows exponentially:

$$d_{\mathrm{H}} \propto \mathrm{e}^{H\Delta t}, \tag{2.15}$$

where Δt is the total duration of the inflationary phase. Clearly, one can make $H\Delta t$ as larger as it is necessary so the particle horizon is consistent with the CMB measurements. In fact, an inflation that lasts approximately 60 e-folds is enough to solve the horizon problem [29].

Flatness problem

Two other topologies that satisfy the cosmological principle are the spherical and the hyperbolic ones. The Friedman equations accounting for a curvature term read

$$H^2 = \frac{\kappa^2}{3}\rho - \frac{K}{a^2}, \tag{2.16}$$

$$\dot{H} = \frac{K}{a^2} - \frac{\kappa^2}{2}(p+\rho), \tag{2.17}$$

where $K = -1, 0, 1$ for negative, flat and positive curvature space-times, respectively. The critical density is defined as

$$\rho_{\mathrm{c}} = \frac{3H^2}{\kappa} \tag{2.18}$$

and replaced in Eq. (2.16) gives

$$1 = \Omega + \Omega_K \tag{2.19}$$

with $\Omega \equiv \frac{\rho}{\rho_c}$ and

$$|\Omega_K| = \frac{|K|}{a^2 H^2}. \tag{2.20}$$

The current observations estimates $\Omega = 1$, which implies a flat Universe. In order to study how the curvature may had evolved, we can differentiate Eq. (2.20) with respect to t to find

$$\frac{\mathrm{d}|\Omega_K|}{\mathrm{d}t} = -2|K|\frac{\ddot{a}}{\dot{a}^3}. \tag{2.21}$$

The curvature contribution grows if $w > \frac{-1}{3}$, which means that after the Big Bang any small deviation from flatness ($|\Omega_K| = 0$), would have increased during the radiation ($w = 1/3$) and and matter epochs ($w = 0$). To be negligible by the time of the LSS and also consistent with the element abundances, the curvature should have a maximum $|\Omega_K| \approx 10^{-16}$ by the time of the electron-positron annihilation and even smaller before [49, 29]. Either the curvature is strictly null since the beginning, or it suffers from a fine tunning in initial conditions. This is called the flatness problem.

Again the inflationary phase can solve the puzzle. The scale factor goes like e^{Ht} and Eq. (2.21) gives

$$|\Omega_K| = \frac{|K|}{H^2}\mathrm{e}^{-2Ht}, \tag{2.22}$$

the exponential decaying is a natural mechanism to control the curvature growth. Observational constraints point to a sufficiently value of 60 e-folds [49, 29] so a unitary curvature term would be negligible by the end of inflation. This limit is also suitable for the horizon problem and inflation seems to be the answer for all Big Bang's conundrums.

The inflationary scenario was proposed by Guth and Linde in the early 80's [50, 51] to solve the aforementioned problems [3].But the most astonishing feature of

[3] Another problem also addressed by Linde's paper of 1982 was the monopole problem [51, 29, 31]. High energy unification theories predict the existence of a relevant amount of objects that we do not detect observationally such as topological defects, exotic particles or primordial black holes. An inflationary phase dissolves the energy density associate with those Big Bang relics and solves this issue. In bounce models it is not yet understood whether those relics are present or not.

inflation was first demonstrated by Mukhanov and Chibisov [52], which is the mechanism for the growth of perturbations.

Their assumption was that, just after the Big Bang, quantum vacuum fluctuations with a Gaussian distribution were amplified due to the accelerated stretch of space-time caused by inflation, yielding a specific predictable spectrum of scalar and tensor perturbations [52].

The simple and most successful inflationary models are based on the slow-roll hypothesis, in which the scalar field responsible for driving inflation slowly rolls down its potential. The origin of primordial perturbation as proposed by [52] together with the slow-roll inflation fits the CMB spectrum and this agreement makes the inflationary scenario a key ingredient of the standard model [38].

Nevertheless, potential-driven inflationary models (at least the ones studied so far) faces some problems [53]. For instance, they need a fine tunning in the potential parameters in order to keep the amplitudes of the primordial fluctuation from growing larger then the values constrained by CMB. Another interesting aspect is the so called “trans-Planckian problem”. Due to the long inflationary phase, large scale comoving distances should have been smaller than the Planck scale during inflation. To assume any known mechanism for the initial fluctuations would imply an extrapolation of the physics for those scales at which we have no current well established theory. It is argued that, when considering high energy models, the predicted spectrum would be very different from the observed one [53, 54, 55].

Finally inflation does not address the singularity problem. One can argue that the singularity theorems are no longer valid because of the violation of the strong energy conditions (SEC) required for the accelerated expansion. Still, inflation is not past-eternal as argued by [46] and the standard cosmological model remains incomplete [29, 53, 21].

2.2 Bouncing models

Bouncing models are characterized by an initially contracting background ($H < 0$) that transits to an expanding phase ($H > 0$). The transition period is called the "bounce phase" and it can be singular[4] or non-singular. In the last case, the scale factor has a inferior limiting value and from now on we will consider only those models. Also, there is no *a priori* reason why the Universe would experience only one bounce. Many bounces or eternal cycles of contraction/expansion are a possibility in certain models.

To produce a non-singular bounce in GR it is necessary that the null energy condition (NEC), $p + \rho \geq 0$, is violated in order to provide $\dot{H} > 0$ for sufficiently long time that the Hubble function goes positive.

Equations (2.16) and (2.17) show that such dynamics can be accomplished by an Universe with positive curvature, $K = 1$. A suitable adjustment of the other energy components allows the curvature to dominate for small scale factors driving the bounce. Those scenarios where investigated and are not so interesting, since the amount of curvature in the expanding phase would have be above the observational limit and would demand an inflationary phase to dissolve it [29, 57, 58, 59, 60].

For a flat Universe, a classical bounce, can be achieved through the introduction of an exotic fluid with a negative energy density, named the ghost scalar fields, as previously studied by [61, 3, 62], or by modifications of GR, for instance Horava-Lifshitz [63] and $F(R)$ [64] gravity.

A very interesting model first studied by refs. [32, 65] is the Ekpyrotic scenario. In this string theory based model, five-dimensional branes collide inducing, in the four dimensional space-time, an effective dynamic in which the Universe bounces, one or even infinite times (cyclic model). Those models were extensively studied

[4] Singular bouncing models present a more involved discussion in what concern the matching conditions for the cosmological perturbations [56], which is outside the scope of the present work.

in the literature [66, 33, 67, 68, 69, 9, 70, 71, 72] and chapter 5 is dedicated to the specific aspect of the growth of anisotropy in this class of models.

Bouncing universes are also found as the cosmological solutions of unification theory models such as string theory [73]. In that context, they present not only an interesting alternative to the inflation paradigm, but also a manner to test those theories at an energy scale impossible to be reached in the laboratory.

As unification theories, quantum gravity models intend to address the behavior of GR when high-energy scales are reached. They also provide consistent cosmological scenarios with one or many bounces. Those are called quantum bounces and they are studied in the context of quantum cosmology. It is the case when loop quantum gravity (LQG) [74] or the canonical quantization for gravity (CQG) [75] are applied to cosmology. The latter is a more conservative approach, which it is believed to describe effective regimes around $10^3\ell_{\rm Pl}$ or more without making use of a more involved quantum gravity theory. This is the one we use in this work.

Whether the bounce is a consequence of an exotic fluid, modification of classical gravity or high energy corrections, the contraction/expansion history is enough to address the problems of the Big Bang scenario discussed previously. Hence, bouncing models are an alternative to inflation that should be well understood: either they are viable scenarios and a realistic model will pass the observational tests, or they can be absolutely discarded. Both outcomes enlighten the path for a consistent theory for the primordial Universe.

In what concerns the Big Bang problems, the **singularity** is avoided by construction in bouncing models with a minimum scale factor.

The **horizon problem** is addressed as follows.

For a Universe dominated by a perfect fluid with a constant EoS w, the background evolves as

$$a \propto t^{\frac{2}{3(1+w)}} \propto \eta^{\frac{1}{3(1+w)}}. \tag{2.23}$$

Hence, particle horizon Eq. (2.11) reads

$$d_{\mathrm{H}}(t) = \pm\frac{3(1+w)}{1+3w}|t|\left(1-\left|\frac{t_0}{t}\right|^{\frac{1+3w}{3(1+w)}}\right) \tag{2.24}$$

for $w > -\frac{1}{3}$, t_0 the initial time and $\pm$ holding for expansion and contraction, respectively. As mentioned before, Eq. (2.24) is limited by the value of t_0 in the BB scenario. If a previous contracting phase is considered, then the horizon is as big as far t_0 is set in the past. There is no a priori reason why t_0 is limited in the past and most of the studied models adopts $t_0 \to -\infty$ resulting in $d_{\mathrm{H}} \to \infty$, which naturally solves the horizon problem.

The **flatness problem** in bouncing scenarios is solved by considering a contracting phase longer than the expansion. In Eq. (2.21), it is clear that a contracting ($\dot{a}^3 < 0$) and decelerated ($\ddot{a} < 0$) phase suppress the curvature growth. Since the Universe have been contracting from $t \to -\infty$, the curvature is sufficiently diluted by the time of the bounce. For a sufficiently symmetric bounce, the expanding phase will start with the same negligible amount of curvature it had by the end of the contracting phase. Hence, the expanding Universe will be sufficiently flat.

Finally, bouncing models have to provide a scenario for the **growth of perturbations**. They have to be able to produce the main features of the large-scale perturbations constrained by CMB: a scale invariant spectrum, amplitudes of order 10^{-10} and a tensor-to-scalar ratio of order $r \lesssim 0.1$ [38].

As in inflation, the origin of the perturbations are the quantum vacuum fluctuations, but in the context of bouncing cosmologies the initial conditions are set in the far past of the contracting phase. Results in [19, 2, 25], and references therein, points to the following. In the far past, if the Universe is dominated by a matter-like energy component then long-wavelength modes entering the horizon during a matter dominated contraction will be scale invariant. The tensor-to-scalar ratio, r, is greater than the CMB estimate for single fluid models when GR is valid during the bounce. The theoretical attempts to decrease r seems to increase the non-Gaussianities in those kinds of models, suggesting a “no-go” theorem for

bouncing cosmologies [26, 25]. However, as we will discuss in Chapter 4, even in the simplest single-field matter contraction one can obtain $r < 0.1$ without any particular fine tuning on the parameters. This last result is published in Ref. [7].

The aforementioned discoveries suggest that the **matter bounce**, i.e., models in which the contracting phase has a matter epoch, is the most tempting scenario. However, one may ask what is the role of DE in the contracting phase. A previous work considering the cosmological constant, shows that its presence may severely change the primordial power spectra by introducing a a kind of running in the spectral index [11]. Considering DE as a cosmological constant is problematic in what concerns the prescription of initial vacuum conditions due to the past DeSitter space. Scenarios in which DE is a transient epoch may properly address both the "DE problem" and the primordial fluctuations in bouncing models. This is a very recent and interesting new bound of bounce cosmology and many efforts are currently been done in that direction, for instance, Refs. [13, 76, 9, 12, 8, 11] including the present work published in Ref. [7].

The anisotropy problem

One can always argue that the initial conditions for the contracting phase are of a perfectly isotropic space-time. However, the robustness of the model can be tested by assuming deviations from isotropy. In that sense bouncing scenarios are not stable. In the literature this is often named as the anisotropy problem.

For the purpose of briefly discussing the anisotropy problem, and to prepare the ground for Chapter 5, we will consider a flat and homogeneous Universe with Bianchi-I metric,

$$\mathrm{d}s^2 = \mathrm{d}t^2 - a^2(t) \sum_i \mathrm{e}^{2\theta_i(t)} \mathrm{d}x^i \mathrm{d}x^i. \tag{2.25}$$

The mean scale factor is a and in the i-th direction the scale factor reads $a\mathrm{e}^{2\theta_i}$, where θ_i holds the anisotropic correction to the background. We can always parametrize those correction to have the relation

$$\sum_i \theta_i = 0. \tag{2.26}$$

Using the Bianchi-I metric in the EFE, Eq. (2.1), the Friedmann equations reads

$$H^2 = \frac{\kappa^2}{3}\rho_{\mathrm{T}} + \frac{\kappa^2}{6}\sigma^2 \quad \text{and} \tag{2.27}$$

$$\dot{H} = -\frac{\kappa^2}{2}(\rho_{\mathrm{T}} + p_{\mathrm{T}}) - \frac{\kappa^2}{2}\sigma^2, \tag{2.28}$$

where σ^2 is the shear defined as

$$\sigma^2 = \sum_i \dot{\theta}_i^2. \tag{2.29}$$

The anisotropy behaves effectively as a stiff-matter component in the Friedmann equations, and we can identify its energy density with

$$\rho_\sigma = p_\sigma = \frac{\sigma^2}{2}. \tag{2.30}$$

That identification shows that the shear density has an EoS $w = 1$, which means it goes as a^{-6}. Considering the regular matter components, dust (a^{-3}), radiation (a^{-4}) and dark energy (a^0), the shear will always dominate for smaller scale factors. It is argued in the literature that the dominance of the shear would imply the BKL instability [28]

For a contracting phase, the growth of anisotropy can have two outcomes: if the regular matter is considered, the anisotropy dominates before the bounce phase leading the Universe to the BKL instability; if other matter components with a constant a EoS $w > 1$ are present they will overcome the anisotropy, but still they have to sufficiently suppress the shear in order to make the expanding phase isotropic.

Ekpyrotic models are tempting in that sense. During the ekpyrotic phase the scalar field behaves effectively as a fluid with EoS $w > 1$, and may suppress the anisotropy [33]. However, the complex dynamics of the previous studied models, may spoil out the ekpyrotic solution for the anisotropy problem. This is the subject of Chapter 5 and is published in [6].

3 Homogeneous Background

For the purpose of this work we consider a canonical scalar field ϕ whose Lagrangian density is given by

$$\mathcal{L} = \sqrt{-g}(\nabla^\nu \phi \nabla_\nu \phi - V(\phi)) \tag{3.1}$$

and the potential $V(\phi)$ is chosen to be the exponential potential

$$V(\phi) = V_0 \mathrm{e}^{-\lambda\kappa\phi}, \tag{3.2}$$

where V_0 is a constant of units mass^4 and λ a positive dimensionless constant.

From alternative models of dark energy and dark matter to modifications of gravity and inflationary scenarios, the exponential potential has vastly assisted cosmologists to address puzzles of the standard model because of its rich dynamics [14, 17, 16, 77]. References [78, 79, 80, 81, 82, 83, 84] are some miscellaneous examples of what was published with exponential potential in the last year.

For instance, a largely explored DE model is a quintessence with an exponential potential. The phase space dynamics presents a future attractor in which the quintessence and, for instance, a second fluid like DM, have scaling solutions. That scenario avoids the so called Big Rip and also addresses the "coincidence problem" [17, 15, 16]. Another application of the exponential potential is in matter bounce scenarios [23, 3, 7]. The contracting phase dominated by the scalar field with exponential potential contains an unstable critical point from where all solutions emerge. By a suitable choice of the parameter λ, the effective EoS of the scalar field in the vicinity of the unstable critical point is that of a matter-fluid. Because it is a critical point, the system can be placed as close as necessary to generate longer or shorter contracting phases.

In previously studied matter bounce models, the bounce was driven by a ghost scalar field that dominates only close to the classical singularity at the end of the contracting phase. In the present work we have a quantum bounce driven by corrections to the background due to the Bohmian quantum potential in the context of the canonical quantization of gravity. Section 3.1 will be dedicated to the formulation of the classical background, based on the implicit analytic solutions of Eqs. (2.6) and (2.7) for the potential (3.2). Section 3.2 discusses the canonical quantization of gravity and the use of the DeBroglie-Bohm (dBB) formulation of quantum mechanics to obtain bounce solutions. In Sec. 3.3 and Sec. 3.4, the full background is constrained and calculated.

3.1 Classical background dynamics

In the case of a single scalar field, λ is the relevant parameter when discussing the global behavior of the background. To determine the asymptotic behavior of the system we perform a dynamical system analysis for which the main technicalities are summarized in appendix A.

The background dynamics is given by the equations

$$\dot{H} = -\frac{\kappa^2}{2}\dot{\phi}^2, \tag{3.3}$$

$$\ddot{\phi} = -3H\dot{\phi} - \frac{\mathrm{d}V}{\mathrm{d}\phi}, \tag{3.4}$$

where Eqs. (3.3) and (3.4) are Eq. (2.6) and (2.7) with ρ and p given by Eqs. (2.3) and (2.4). Equation (3.4) is the so called Klein-Gordon equation. The above system is more treatable through a choice of dimensionless variables that allows us to rewrite the coupled second order equations (3.3) and (3.4) as a planar system [85]. The new variables are

$$x = \frac{\kappa\dot{\phi}}{\sqrt{6}H}, \tag{3.5}$$

$$y = \frac{\kappa\sqrt{V}}{\sqrt{3}H}. \tag{3.6}$$

x	y	w
-1	0	1
1	0	1
$\frac{\lambda}{\sqrt{6}}$	$-\sqrt{1-\frac{\lambda^2}{6}}$	$\frac{1}{3}\left(\lambda^2-3\right)$
$\frac{\lambda}{\sqrt{6}}$	$\sqrt{1-\frac{\lambda^2}{6}}$	$\frac{1}{3}\left(\lambda^2-3\right)$

Table 3.1.: Critical points of the planar system Eqs. (3.8) and (3.9).

In those new variables the Friedmann constraint, Eq. (2.5), reads:

$$x^2 + y^2 = 1 \tag{3.7}$$

and the effective EoS reads

$$w = 2x^2 - 1.$$

The above definitions applied to the systems of Eqs. (3.3) and (3.4) lead to the planar system:

$$\frac{\mathrm{d}x}{\mathrm{d}\alpha} = -3x(1-x^2) + \lambda\sqrt{\frac{3}{2}}y^2, \tag{3.8}$$

$$\frac{\mathrm{d}y}{\mathrm{d}\alpha} = xy\left(3x - \lambda\sqrt{\frac{3}{2}}\right), \tag{3.9}$$

where $\alpha \equiv \ln(a)$. The critical points are listed in Tab. 3.1.

From the definition (3.6), the contracting phase, $H < 0$, are trajectories with $y < 0$ and the expanding phase, $H > 0$, trajectories with $y > 0$, lower and upper quadrants of Figs. 3.1, 3.3 and 3.4. At the critical points where $w = 1$, the background evolves as a^{-6}, i.e., the scalar field behaves like a stiff-matter fluid. They are space-time singularities and the semi-circles of Fig. 3.1 are disconnected. Those critical points will be further referred to as $S_{\pm}$, the plus sign for $x = 1$ and the minus sign for $x = -1$. For those where the effective EoS is $w = \frac{1}{3}\left(\lambda^2 - 3\right)$, the background evolves as $a^{-\lambda^2}$.

The qualitative behavior of the system can be studied with the tools described in [85, 86, 87], for a detailed analysis see [77, 17, 16, 23]. For $\lambda < \sqrt{6}$, the first two critical points, $x = \pm 1$ and $y = 0$, are unstable (repellers) during expansion and stable (attractors) during contraction; for $\lambda > 0$, $x = \frac{\lambda}{\sqrt{6}}$ and $y = \sqrt{1 - \frac{\lambda^2}{6}}$ is an attractor and $x = \frac{\lambda}{\sqrt{6}}$ and $y = -\sqrt{1 - \frac{\lambda^2}{6}}$ a repeller.

Ir order to produce a matter bounce model, which is the most appropriate for generating adiabatic scale invariant spectra, we choose $\lambda = \sqrt{3}$. The two last critical points now read:

$$x_c = \frac{\sqrt{2}}{2} \quad \text{and} \quad y_c = \pm\frac{\sqrt{2}}{2}.$$

As a consequence the scalar field behaves as a matter-fluid, $w = 0$, close to the repeller $(\frac{\sqrt{2}}{2}, -\frac{\sqrt{2}}{2})$, further on referred to as M_-. Since the critical points are symmetric, the choice of λ implies that in the future attractor, $(\frac{\sqrt{2}}{2}, \frac{\sqrt{2}}{2})$, the scalar field also behaves as matter-like fluid. From here on this critical point will be referred to as M_+. In Fig. 3.1 we have the phase space for the planar system of Eqs. (3.8) and (3.9).

The contraction history goes as follows. The Universe starts close to the critical point M_- with $x_{\rm ini} = \frac{\sqrt{2}}{2} \pm \epsilon$ for $0 < \epsilon \ll 1$. The plus sign and the minus sign lead the contraction to the stable point S_+ or S_-, respectively. Close to $S_\pm$ the final EoS is $w = 1$, hence the background goes as a^{-6} and the contraction finishes in a singularity. Classically, there is no possible bounce solution when the system arrives at the critical points $S_\pm$.

The DE epoch is characterized by $w < -\frac{1}{3}$, which happens when

$$-\frac{\sqrt{2}}{3} < x < \frac{\sqrt{2}}{3}.$$

In the contracting phase, the DE belongs to the trajectory $M_- \longrightarrow S_-$ and in expanding phase to the trajectory $S_- \longrightarrow M_+$.

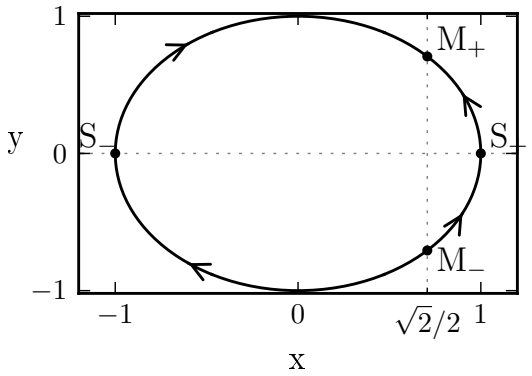

Figure 3.1.: Phase space for the planar system of Eqs. (3.8) and (3.9). The critical points are indicated by $M_{\pm}$, for a scalar field with a matter-type effective EoS and $S_{\pm}$ for a stiff-matter-like one. For $y < 0$ he have the contracting phase and for $y > 0$ the expanding phase. The lower and upper quadrants are not physically connected, because there is no classical mechanism that could drive a bounce between the contraction and expanding phases.

At the critical points $M_{\pm}$, Eq. (3.5) gives

$$H = \frac{\kappa\dot{\phi}}{\sqrt{3}},$$

represented as a straight line in the qualitative phase space in Fig. 3.2. Close to $S_{\pm}$ one has

$$\phi \propto \alpha, \quad \dot{\phi} \propto H \quad \text{and} \quad H \propto \exp^{-3\alpha},$$

deduced from Eqs. (2.5), (3.5) and from the fact that $H = \dot{\alpha}$. Close to the singularity $\alpha \to -\infty$, for the contracting phase

$$\lim_{x\to\pm1} \begin{cases} H & \to -\infty, \\ \phi & \to \pm\frac{\sqrt{6}}{\kappa}\alpha \quad \to \mp\infty, \\ \dot{\phi} & \to \pm\frac{\sqrt{6}}{\kappa}H \quad \to \mp\infty, \end{cases} \tag{3.10}$$

and for the expanding phase

$$\lim_{x\to\pm1} \begin{cases} H & \to \infty, \\ \phi & \to \pm\frac{\sqrt{6}}{\kappa}\alpha \quad \to \mp\infty, \\ \dot{\phi} & \to \pm\frac{\sqrt{6}}{\kappa}H \quad \to \pm\infty. \end{cases} \tag{3.11}$$

To understand the schemes (3.10) and (3.11) let's consider the contracting phase ending at the critical point S_+, which happens for $x \to +1$ (upper signs in the previous expressions). When $\alpha \to -\infty$ in the end of contracting phase, then $\dot{\phi} \to \infty$. However, when $\alpha \to -\infty$ in the beginning of expanding phase $\dot{\phi} \to -\infty$. Any possible trajectory in the phase space of H and $\dot{\phi}$ that connects $\phi \to -\infty$ with $\phi \to \infty$ would necessarily cross the other solutions, for instance, the straight line representing the solution at the critical point $M_\pm$. The same analysis can be performed for a contracting phase ending at S_-. The existence and uniqueness theorem for differential equation guarantees that trajectories do not cross in phase space. Figure (3.2) qualitatively depicts these arguments. Hence, there is no way a bounce could connect a contraction ending in the same critical point from which the expansion begins, i.e., there is no solution in the complete phase space where the Universe contracts in the direction of S_- (S_+) and expands from S_- (S_+).

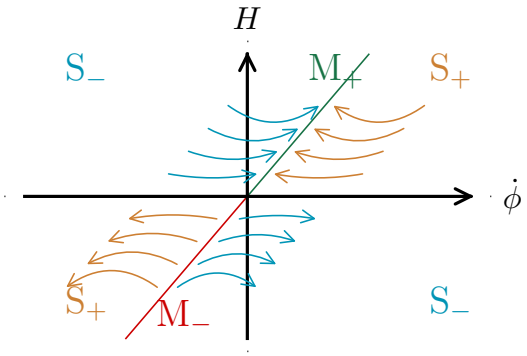

Figure 3.2.: Illustration of the solutions for H and $\dot{\phi}$ close to the critical points $S_\pm$ and $M_\pm$. In a full quantized system in which the Universe bounces due to quantum corrections close to the Planck scale, the allowed phase space connect the contraction finishing at $S_\pm$ with the expansion starting at $S_\mp$.

The bounce is still possible, though. A solution in the phase space of H and $\dot{\phi}$ that satisfies the uniqueness and existence criteria would be the one connecting the contracting phase ending at S_+ (S_-) with the expansion from S_- (S_+). For the model in consideration, we have then two possible histories of the Universe showed in Figs. 3.3 and 3.4.

In the case of Fig. 3.3, a contracting phase starts close to M_-, $x_{\rm ini} = \frac{\sqrt{2}}{2} - \epsilon$, passes through a DE epoch and approaches S_-. Around S_- a new physics takes place performing a bounce and the Universe starts expanding from S_+ and ends in matter-like expansion at M_+. In the trajectory $S_+ \to M_+$ one has $x > \frac{\sqrt{2}}{3}$, which means that there is not a DE epoch in the expanding phase.

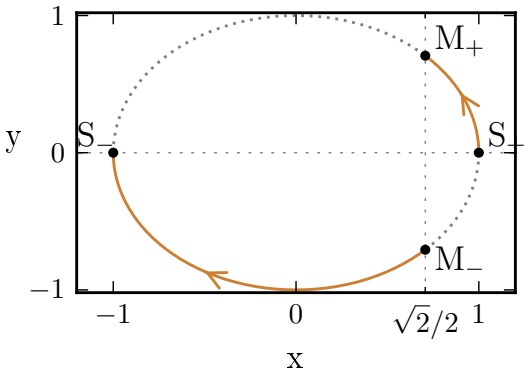

Figure 3.3.: Case A: the scale field has a DE-type EoS during the contracting phase. By means of the quantum bounce, this system can not address the DE in the future, since the matter attractor is reached after the stiff-matter expansion.

The case of Fig. 3.4 is the opposite. The contracting phase starts close to M_- with $x_{\rm ini} = \frac{\sqrt{2}}{2} + \epsilon$ and goes to S_+. Since $x > \frac{\sqrt{2}}{3}$ all along the trajectory $M_- \to S_+$, there is no DE epoch during the contraction. Around S_+ a new physics avoids the singularity and transits the Universe to an expansion that starts in S_-. From S_- the Universe passes by a DE epoch and ends finally in the matter expansion, the attractor M_+.

The two above mentioned scenarios are very interesting. From here on we name case **A** the one with DE in the contracting phase and case **B** the one the DE epoch in the expanding phase, Figs 3.4 and 3.3, respectively.

Case **A** is an academic exercise of how a scalar field could perform both the matter contraction and the DE epoch. It could be used as a toy model to study how a transient DE epoch affects the primordial power spectra, but it cannot be a realistic scenario since there is no DE epoch in the expanding phase.

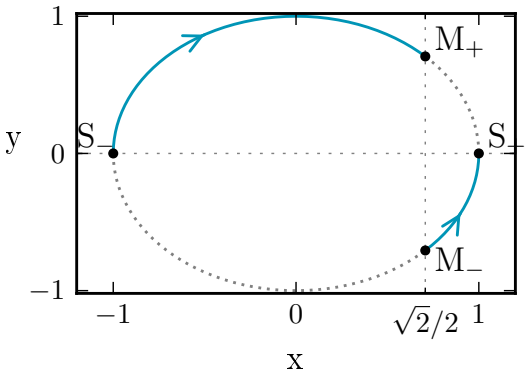

Figure 3.4.: Case B: the contracting phase begins close to the instable point M_-, in which the scalar field has a matter-type EoS. After the quantum bounce, the expanding phase starts in S_- and has a DE epoch before it reaches the future attractor M_+.

Case **B** is a more realistic one and is a very interesting scenario: the same scalar field that drives the matter contraction accomplishes for the bounce and for the DE epoch in the expanding phase. This is the one we will focus in this work.

As we mentioned earlier, there is no classical bounce in the previous described backgrounds. Close to the attractor of the contracting phase (S_+ in case A and S_- in case B) $H \propto -\exp^{-3}$ and when $a \to 0$ the Universe approaches a singularity. This happens precisely because the kinetic term dominates the Lagrangian of the scalar field. However, in the case the kinetic term dominates it has already been demonstrated a quantum bounce solution. In the next section, we develop the results from [27] and show how they can be applied to our cases avoiding the singularity and connecting $S_\pm$ with $S_\mp$.

3.2 The quantum bounce

Quantum cosmology is the field of research in which quantum theory is applied to the Universe and should have the standard cosmological models as its classical limit. This interesting and challenging topic, not only enlightens fundamental problems of

cosmology, such as the singularity problem, but also allows fundamental quantum mechanics to be tested at the cosmological level [88, 89, 90, 91, 92].

A quantum description of gravity, besides facing mathematical problem because of the non-renormalizable aspect of GR [93], also suffers from fundamental issues in what concerns the application of a quantum theory of gravity to the description of the Universe. In order to accomplish a quantum theory of the Universe, the traditional Copenhagen interpretation of quantum mechanics has to be replaced.

The main limitation of the Copenhagen interpretation is the postulate of the collapse of the wave function, i.e., the need of an external classical system that performs the collapse. Since quantum gravity is applied to the Universe, by definition, there is no such external observer.

Any alternative to the Copenhagen interpretation applicable to Cosmology should agree with the results from experimental particle physics, but should also dispense the need of an exterior classical world. There are many proposals of quantum gravity that satisfy those criteria and were already applied to Cosmology such as: the consistent histories [94, 95], collapse model of the wave-function [96, 91, 92], many worlds interpretation [97, 98] and the DeBroglie-Bohm (dBB) interpretation [99, 100], which is the one we will adopt here.

The canonical quantization of gravity by means of the ADM formalism, which would be an effective limit of more fundamental unification theories, can be interpreted using the de Broglie-Bohm (dBB) formulation of quantum mechanics. The solution for the Wheeler-de Witt equation are Bohmian trajectories with an objective reality, hence there is no problem of collapse of the wave-function [99, 101].

A flat, homogeneous and isotropic space-time in the presence of a scalar-field with a dominant kinetic term, have already been quantized in the literature [27]. The superposition of the Bohmian trajectories for the system lead to bounce solutions. Both models described in the previous section, cases **A** and **B** have in common

the stiff-matter domination phase before and after the bounce. A stiff-matter like EoS means that the kinetic term dominates the exponential potential $V(\phi)$ in the previously discussed scenarios and, in the vicinity of $S_{\pm}$, our model has the same physical conditions as the one quantized in [27].

To perform Dirac's canonical quantization procedure, a Hamiltonian formulation of GR is needed. The simplest and most common approach is the ADM (Arnowitt-Misner-Deser) formalism. For a recent republication see Ref. [102]. In the ADM decomposition, the four dimensional space-time manifold is foliated in three-dimensional hypersurfaces of constant time and the usual Einstein-Hilbert action

$$\mathcal{S} = \int \sqrt{-g}\mathrm{R}\mathrm{d}^4x$$

is rewritten in terms of the ADM canonical variables, N, N^i and h_{ij}. They are related to the original four-dimensional metric, g_{ij}, as follows:

$$g_{ij} = h_{ij} \tag{3.12}$$

$$g_{0i} = N_i \tag{3.13}$$

$$g_{00} = -N^2 + N^i N_i. \tag{3.14}$$

In the above equations N is the lapse function, N^i the shift function and h_{ij} the three-metric of the hypersurfaces. For closed spatial sections[1], the decomposed action reads

$$\mathcal{S} = \int \mathrm{d}t\mathrm{d}^3x N\sqrt{h}\left({}^{(3)}\mathrm{R} + \mathrm{K}_{ij}\mathrm{K}^{ij} - \mathrm{K}_2\right), \tag{3.15}$$

where

$$\mathrm{K}_{ij} = \frac{1}{2N}\left(2D_{(i}N_{j)} - \frac{\partial h_{ij}}{\partial t}\right) \tag{3.16}$$

[1] On close spatial section the calculations for the ADM formalism are more straightforward, since surface terms are eliminated all along the construction of GR's Hamiltonian. For open spatial section, surface terms have to be evaluated, but this discussion is not relevant for the further developments of this thesis.

is the extrinsic curvature, D_i the covariant derivative and ${}^{(3)}\mathrm{R}$ the Ricci scalar, both calculated using the three-metric h_{ij}. The conjugate momenta read

$$\Pi \equiv \frac{\partial \mathcal{L}}{\partial \dot{N}} \approx 0, \tag{3.17}$$

$$\Pi_i \equiv \frac{\partial \mathcal{L}}{\partial \dot{N}_i} \approx 0, \tag{3.18}$$

$$\Pi_{ij} \equiv \frac{\partial \mathcal{L}}{\partial_t \dot{h}_{ij}} = -\sqrt{h}\left(\mathrm{K}_{ij} - h_{ij}\mathrm{K}\right), \tag{3.19}$$

where $\mathcal{L}$ is the Lagrangian density in (3.15), revealing that the only dynamical variable is the metric h_{ij}. Equations (3.17) and (3.18) are first order constraints and Dirac formalism for constrained Hamiltonian systems has to be applied [103]. In Dirac's terminology, "weakly zero" in Eqs. (3.17) and (3.18), means that those constraints are null only for a subset of the phase-space.

When checking the conservation in time of the constraints in Eqs. (3.17) and (3.18), two second order constraints are identified

$$\mathcal{H} = G_{ijkl}\Pi^{ij}\Pi_{ij} - {}^{(3)}R\sqrt{h} \approx 0, \tag{3.20}$$

$$\mathcal{H}^j = -2D_i\Pi^{ij} \approx 0, \tag{3.21}$$

named the superhamiltonian and the supermomenta, respectively. In Eq. (3.20), G_{ijkl} is called the DeWitt metric and it is defined as

$$G_{ijkl} = \frac{1}{2\sqrt{h}}\left(h_{ik}h_{jl} + h_{il}h_{jk} - h_{ij}h_{kl}\right). \tag{3.22}$$

One can verify that N and N^i are merely Lagrange multipliers for the superhamiltonian and the supermomenta and also that (3.29), (3.30), (3.20) and (3.21) are first class constraints, which means they are related to the gauge freedom of the theory. The final Hamiltonian of GR reads

$$H_{\mathrm{GR}} = \int \mathrm{d}^3x \left(N\mathcal{H} + N_j\mathcal{H}^j\right), \tag{3.23}$$

Dirac's quantization procedure considers the canonical variables as operators acting in the wave functional $\Psi[h_{ij}, t]$, and when composed in the total Hamiltonian gives the Schrödinger equation

$$i\hbar\frac{\partial\Psi}{\partial t} = \hat{H}_{\rm GR}\Psi. \tag{3.24}$$

However, $\hat{H}_{\rm GR}$ is a function of first class constraints and the above equation leads to no dynamics. For constrained Hamiltonians systems, Dirac prescribes the following relations to the wave functional:

$$\hat{\mathcal{H}}\Psi[h_{ij}, t] = 0, \tag{3.25}$$

$$\hat{\mathcal{H}}^i\Psi[h_{ij}, t] = 0, \tag{3.26}$$

which implies that Eq. (3.24) is null and, therefore, the wave-functional doesn't depend on time. This is the so-called time issue in quantum gravity. For a homogeneous Universe, $\mathcal{H}^i$ is identically zero and Einstein's equation can still be recovered if one sets $N_i = 0$. Hence, the relevant equation for the wave functional, from here on referred to as the Wheeler-De Witt equation (WdW), reads

$$\hat{\mathcal{H}}\Psi[h_{ij}, t] = 0. \tag{3.27}$$

The above equation is a very complicated set of functional differential equations not well-defined mathematically. Therefore, in order to solve Eq. (3.27) in the cosmological context, the degrees of freedom of the metric and of the scalar field are reduced. This simplification is done by selecting amongst the superspace of all equivalent metrics h_{ij} those that satisfy the required symmetries, for instance isotropy and homogeneity, which in the present case reduces the infinite degrees of freedom to only two, the scalar factor and the scalar field amplitude [99, 104]. This is the so-called minisuperspace model. Even though it is a working hypothesis, most of the important and relevant issues of quantum cosmology can be addressed by the minisuperspace models, such as the time issue and the avoidance of the singularity by quantum corrections of the background.

Avoiding the technicalities, which can be found in Refs. [105, 99, 104], the specialization of the total Hamiltonian (GR + matter field with $V = 0$) in the minisuperspace model for the metric FLRW (2.2) reads:

$$H = N\mathcal{H} = \frac{N\kappa^2}{12V_l \mathrm{e}^{3\alpha}}\left(-\Pi_\alpha^2 + \Pi_\phi^2\right), \tag{3.28}$$

with the associated momenta

$$\Pi_\alpha = -\frac{6V_l}{N\kappa^2}\mathrm{e}^{3\alpha}\dot{\alpha}, \tag{3.29}$$

$$\Pi_\phi = \frac{6V_l}{N\kappa^2}\mathrm{e}^{3\alpha}\dot{\phi}. \tag{3.30}$$

In the above equations, and from here on, we will adopt

$$\phi = \phi \to \frac{\kappa\phi}{\sqrt{6}}$$

and $\alpha = \ln a$ as before. For a flat hypersurfaces, V_l, which is the total volume of the hypersurfaces divided by a^3, can have any value [27, 106] and we will choose $V_l = \frac{4\pi\ell_{\mathrm{Pl}}^3}{3}$ in order to have $a \to a/\ell_{\mathrm{Pl}}$ [7]. The WdW equation, Eq. (3.27), reads

$$\left[-\frac{\partial^2}{\partial\alpha^2} + \frac{\partial^2}{\partial\phi^2}\right]\Psi(\alpha,\phi) = 0, \tag{3.31}$$

whose solution is

$$\begin{aligned}\Psi(\alpha,\phi) &= F(\phi+\alpha) + G(\phi-\alpha) \\ &\equiv \int \mathrm{d}k\Big\{f(k)\exp\left[ik(\phi+\alpha)\right] + g(k)\exp\left[ik(\phi-\alpha)\right]\Big\},\end{aligned} \tag{3.32}$$

where f, g are arbitrary functions.

In the context of minisuperspace models, the dBB formulation of quantum mechanics eliminates the time issue [99], and cosmological solutions are the Bohmian trajectories, which have an objective reality [107, 99, 100, 27].

In order to construct the Bohmian trajectories, one starts by rewriting the solution (3.32) in the polar form

$$\Psi = R\exp(iS),$$

which replaced in Eq. (3.28) yields

$$\left(\frac{\partial S}{\partial \alpha}\right)^2 - \left(\frac{\partial S}{\partial \phi}\right)^2 - \frac{1}{R}\left(\frac{\partial^2 R}{\partial \alpha^2} - \frac{\partial^2 R}{\partial \phi^2}\right) = 0. \tag{3.33}$$

The last term on the LHS is the quantum potential,

$$Q = -\frac{1}{R}\left(\frac{\partial^2 R}{\partial \alpha^2} - \frac{\partial^2 R}{\partial \phi^2}\right), \tag{3.34}$$

and when Q is negligible, the Bohmian trajectories coincide with the usual background solution from the Friedmann equations for a stiff-matter-like fluid.

The Bohmian trajectories $\alpha(t)$ and $\phi(t)$ are obtained by imposing the dBB guidance relations

$$\Pi_{(\alpha,\phi)} = \frac{\partial S}{\partial(\alpha,\phi)},$$

which for Eqs. (3.29) and (3.30) are

$$\Pi_\alpha = \frac{\partial S}{\partial \alpha} = -\ell_{\rm Pl}\mathrm{e}^{3\alpha}\dot{\alpha}, \tag{3.35}$$

$$\Pi_\phi = \frac{\partial S}{\partial \phi} = \ell_{\rm Pl}\mathrm{e}^{3\alpha}\dot{\phi}, \tag{3.36}$$

The cosmic time was adopted by setting $N = 1$.

In Ref. [27], the authors use a Gaussian superposition of plane-waves by choosing

$$f(k) = g(k) = \exp\left[\frac{-(k-d)^2}{\sigma^2}\right]. \tag{3.37}$$

Integrating Eq. (3.32) and writing Ψ in the polar form, one can express $S = S(\alpha, \phi)$ and replace it in the guidance relation to obtain

$$\dot{\alpha} = \frac{R_H}{\ell_{\rm Pl}} \frac{\phi\sigma^2 \sin(2d\alpha) + 2d \sinh(\sigma^2\alpha\phi)}{2\mathrm{e}^{3\alpha}\left[\cos(2d\alpha) + \cosh(\sigma^2\alpha\phi)\right]}, \tag{3.38}$$

$$\dot{\phi} = \frac{R_H}{\ell_{\rm Pl}} \frac{-\alpha\sigma^2 \sin(2d\alpha) + 2d\cos(2d\alpha) + 2d\cosh(\sigma^2\alpha\phi)}{2\mathrm{e}^{3\alpha}\left[\cos(2d\alpha) + \cosh(\sigma^2\alpha\phi)\right]}. \tag{3.39}$$

The above equations determines the Bohmian trajectories for α and ϕ and the constant $\frac{R_H}{\ell_{\rm Pl}}$, where $R_{\rm H} = H_0^{-1}$, is used so the time is measured in units of H_0^{-1}.

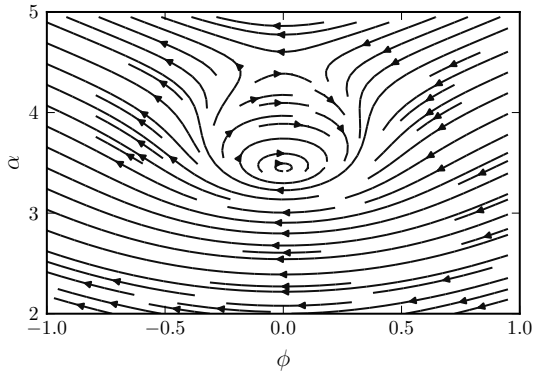

Figure 3.5.: Phase space for the system of Eqs.(3.38) and (3.39) for $d = -1$ and $\sigma = 1$. We can notice the bounce solutions and the cyclic solutions around the centers.

In Fig. 3.5 we have the phase space for the Eqs. (3.38) and (3.39). We can notice the presence of bounce solutions and cyclic solutions. It is easy to calculate the nodes and centers, and they happen all along the line $\phi = 0$ for $d\alpha = (2n+1)\pi/2$, nodes, and $\sigma^2\alpha/2d = \cot(d\alpha)$, centers [27].

The classical limits of Eqs. (3.38) and (3.39) are obtained for large α, when the hyperbolic function dominates. From the definition of x, (3.5), the following relations are straightforward:

$$x \approx \coth\left(\sigma^2\alpha\phi\right), \tag{3.40}$$

$$\frac{H}{H_0} \approx \frac{R_H}{\ell_{\rm Pl}} \frac{d\mathrm{e}^{-3\alpha}}{x}, \tag{3.41}$$

$$\dot{\phi} \approx \frac{R_H}{\ell_{\rm Pl}} d\mathrm{e}^{-3\alpha}. \tag{3.42}$$

These equations imply that ϕ and x have the same sign, and $\dot{\phi}$ the same sign as d in the classical limit. This means that in case **A**, since its contraction ends in $x \to -1$, Eq. (3.41) is satisfied only if $d > 0$. Similarly, case **B** requires $d < 0$. This result is consistent with our discussion in Sec. 3.1. In case **A**, the quantum dynamics starts with $x \approx -1$ ($\phi \ll -1$), ending in $x \approx 1$ ($\phi \gg 1$). The opposite happens in case **B**, i.e., our bouncing dynamics always connects the classical critical points S_- (S_+) with S_+ (S_-). In practice, the sign of d determines in which direction time evolves, thereby selecting between cases **A** or **B**.

3.3 Matching of the background

Previously we exposed the quantum correction to the system when the kinetic term of the scalar field dominates. In order to construct a complete background we should be able to match the solutions from the classical evolution, described in Sec. 3.1, with the quantum solution from the system of equations (3.38).

The nomenclature in what follows may be confusing and we will adopt "quantum/ classical solutions" to name the dynamics described by Eqs. (3.38) and (3.39) and the one described by Eqs. (3.8) and (3.9) respectively. To make reference to the period at which the quantum potential is relevant we will adopt *quantum phase* in opposition to the *classical phase*, in which the quantum potential is irrelevant. This nomenclature should not be taken strictly since, in the complete dBB formulation, we have the Bohmian trajectories that account for the complete background regimes, which would be the case if the Hamiltonian in (3.28) had the exponential potential, Eq. (3.2). The full quantum description of this system can be found in Ref. [108] showing the phase space that contains bounce solutions. The present approach by means of a matching between the classical and quantum solutions leads to the same results as their rigorous approach, but avoids the technical difficulties in explicitly calculating the background evolution, allowing us to address the problem of the primordial perturbations directly with no loss of relevant information.

The complete background solution has three branches. The first one is the classical contraction that starts with $x \approx 1/\sqrt{2}$ and ends at $x \to \pm 1$. The second branch is the quantum background that starts at $x \approx \pm 1$ and bounces to $x \approx \mp 1$. The third branch, the classical expansion, starts with $x \to \mp 1$ and ends with $x \to 1/\sqrt{2}$. The lower signs holding for the case A and the upper signs for the case B.

The match is performed guaranteeing the continuity of the solutions at the time they transit from one regime to another, which happens when the quantum solution reaches its classical limit, Eqs. (3.40) and (3.41).

However, the classical limit of the quantum regime happes when $x = \pm 1$, which is a critical point of the classical equations, Eqs. (3.8) and (3.9). To start the classical phase at a critical point means that the Universe would be stuck in the stiff-matter epoch. We will parametrize x in the vicinity of the stiff critical points by $x_\pm = \pm(1 - \epsilon_\pm)$. At the matching point, $\epsilon_\pm$ should be small enough to justify the classical limit of the quantum regime, the plus sign holds for the vicinity of the S_+ and the minus sign for the vicinity of S_-.

If the background was obtained by the Bohmian trajectories in the full quantized system, the initial conditions would be given in the far past of the contraction phase. For instance, the system would evolve from a $x_{\rm ini}$ close to the unstable point M_-. The proximity between $x_{\rm ini}$ and M_- dictating the duration of the matter epoch and selecting between cases **A** and **B** if $x_{\rm ini} \lessapprox x_{\rm c}$ or $x_{\rm ini} \gtrapprox x_{\rm c}$, respectively. The choice of the parameter d should be in agreement with the choice between the cases: $d > 0$ demands $x_{\rm ini} \lessapprox x_{\rm c}$, and $d < 0$, $x_{\rm ini} \gtrapprox x_{\rm c}$. Also, one would have to choose an initial scale factor, $a_{\rm ini}$, and a Hubble constant, $H_{\rm ini}$ ($\phi_{\rm ini}$ and $\dot{\phi}_{\rm ini}$ are constrained by the value of $x_{\rm ini}$ and V_0 through the Friedmann equation). With that all set, the Bohmian trajectories would describe the whole evolution until the expanding phase. Therefore, the main characteristics of the background as the minimum scale factor of the bounce, the energy scale of the DE epoch and the duration of the quantum bounce, would be a consequence of the model parameter V_0, the wave-function and the initial conditions.

Because of our matching procedure, things are a little more subtle. We not only have the choice of initial conditions, rather of the quantum bounce parameters, d and σ, but also contracting and expanding matching parameters, respectively $\epsilon_{\rm c}$ and $\epsilon_{\rm e}$. In what follows we will rewrite the system in terms of new parameters that will assist us with writing the full background solution. The new parameters will also control the physical aspects of the background that are relevant to the discussion on the cosmological perturbations, such as, the duration of the matter epoch, the energy scale of the DE phase and the depth of the bounce.

Using Eq. (3.5) to integrate Eq. (3.3) in x we have:

$$\frac{\mathrm{d}H}{\mathrm{d}\alpha} = -3x^2 H. \tag{3.43}$$

Using Eqs. (3.8) and (3.7) we can integrate the above expression in x to find:

$$\log(H) = \sqrt{2}\tanh^{-1}(x) + \log\left(\frac{\frac{1}{\sqrt{2}} - x}{1 - x^2}\right) + \mathcal{C}_1 \tag{3.44}$$

Because, $H = \dot{\alpha}$, from (3.44) we have the evolution of the scale factor with x:

$$3\log(a) = -\sqrt{2}\tanh^{-1}(x) - \log\left(\frac{\left(\frac{1}{\sqrt{2}} - x\right)^2}{1 - x^2}\right) + \mathcal{C}_2. \tag{3.45}$$

In the above equations $\mathcal{C}_{1,2}$ are integration constants and we can combine them to write:

$$a^6 H^2 = \frac{\bar{\mathcal{C}}_1}{\left(\frac{1}{\sqrt{2}} - x\right)^2} \quad \text{and} \tag{3.46}$$

$$a^3 = \frac{\bar{\mathcal{C}}_2 (1-x)^{\gamma_+} (1+x)^{\gamma_-}}{\frac{1}{\sqrt{2}} - x}, \tag{3.47}$$

where $\bar{\mathcal{C}}_1$ and $\bar{\mathcal{C}}_1$ are constants. We will use H in units of H_0, the Hubble parameter today, and parametrize a by an a_0, which for now is just a meaningless number not necessarily connected to H_0. The above equation becomes

$$\left(\frac{a}{a_0}\right)^6\left(\frac{H}{H_0}\right)^2 = \frac{C_1}{\left(\frac{1}{\sqrt{2}}-x\right)^2} \quad \text{and} \tag{3.48}$$

$$\left(\frac{a}{a_0}\right)^3 = \frac{C_2\,(1-x)^{\gamma_+}\,(1+x)^{\gamma_-}}{\left(\frac{1}{\sqrt{2}}-x\right)^2}, \tag{3.49}$$

where $\gamma_\pm \equiv 1 \pm \frac{1}{\sqrt{2}}$ The introduction of H_0 and a_0 can be absorbed in to C_1 and C_2 preserving the degrees of freedom.

The numerical calculation was performed as follows: initial conditions were chosen in the bounce and the expansion and contracting phases were evolved from it until the classical regime of the quantum equations was reached. During the period at which $x \approx \pm 1$ quantum and classical background were matched guaranteeing the continuity of the solutions. Due to some particularities, the matching procedure will be presented in the two following subsections: the first one will consider the energy scale of the matter epoch and the second one the energy scale of the DE epoch. In the diagram of Fig. 3.6 we show the epochs in each case A and B, and the different regimes, classical and quantum.

Matching with the matter domination scale

The matching between the quantum and the classical solutions have to take place close to the critical points $S_\pm$, i.e., for a $x(a_\pm) = \pm(1-\epsilon(a_\pm))$ with $a_\pm$ the scale factor at which the classical equations start to be evolved. The parameter $\epsilon_\pm$ controls the quality of the matching, $0 < \epsilon \ll 1$. In Eqs. (3.48) and (3.49), we will consider a_0 the scale factor at which the Universe is at the matter epoch. Since it happens at a critical point, we have an infinite set of a_0 that satisfies $x(a_0) = \frac{\sqrt{2}}{2} + \epsilon_{\rm c}(a_0)$, with $0 < \epsilon_{\rm c} \ll 1$.

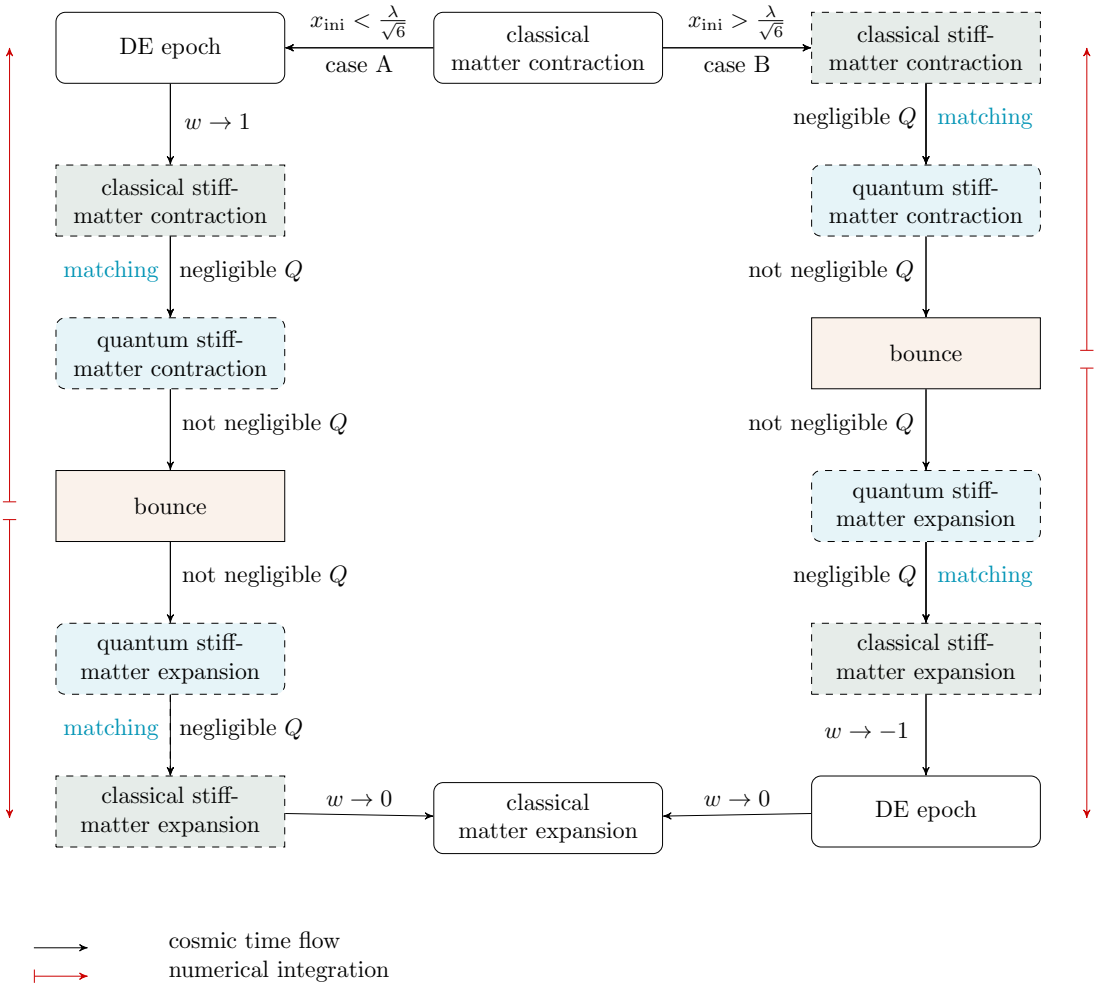

Figure 3.6.: The epochs of the Universe in case A and B. The cosmic time runs in the direction of the black full lines from the matter contraction to the matter expansion. The numerical integration is performed in the direction of the red lines: from the bounce to the expansion and contracting phases.

The Hubble parameter around $x_\pm$ reads

$$\left(\frac{H_\pm}{H_0}\right)^2 \approx \frac{C_1}{\gamma_\mp^2}\left(\frac{\bar{a}_0}{a_\pm}\right)^6. \tag{3.50}$$

The continuity condition implies that $H_\pm = H_{qt}$, where H_{qt} is the classical limit of the quantum solutions, Eq. (3.41). This equality gives

$$C_1 = \frac{R_H^2}{\ell_{\rm Pl}^2}\frac{d^2\gamma_\mp^2}{\mathcal{X}_{\rm b} a_{\rm b}^6}. \tag{3.51}$$

All the above parameters are model parameters, with exception of a_0, which is arbitrary. For future proposes, it is convenient to set a_0 in term of the variable $\mathcal{X}_{\rm b}$, defined as

$$\mathcal{X}_{\rm b} \equiv \frac{a_0}{a_{\rm b}}. \tag{3.52}$$

This new parameter controls the number of e-folds between the matter epoch and the bounce and will be a key parameter to discuss the influence of that duration in the spectrum of the primordial perturbations.

Expanding the Eq. (3.49) around $x_\pm$ one obtains

$$C_2 = \frac{\gamma_\mp^2}{2^{\gamma_\mp}\epsilon_\pm^{\gamma_\pm}}\left(\frac{a_\pm}{\bar{a}_0}\right)^3. \tag{3.53}$$

Now, C_1 and C_2 are fixed in terms of the model parameters, d and σ, the matching parameters $a_\pm$ and $\epsilon_\pm$ and a sort of initial condition a_0 through the parameter $\mathcal{X}_{\rm b}$.

However, the matching point is still arbitrary and any value of $a_\pm$ and $\epsilon_\pm$ is accepted as long as $w = 1$ and the classical regime of the quantum solution is valid. In order to constrain the matching point, we will introduce another parameter, $\Omega_{\rm m}$ with a very neat physical meaning. Close to the matter epoch the zeroth order Hubble parameter reads, from Eq. (3.46),

$$\left(\frac{H}{H_0}\right)^2 \approx \frac{C_1}{C_2\gamma_-^{\gamma_+}\gamma_+^{\gamma_-}}\left(\frac{\bar{a}_0}{a}\right)^3. \tag{3.54}$$

The last expression motivates the definition of the parameter $\Omega_{\rm d}$ as

$$\Omega_d = \frac{C_1}{C_2\gamma_-^{\gamma_+}\gamma_+^{\gamma_-}} = \frac{R_H^2}{\ell_{\rm Pl}^2}\frac{d^2\gamma_\mp^2}{C_2\gamma_-^{\gamma_+}\gamma_+^{\gamma_-}a_0^6}. \tag{3.55}$$

Hence, for $a = a_0$ one has

$$H^2(a = a_0) \approx H_0^2\Omega_{\rm d}$$

To choose $\Omega_{\rm d}$ is to choose the energy scale of the matter epoch. For instance, $\Omega_{\rm d} = 1$ means that the matter epoch happens at the same energy scale as the current Universe.

In terms of the physical variables Ω_d and $\mathcal{X}_{\rm b}$, the constant C_2 reads,

$$C_2 = \frac{R_H^2}{\ell_{\rm Pl}^2}\frac{d^2\gamma_{\mp}^2}{\Omega_{\rm d}\gamma_-^{\gamma_+}\gamma_+^{\gamma_-}a_{\rm b}^6\mathcal{X}_{\rm b}^6}. \tag{3.56}$$

This expression is completely determined by our choices of the quantum initial condition a_b and the constants Ω_d and $\mathcal{X}_{\rm b}$. Plugging it into Eq. (3.53), we obtain our matching time

$$\frac{a_{\pm}}{\epsilon_{\pm}^{\gamma_{\pm}/3}} \approx \frac{1}{\mathcal{X}_{\rm b}a_{\rm b}}\left(\frac{R_H^2 d^2 2^{\gamma_{\mp}}}{\ell_{\rm Pl}^2\gamma_-^{\gamma_+}\gamma_+^{\gamma_-}\Omega_d}\right)^{1/3}. \tag{3.57}$$

The above equation is a consistency relation between the initially arbitrary parameters $a_{\pm}$ and $\epsilon_{\pm}$ and the given parameters d, σ, $\mathcal{X}_{\rm b}$ and $\Omega_{\rm d}$. It will be used as the criterium to stop the quantum evolution and switch to the classical equations. It should be noticed that the consistency relation depends on the product $\Omega_d\mathcal{X}_{\rm b}$, so one can fix $\Omega_{\rm d} = 1$ without loss of generality leaving the control of the matter duration with the parameter $\mathcal{X}_{\rm b}$. The constants C_1 and C_2 are already determined in Eqs. (3.51) and (3.56) and with Eqs. (3.48) and (3.49) allow us to calculate the classical background.

Matching in the DE branch

For the classical branch with a DE epoch we can set, alternatively, a_0 and the scale factor at which DE takes place. It happens for $x = 0$ and $w = -1$ and Eqs. (3.48) and (3.49) read

$$\left[\frac{H(a=\bar{a}_0)}{H_0}\right]^2 = 2C_1 \equiv \Omega_\Lambda, \qquad 2C_2 = 1, \tag{3.58}$$

where the parameter Ω_Λ is introduced and has the same meaning as $\Omega_{\rm d}$, i.e., it gives the energy scale of the DE epoch. If $\Omega_\Lambda = 1$, then $H(a_0) = H_0$ by the time

$w = -1$. When choosing the DE scale to do the matching there is no ambiguity, since it happens for a specific time, contrarily to the matter epoch, which happens for the infinite time that the system can remain at the critical point. By fixing Ω_Λ, the values of C_1 and C_2 in Eqs. (3.58) determine completely the classical solution in Eqs. (3.48) and (3.49). The consistency relation for that case can be calculated with Eqs. (3.51) and (3.56):

$$\frac{a_-}{\epsilon_-^{\gamma_-/3}} \approx \left(\frac{R_H|d|2^{\gamma_+}}{\ell_{\rm Pl}\sqrt{2\Omega_\Lambda}\gamma_+}\right)^{1/3}. \tag{3.59}$$

The above equation gives the value of a_- at which the quantum evolution stops and the classical solution starts. The minus sign is justified by the fact that the trajectories containing a DE epoch are those connected S_-, i.e., $x_- = -(1-\epsilon_-)$.

Initial conditions at the bounce

In Sec. 3.2 we have the equations of motion for the quantum branch, Eqs. (3.38) and (3.39). The bounce happens when $\alpha_{\rm b}$ and $\phi = 0$, which is a node of the planar system. We are obliged to give initial conditions close to the node in order to have non-trivial solutions. From now on we will consider the following time variable:

$$\alpha = \alpha_{\rm b} + \frac{\tau^2}{2}, \tag{3.60}$$

which leads to $\mathrm{d}\tau/\mathrm{d}t = H/\tau$ and $\mathrm{d}\alpha = \tau\mathrm{d}\tau$. The above parametrization accounts for the existence of a minimum scale factor, $\alpha_{\rm b}$, setting the bounce to happen when $\tau = 0$. Also, from Fig. 3.5, Eq. (3.60) is coherent with the fact that α does not change sign, which means that α attains its smallest value in the bounce. Expanding Eqs. (3.38) and (3.39) around the bounce, we get the leading order approximations

$$\frac{\mathrm{d}\tau}{\mathrm{d}t_Q} = \frac{\phi}{\tau}D_1, \tag{3.61}$$

$$\frac{\mathrm{d}\phi}{\mathrm{d}t_Q} = D_2, \tag{3.62}$$

where we rewrote the equation in terms of τ and the convenient dimensionless time variable $\mathrm{e}^{3\alpha}\ell_{_{\mathrm{Pl}}}\mathrm{d}t_Q = \mathrm{d}t$. The two constants D_1 and D_2 are

$$D_1 = \frac{\sigma^2\left[\sin(2d\alpha_{\mathrm{b}}) + 2d\alpha_{\mathrm{b}}\right]}{2\left[2\cos(2d\alpha_{\mathrm{b}}) + 1\right]},$$
$$D_2 = \frac{-\alpha_{\mathrm{b}}\sigma^2\sin(2d\alpha_{\mathrm{b}}) + 2d\cos(2d\alpha_{\mathrm{b}}) + 2d}{2\left[2\cos(2d\alpha_{\mathrm{b}}) + 1\right]}.$$

These equations can be easily integrated to give

$$\tau = t_Q\sqrt{D_1 D_2}, \qquad \phi = t_Q D_2, \tag{3.63}$$

where the sign of τ was chosen to coincide with the sign of t_Q. To start the calculations we have to chose a t_Q very small in order for the approximations Eq. (3.63) to be valid, for instance, $t_Q^{\mathrm{ini}} \propto \pm\mathcal{O}(10^{-50})$. For a plus sign we are integrating the expansion and for the minus sign the contracting phase.

After choosing α_{b}, d, σ, $\mathcal{X}_{\mathrm{b}}$ and Ω_Λ Eq. (3.63) gives the initial conditions for Eqs. (3.38) and (3.39). If $d > 0$ we have case **A** in which the DE epoch happens for the contracting phase and the matching can be performed using the DE domination scale. Hence, from $t_Q^{\mathrm{ini}} > 0$ the quantum solutions evolve from the bounce until the consistency condition Eq. (3.59) is satisfied and from there on the classical solutions are built with Eqs. (3.48) and (3.49). For $t_Q^{\mathrm{ini}} > 0$ the system enters the expanding phase, which can be matched using the matter domination scale. Again, the quantum solutions takes place until the consistency relation is satisfied, now, Eq. (3.57). From there on the classical solutions are used to complete the background.

If $d < 0$ we are in case **B**, i.e, DE in the expanding phase. The numerical integration goes much in the same way as described before, but now the contracting phase is matched with the matter domination scale, and the expansion, with the DE domination scale.

d	σ	$\alpha_{\rm b}$	$\mathcal{X}_{\rm b}$	Ω_Λ
10^{-5}	5×10^{-2}	$\mathbf{10^{-40}}$	10^{10}	$\mathbf{1}$
$\mathbf{10^{-1}}$	$\mathbf{5\times10^{-1}}$	10^{-5}	10^{20}	10^{20}
10	5	1	$\mathbf{10^{30}}$	10^{40}

Table 3.2.: The parameters of the numerical solutions, Figs. 3.7 to 3.12. The bold values in the table are fixated when one parameter is varied. For example, in Fig. 3.7, d assumes the three different values, but the other parameters were the one in bold letters, i.e., $\sigma = 0.5$, $\alpha_{\rm b} = 10^{-40}$, $\mathcal{X}_{\rm b} = 10^{30}$ and $\Omega_\Lambda = 1$.

3.4 Numerical solutions for the background

In this section we will explore the parameters space and see its influence on the complete background that will be used in the perturbative study. The bold values in Table 3.2 were fixed when just one parameter was varied. For instance, the variation of d for the case B, Fig. 3.7, was calculated with $\sigma = 0.5$, $\alpha_{\rm b} = 10^{-40}$, $\mathcal{X}_{\rm b} = 10^{30}$ and $\Omega_\Lambda = 1$.

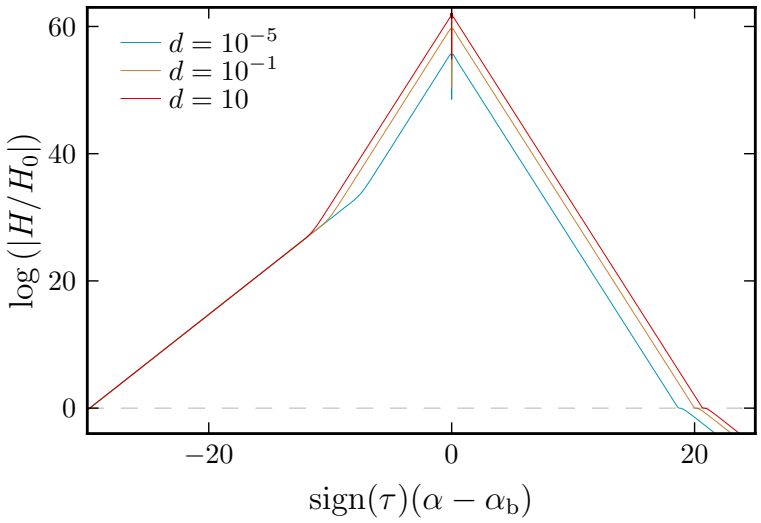

Figure 3.7.: Case **A**: the dependence of the background dynamics with the parameter d. Bigger values of d implies longer stiff-matter domination phase, which results in shorter matter contraction/expansion when $\mathcal{X}_{\rm b}$ is fixed..

In what concerns the study of the cosmological perturbations, the background dynamics can be fully understood by the plot of H with α, Figs. 3.7 to 3.11. We show the bounce asymmetry by choosing the horizontal axis to be

$$\mathrm{sign}(\tau)(\alpha - \alpha_{\mathrm{b}}).$$

The contracting phase is $\tau < 0$ and the expanding phase $\tau > 0$.

For a perfect fluid with $p = w\rho$, the evolution of H is:

$$\ln|H| \propto \pm\frac{3}{2}(w+1)\alpha, \tag{3.64}$$

with the minus sign for contraction and the plus sign for expansion. In the matter epoch, the effective EoS of the scalar field is $w = 0$, and in the stiff matter one it is $w = 1$, implying different slopes in Figs. 3.7 to 3.12. The duration of the epochs is connected with the size of the Universe at which we see the transition from one slope to another. The closer to the bounce the transition happens, the longer is the matter epoch. This is very important since we are interested in controlling the matter contraction duration to confirm its influence on the relevant modes.

The DE epoch happens when $x = 0$ corresponding to a short plateau between the matter and stiff-matter phases, for example, in Fig. 3.7 around $\alpha = 20$.

Except for Fig. 3.8, all the scenarios are solutions for case **B**, since we will focus on its property to discuss the primordial perturbations. Case **A** can be obtained from it by choosing

$$\mathrm{sign}(\tau)(\alpha - \alpha_{\mathrm{b}}) \to -\mathrm{sign}(\tau)(\alpha - \alpha_{\mathrm{b}}).$$

As we've mentioned before, it makes no sense to change Ω_Λ in case **B**, since it is a observational constraint. On the other hand, in case **A**, this is exactly the parameter we are interested in order to study perturbations during a DE epoch. Therefore, Fig. 3.8 is a plot for case **A**. This scenario is subject for further studies.

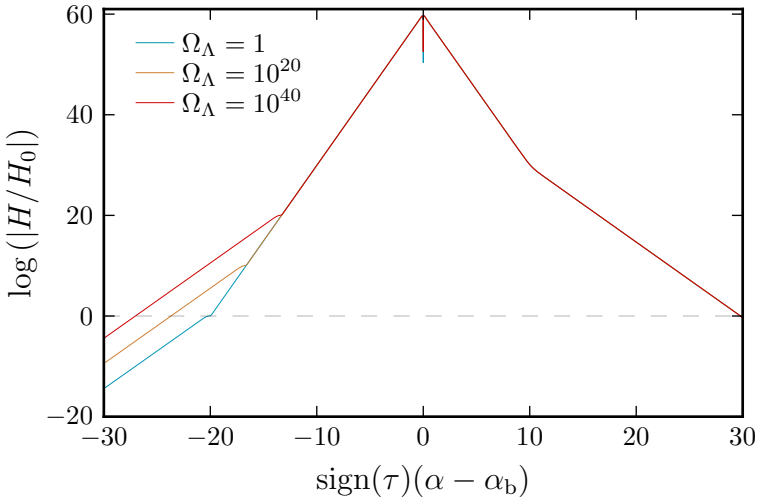

Figure 3.8.: For case **A**: the dependence of the DE epoch with the parameter Ω_Λ. Smaller values leads to earlier and less energetic DE epochs. For case B, Ω_Λ is an observational constraint, but if it could be changed, smaller Ω_Λ would imply in latter and less energetic DE epoch.

The bounce happens at $\tau = 0$ and the two peaks, better noticed in Figs. 3.9, 3.10 and 3.11, represent the maximum values of H reached by the system, further on referred to as H_ext. The peaks are at $\dot{H} = 0$ and we can use them to define the duration of the bounce, δ_b. The closer the peaks are in the plots, the smaller is δ_b (faster bounce). For instance, in Fig. 3.10, the red curve presents a faster bounce than the blue curve.

In what concerns the quantum solutions, the variation of the parameters d, σ and α_b directly changes the time and energy scales of the bounce. When increasing d, the frequency in the trigonometric functions of Eqs. (3.38) and (3.39) is higher and it is possible that the background oscillates close to the bounce, Fig. 3.9.

Another important influence of d is in the duration of the matter domination phase. For the branch matched with the matter domination scale, in case **B** of Fig. 3.7 its the contracting phase, Eq. (3.57) shows that, after fixing all the parameters, we have $a_\pm \propto d^{\frac{2}{3}}$. For bigger values of d, longer it will be the stiff-matter phase between the bounce and the matter domination. For a fixed value of $\mathcal{X}_\mathrm{b}$, it implies in shorter matter epochs. For the branch matched with the DE domination scale, in case B the expanding phase, Eq. (3.59) gives $a_- \propto |d|^{\frac{1}{3}}$, and again a longer

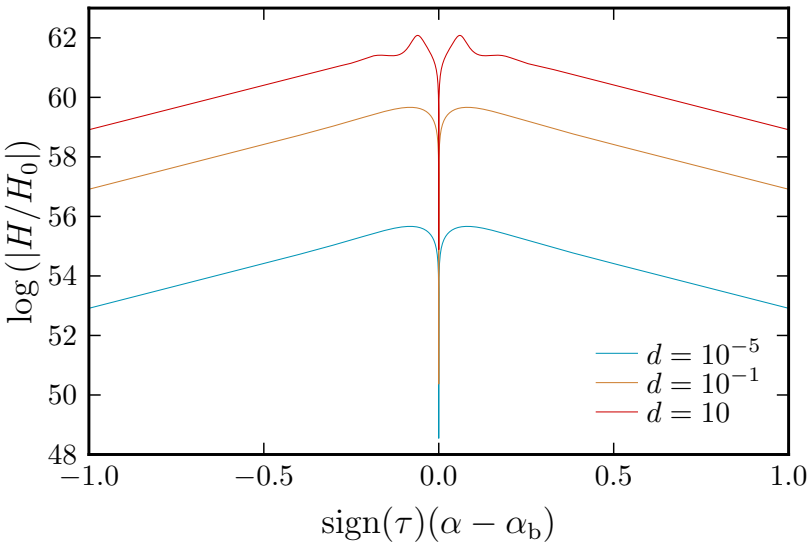

Figure 3.9.: For case B, the dependence of H_{ext} with the parameter d: faster bounces happens for bigger values of d, which leads to more energetic transitions. This behavior is also noticed in case A.

stiff-matter phase is expected when increasing d, consequently a later DE epoch and a later matter phase.

The parameter σ is relevant only in the quantum phase. Fig. 3.10 shows that bigger σ implies higher energy and in shorter time scales in the bounce. This can be easily understood looking again at Eqs. (3.38) and (3.39). The hyperbolic functions have the argument $\sigma^2\alpha\phi$, and they saturate when the argument is of the order of 11 (for instance, $\tanh(11) \approx 1 - 10^{-10}$). For this value to be achieved, a bigger σ would demand a smaller α, which means that the classical regime of the quantum solution still holds very close to the bounce. As a consequence, the Universe contracts for a longer time and a higher value of $|H_{\mathrm{ext}}|$ is reached by the system. Also, since the classical regimes happens very close to the minimum scale factor, the window for the quantum solution to drive the background to the expanding phase is very small and faster bounces are observed when σ is bigger.

A similar argument for the higher values of $|H_{\mathrm{ext}}|$ can be used when analyzing the influence of α_b, Fig. (3.11). Deeper bounces implicate a longer contraction, hence more time for $|H|$ to grow.

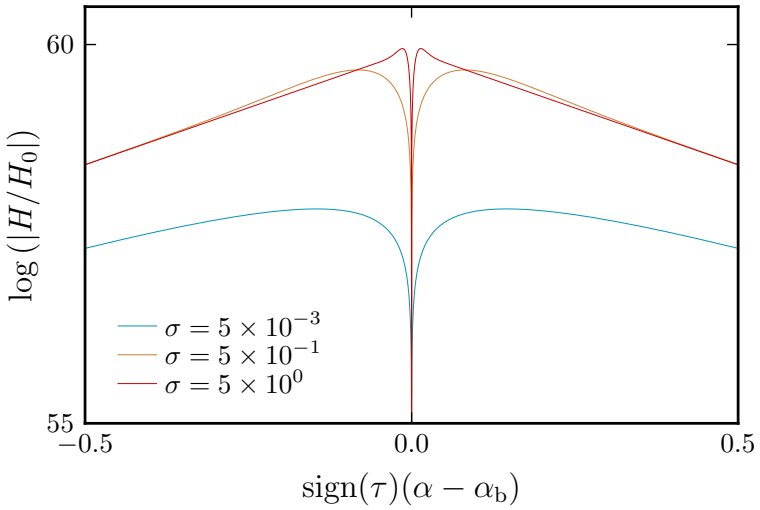

Figure 3.10.: For case B, the dependence of the H_{ext} with σ. H_{ext} is an important parameter in order to determine the validity of the canonical quantization, since we should maintain the energy scale of the bounce below Planck scale.

The parameter that influences the most the matter phase is $\mathcal{X}_\mathrm{b}$. In Fig. 3.12 we can see that longer matter epochs are attained by bigger values of $\mathcal{X}_\mathrm{b}$, which is to be expected due to the definition in Eq. (3.52). Amongst the parameters presented in this section, $\mathcal{X}_\mathrm{b}$ influences the classical background the most, and it will be a key ingredient to generate scenarios with consistent primordial power spectra.

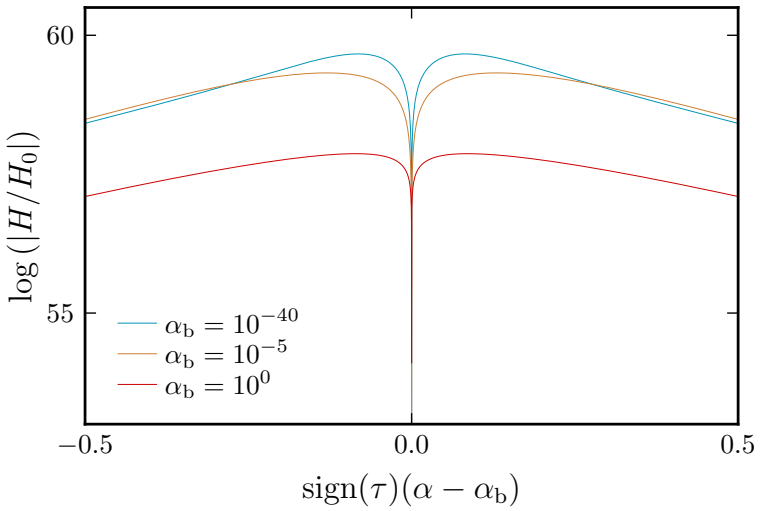

Figure 3.11.: The scale factor at the bounce, α_b, changes the maximum value of H achieved by the system. Smaller α_b, implies contractions before the bounce and, consequently, $|H|$ has more time to increase, as depicted in the plot for case **B**.

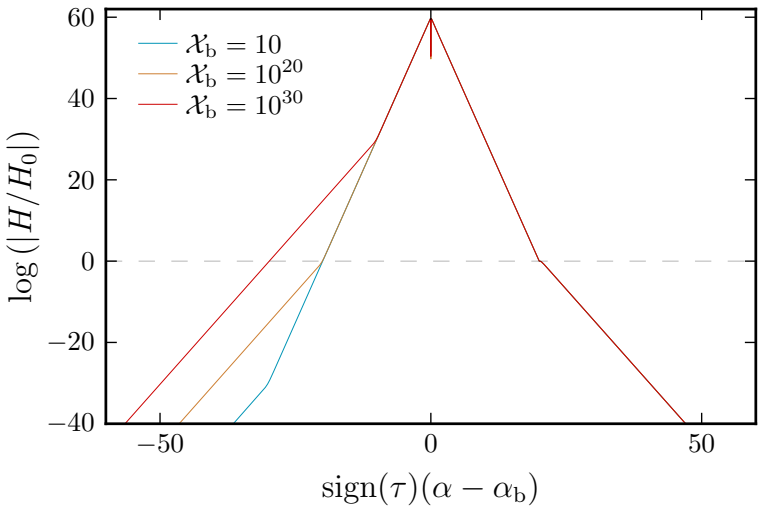

Figure 3.12.: The duration of the matter contraction is mostly sensible to the parameter $\mathcal{X}_b$. Longer matter contractions are obtained using bigger values of $\mathcal{X}_b$, as depicted in the plot for case **B**.

4 Primordial Perturbations

When the cosmological principle is invoked to assist us in the study of the background dynamics, it is not only a working hypothesis, but actually a reliable picture of the Universe for scales larger than a hundred megaparsec. In order to study the smaller scales we have to consider the deviations from homogeneity and isotropy. As we look deeper and deeper into the redshift space, those deviations becomes smaller and to study their evolution we can make use of the first order perturbed Einstein's equations.

In the standard cosmological model those deviations are seeded by the quantum fluctuations of the Minkowsky vacuum at some time very early in the beginning of inflationary phase. They evolve throughout the primordial Universe leaving a very specific fingerprint in the temperature fluctuations of the CMB.

From the temperature fluctuations of CMB, the primordial power spectra can be recovered, i.e., the distribution of amplitudes per characteristic wave-numbers of perturbations. The own nature of gravity implies the coupling between the metric and the energy-tensor fluctuations. That said, there are many ways to cast together those two components, but attention should be made to the existence of non physical modes that appear due to the gauge dependence of GR. Linear perturbation theory addresses those issues and offers a clean approach to study primordial perturbation.

In what follows we will develop the necessary tools to study the spectra that arise after the bounce. In those scenarios, the seeds of the perturbations are the quantum vacuum fluctuations in the far past history of the contracting phase.

4.1 Linear Perturbation Theory

Perturbing Einstein's equations, Eq. (2.1), and linearizing up to first order leads to the following relations:

$$\delta G^{\mu}_{\nu} = 8\pi G \delta T^{\mu}_{\nu}. \tag{4.1}$$

The Einstein tensor contains the metric and its derivatives. The flat FLRW metric expanded to linear order about the background reads

$$\begin{aligned} \mathrm{d}s^2 &= a(\eta)^2 \Big\{ -(1+\phi)\mathrm{d}\eta^2 + 2(B_{,i} + S_i)\mathrm{d}\eta \mathrm{d}x^i + \\ &\quad + \Big[(1-2\psi)\delta_{ij} + 2E_{,ij} + 2F_{(i,j)} + 2h_{ij} \Big] \mathrm{d}x^i \mathrm{d}x^j \Big\}, \end{aligned} \tag{4.2}$$

where η is the conformal time satisfying

$$\mathrm{d}\eta \equiv \frac{1}{a}\mathrm{d}t$$

and from here on $\prime \equiv \frac{\mathrm{d}}{\mathrm{d}\eta}$.

Here the decomposition theorem is invoked to write the perturbed metric into its scalar (S), vector (V) and tensor (T) components. The scalars are A, B, ψ and E; the vectors S_i and F_i, both with zero divergence; and the tensor h_{ij} satisfying

$$h^i_i = 0, \qquad h^i_{j,i} = 0. \tag{4.3}$$

The perturbation in the space-time manifold can be understood as the deviation between the physical manifold and the homogeneous one, identified by the superscript 0:

$$g_{\mu\nu} = g^0_{\mu\nu} + \delta g_{\mu\nu}. \tag{4.4}$$

To evaluate that deviation one should build an identification one-to-one between the points in the manifolds, note that such identification is arbitrary. The arbitrariness of that local correspondence introduces non physical degrees of freedom. This is known as the gauge problem: gauge transformations, i.e., the change in the

local correspondence between the manifolds, may produce non-physical (gauge) modes, disabling us from studying the physical perturbations[109, 110].

To overcome this problem, the most common approach is to express the perturbed quantities in term of gauge-invariant variables. We can deduce the gauge transformations from each of the STV components and combine them in a gauge invariant manner [111, 109, 110]:

$$\Phi \equiv \phi - \frac{1}{a}\left[a(B-E')\right]', \tag{4.5}$$

$$\Psi \equiv \psi + \mathcal{H}(B-E'), \tag{4.6}$$

$$\mathbf{V}_i \equiv S_i - F_i' \qquad \text{and} \tag{4.7}$$

$$h_{ij} = h_{ij} \tag{4.8}$$

In Eq. (4.3) we had 10 degrees of freedom, ϕ, Ψ, B, E, S_i, F_i and h_{ij}. Their gauge-invariant composition reduces the system to 6 degrees of freedom, Φ, Ψ, $\mathbf{V}_i$ and h_{ij}. By rewriting the perturbation in a gauge-invariant manner, 4 fictitious, non-physical modes were excluded.

To study the evolution of the fluctuations, the metric and its derivative have to be replaced in the gauge-invariant version of Eq. (4.1). Linearizing up to the first order, the $\binom{0}{0}$, $\binom{0}{j}$ and $\binom{i}{j}$ components give the equations for the perturbations for a given energy-momentum tensor [49, 111, 112]. The set of equations relevant for the scalar modes is:

$$\Delta\Psi - 3\mathcal{H}(\Psi' + \mathcal{H}\Phi) = 4\pi G a^2 \delta\mathbf{T}^{\mathbf{0}}_{\mathbf{0}}, \tag{4.9}$$

$$(\Psi' + \mathcal{H}\Phi)_{,i} = 4\pi G a^2 \delta\mathbf{T}^{\mathbf{0}}_{\mathbf{i}}, \tag{4.10}$$

$$\Big[\Psi'' + \mathcal{H}(2\Psi+\Phi)' + (2\mathcal{H}' + \mathcal{H}^2)\Phi + \\ + \frac{1}{2}\Delta(\Phi-\Psi)\Big]\delta_{ij} - \frac{1}{2}(\Phi-\Psi)_{,ij} = -4\pi G a^2 \delta\mathbf{T}^{\mathbf{j}}_{\mathbf{i}}, \tag{4.11}$$

where $\delta\mathbf{T}_{\mu\nu}$ is the gauge-invariant version of the energy-momentum tensor. For a perfect fluid and, analogously, for canonical scalar fields, $\delta\mathbf{T}^{\mathbf{i}}_{\mathbf{j}} = 0$ for $i \neq j$, and $\Psi = \Phi$.

For the tensor modes the equation reads

$$h''_{ij} + 2\mathcal{H}h'_{ij} - \Delta h_{ij} = 16\pi G a^2 \delta \mathbf{T}^{\mathrm{T}}_{\mathbf{ij}} \tag{4.12}$$

in which $\delta \mathbf{T}^{\mathrm{T}}_{\mathbf{ij}}$ is the component of $\delta \mathbf{T}_{\mathbf{ij}}$ with the same symmetries as h_{ij}, which means that for a matter content with no anisotropic pressure (as the perfect fluid and the scalar field)[1], $\delta \mathbf{T}^{\mathrm{T}}_{\mathbf{ij}} = 0$ [110].

The vector mode decays as $1/a^2$ and is not relevant when the Universe is isotropic.

Tensor modes

Because of the translation symmetry of the perturbations, it is useful to study their dynamics in the Fourier space. The final equation for the tensor perturbations reads

$$h''_k + 2\frac{z'_h}{z_h}h'_k - k^2 h_k = 0, \tag{4.13}$$

where h_k is the amplitude of any of the two polarization modes and, for further use, the quantity z_h is defined as

$$z_h = a.$$

Another useful way to recast the tensor perturbation is by making use of Mukhanov-Sasaki variable $\mu = ha$, which implies

$$\mu''_k + (k^2 - \frac{z''_h}{z_h})\mu_k = 0. \tag{4.14}$$

When discussing the initial conditions, this is the interesting variable to quantize the tensor perturbations in the far past.

[1] The same STV decomposition made for the metric tensor can be applied to $T_{\mu\nu}$. The tensorial components are called anisotropic pressure, $\pi_{\mu\nu}$ with $\pi^{\mu}_{\mu} = 0$ and $\pi^{\nu}_{\mu,\nu} = 0$ [110].

Scalar modes

In the following developments we will choose the longitudinal gauge,

$$E = B = 0 \tag{4.15}$$

which simply gives $\Phi = \phi$, $\Psi = \psi$ and $\delta\mathbf{T}_{\mu\nu} = \delta T_{\mu\nu}$. For the the canonical scalar field φ with a potential $V(\varphi)$, $\delta\mathbf{T}_{\mu\nu}$, the perturbed energy-momentum tensor reads:

$$\delta T_0^0 = \frac{\rho + p}{c_s^2}\left[\left(\frac{\delta\varphi}{\varphi_0'}\right)' + \mathcal{H}\frac{\delta\varphi}{\varphi_0'} - \Psi\right] - 3\mathcal{H}(\rho + p)\frac{\delta\varphi}{\varphi_0'} \tag{4.16}$$

$$\delta T_i^0 = (\rho + p)\left(\frac{\delta\varphi}{\varphi_0'}\right)_{,i}, \tag{4.17}$$

where

$$\rho = \frac{\varphi_0^2}{2} + V(\varphi_0) \tag{4.18}$$

$$p\rho = \frac{\varphi_0^2}{2} + V(\varphi_0). \tag{4.19}$$

In the above equations, the scalar metric perturbation is Ψ ($\Psi = \Phi$) and φ is the scalar field: φ_0 the its background value and $\delta\varphi$ the deviation from homogeneity.

Equations (4.9), (4.10), (4.11), (4.16) and (4.17) can be recast in a very simple and objective manner by combining the scalar perturbation Ψ and the field perturbation $\delta\phi$ by means of the Mukhanov-Sasaki variable, v [111, 112]:

$$v = a\left(\delta\varphi + \frac{\varphi_0'}{\mathcal{H}}\Psi\right). \tag{4.20}$$

The final equation of motion in terms of v in Fourier space reads

$$v_k'' + \left(c_s^2 k^2 - \frac{z''}{z}\right) v_k = 0, \tag{4.21}$$

where

$$z^2 = \frac{a^2\varphi_0^2}{\mathcal{H}^2}. \tag{4.22}$$

From the definition (3.5), z^2 can be written as

$$z^2 = \frac{3a^2x^2}{\kappa^2}. \tag{4.23}$$

Since v_k and μ_k are guided by the same wave-equation, Eqs. (4.21) and (4.14) have the same long-wave limit solution

$$v_k(\eta) \approx C_1^k z + C_2^k z \int \frac{\mathrm{d}\eta}{z^2}, \tag{4.24}$$

with the tensor modes recovered by changing $v_k \to \mu_k$ and $z \to z_h$. One should notice that the dynamics of the tensor and scalar modes will differ essentially by a factor of x due to the definitions of z and z_h.

Initial vacuum perturbations

The most natural proposal for the origin of the inhomogeneities in the current Universe is the primordial vacuum quantum fluctuations. In the inflationary scenario, the exponential growth of the scale factor is responsible for amplifying those quantum fluctuations. They become classical fluctuations [113] and after a 60 e-fold expansion they have enough amplitude to fit the CMB observations.

Bounce models assume the same mechanism for the origin of inhomogeneities, but placed in the far past of the contracting phase. Some scenarios may find difficulty in providing the Minkowsky vacuum as initial conditions. This is the case when the cosmological constant is considered [11]. In the present model, the choice of $\lambda = \sqrt{3}$ guarantees a past matter domination epoch and the standard vacuum initial conditions can be assumed.

The action that gives the dynamics for the perturbations comes from the first order perturbed Einstein-Hilbert action and reads:

$$S = \frac{1}{2}\int \left(v' + v\Delta v + \frac{z''}{v^2} \right) \mathrm{d}\eta \mathrm{d}x^3. \tag{4.25}$$

The equation of motion for v, Eq. (4.21), is obtained through the variational principle.

In the present case the scalar field behaves like a matter fluid and the usual quantization of the adiabatic vacuum fluctuations in a Minkowsky space-time coincides with the WKB solution with positive energy [111, 112]. Equation (4.21) can be written

$$v_k'' + w_k^2 v_k = 0, \tag{4.26}$$

where,

$$w_k^2(\eta, k) \equiv k^2 - \frac{z''}{z}. \tag{4.27}$$

A solution to the above equation can be expressed in terms of the WKB approximation [110], which has a certain limiting validity. Let us define,

$$Q_{\mathrm{WKB}} = \frac{3}{4}\left(\frac{w_k'}{w_k}\right)^2 - \frac{1}{2}\frac{w_k''}{w_k}. \tag{4.28}$$

In the regime for which.

$$\left| \frac{Q_{\mathrm{WKB}}}{w_k^2} \right| \ll 1, \tag{4.29}$$

the solution is

$$\tilde{v}_k^{\mathrm{WKB}}(\eta) = \frac{1}{\sqrt{2w_k}} \exp^{\pm i \int_{\eta_0}^{\eta} w_k(k,\bar{\eta}) \mathrm{d}\bar{\eta}}. \tag{4.30}$$

The matter contraction satisfies Eq. (4.29) and Eq. (4.30) not only gives the initial conditions, but also a good approximation for the solution of Eq. (4.21) while condition (4.29) is satisfied.

For $k^2 >> \frac{z''}{z}$ the initial vacuum conditions are reduced to :

$$v_{\rm ini} = \frac{1}{\sqrt{2k}} \quad \text{and} \tag{4.31}$$

$$v'_{\rm ini} = i\sqrt{2k}, \tag{4.32}$$

where the phase factor was set equal to zero.

The tensor modes h can be quantized in terms of the variable μ, which satisfies the same action (4.25), but with $z \to z_h = a$. The same treatment given to the quantization of v can be performed for μ, and the initial conditions are equivalent for the tensor modes.

In the adiabatic limit, the perturbations are in a highly oscillatory regime and the numerical calculations have a hard time pursuing the solutions. A very common approach to numerically solve the perturbations is to consider the WKB solution until $k^2 \approx \frac{z''}{z}$ and to switch to the numerical calculation just before $k^2 = \frac{z''}{z}$. However, if the calculation starts very deep in the adiabatic regime, the high oscillatory behavior will demand a long computational time and the accumulated error when condition (4.29) begins to break may spoil important estimations in the final spectra [114]. To circumvent those problems, in the the next section, the action angular variable will be used to solve numerically the perturbations.

Besides the linearity condition, i.e, small fluctuations, isotropy is another key ingredient to the validity of the perturbation theory presented here. As mentioned in the chapter 3, bouncing models suffer from a significantly growth of anisotropies during the contracting phase if the background is not Friedmann. In the case the background is homogeneous and isotropic, there is no such problem, see Ref. [115]. In what concerns the perturbations, the authors in Ref. [116] made a very rigorous calculation of the equations describing the evolution of the perturbations in a Bianchi space-time. They show that even at first order the STV modes are coupled, which means that the theory presented in this section would be no longer valid, if the background is not homogeneous and isotropic.

4.2 Numerical Results

The relevant quantities to be constrained by observations are related to the curvature scalar, defined as

$$\zeta_k = \frac{v_k}{z},$$

and the amplitude of the tensor modes, h_k. Also, to make use of the background developed in Chapter 3, the adopted time parameter to solve the perturbations will be τ. The lapse function is

$$N \equiv \frac{\tau}{H} = \frac{\mathrm{d}t}{\mathrm{d}\tau}, \tag{4.33}$$

from now on $' \to \frac{\mathrm{d}}{\mathrm{d}\tau}$, and k is measured in units of the Hubble radius, R_H.

The equations of motion for ζ_k and h_k in terms of τ can be easily deduced from Eqs. (4.21) and (4.13) and read

$$\zeta_k'' + 2\frac{z'}{z}\zeta_k' + \nu^2\zeta_k = 0, \tag{4.34}$$

$$h_k'' + 2\frac{z_h'}{z_h}h_k' + \nu^2 h_k = 0, \tag{4.35}$$

with

$$z^2 \to z^2 = \frac{3a^3x^2}{\kappa^2 N}, \tag{4.36}$$

$$z_h^2 \to z_h^2 = \frac{a^3}{4\kappa^2 N}, \tag{4.37}$$

and

$$\nu^2 = \frac{N^2k^2}{R_H^2 a^2}. \tag{4.38}$$

The initial conditions for Eqs. (4.34) and (4.35) can be obtained from Eqs. (4.31) and (4.32) with respect to τ. For the scalar mode they are

$$v_{\rm ini} = \frac{1}{\sqrt{2k}}\sqrt{\frac{aR_H}{N}}, \tag{4.39}$$

$$\left.\frac{{\rm d}v}{{\rm d}\tau}\right|_{\rm ini} = i\sqrt{2k}\sqrt{\frac{N}{aR_H}}. \tag{4.40}$$

The constrained quantities are the power spectra

$$\Delta_{\zeta_k} \equiv \frac{k^3|\zeta_k|^2}{R_H^3 2\pi^2} = \frac{\ell_{\rm Pl}^2}{R_H^2}\frac{4k^3|\tilde{\zeta}_k|^2}{3\pi}, \tag{4.41}$$

$$\Delta_{h_k} \equiv \frac{k^3|h_k|^2}{R_H^3 2\pi^2} = \frac{\ell_{\rm Pl}^2}{R_H^2}\frac{16k^3|\tilde{h}_k|^2}{\pi}, \tag{4.42}$$

the scalar and tensor spectral index, respectively

$$n_{\rm s} - 1 \equiv \left.\frac{{\rm d}\log(\Delta_{\zeta_k})}{{\rm d}\log k}\right|_{k=k_*}, \tag{4.43}$$

$$n_{\rm T} \equiv \left.\frac{{\rm d}\log(\Delta_{h_k})}{{\rm d}\log k}\right|_{k=k_*}, \tag{4.44}$$

and the tensor-to-scalar ratio,

$$r \equiv 2\left.\frac{\Delta_{h_k}}{\Delta_\zeta}\right|_{k=k_*}. \tag{4.45}$$

In the above equations the dimensionless mode functions were introduced,

$$\zeta_k \equiv \sqrt{\frac{\kappa^2 R_H}{3}}\tilde{\zeta}_k, \qquad h_k \equiv \sqrt{4\kappa^2 R_H}\tilde{h}_k, \tag{4.46}$$

and $k_* = 0.05 R_H {\rm Mpc}^{-1}$ is the pivotal scale as in [38]. The latest Planck Collaboration release, estimates for long-wave-lengths $\Delta_{\zeta_k} \approx 10^{-10}$, $n_{\rm s} \approx 0.96$ and $r < 0.1$ [38]. Those are the estimations that the present model should be confronted with.

The numerical solutions of Eqs. (4.34) and (4.35) will be calculated using the **action angle variables** (AA variables), which are a set of variables suitable to

integrate highly oscillatory systems [117, 118, 119]. In analogy with the harmonic oscillator, the new set of variables are obtained by identifying the mass term m, and the frequency ν of the system. The full development of the set of equations solved numerically can be found in Appendix B. For instance, the frequency and the mass term for the scalar modes are, respectively, Eq. (4.38) and

$$m = \frac{\kappa^2 R_H z^2}{3}.$$

The calculations were performed using the library NumCosmo [120]. The object NcHICosmoVexp solves the background described in Chapter 3 and by means of the objects NcHIPertAdiab and NcHIPertGW (scalar and tensor modes, respectively) furnishes the mass m and the frequency ν in order for the object NcmHOAA [121] to implement the AA variables and to calculate the spectra.

The focus of the present results is on case B, which is a complete background that addresses the problem of DE in bounce models by means of a single scalar field. Hence, for the numerical solutions, $\Omega_\Lambda = 1$ and $\Omega_\mathrm{d} = 1$.

The present model belongs to the category of "matter bounce models" and, as discussed in chapters 1 and 2, the current results regarding the primordial perturbations can be summarized as follows: the power spectrum is scale invariant; the tensor-to-scalar ratio is larger than measured in CMB if the scalar field is canonical and the bounce is symmetric; attempts to solve this problem, assuming the validity of GR all along, result in the increase of non-Gaussianities, which seems to suggest a no-go theorem for bounce cosmologies [25, 122, 26, 23, 123, 61, 3, 19, 124, 125, 20]. In previous works the bounce phase was obtained by means of a second scalar field with a ghost-type Lagrangian. Choosing wisely the parameters of the ghost scalar field, it takes place only very close to the singularity and the perturbations are studied without taking it into account.

In the model presented in this work, the matter contraction is followed by a quantum bounce and the numerical calculations take into account all the background

without any simplification until the expanding phase. Four sets of parameters listed in Table 4.1 are used to discuss the main features of the perturbations. As mentioned before, the parameter choices are implicit determinations of the background model initial conditions (including the wave function parameters).

	d	σ	$\alpha_{\rm b}$	$\mathcal{X}_{\rm b}$
set1	-9×10^{-4}	9	8.3163×10^{-2}	2×10^{36}
set2	-9×10^{-4}	100	7.4847×10^{-3}	4×10^{36}
set3	-0.1	4	10^{-5}	6×10^{37}
set4	-0.1	4	10^{-7}	6×10^{37}

Table 4.1.: Model parameters for four different cases in which the present model produces Δ_ζ close to 10^{-10}, and scale invariant spectra. The relevant background quantities are presented in Fig. (4.2) through (4.5), while the modes evolution can be seen in Fig. (4.1). The DE scale is fixed at $\Omega_\Lambda = 1$.

The numerical results for the power spectra at the pivotal mode k_* are:

$$\begin{aligned}
&\text{set1}: && \Delta_{\zeta_k}|_{k=k_*} = 1.4\times10^{-10},\ r = 1.9\times10^{-7},\\
&\text{set2}: && \Delta_{\zeta_k}|_{k=k_*} = 4.6\times10^{-11},\ r = 1.3\times10^{-5},\\
&\text{set3}: && \Delta_{\zeta_k}|_{k=k_*} = 1.2\times10^{-14},\ r = 56,\\
&\text{set4}: && \Delta_{\zeta_k}|_{k=k_*} = 1.7\times10^{-14},\ r = 59,
\end{aligned}$$

and the time evolution is plotted in Fig. 4.1, where the superscripts a and b holds for the real and the imaginary part of ζ_k and h_k.

The scalar spectral index is close to scale invariant in the fours sets, hence the main differences between them, as showed in the previous estimations, are the amplitude and the tensor-to scalar ratio.

To understand the influence of the model parameters in the spectra, the long wave-length solution, Eq. (4.24), can be rewritten for ζ_k and h_k. Using τ as the time parameter and the definitions of ζ_k and h_k one can easily obtain:

$$\zeta_k \approx A_1^k + A_2^k \frac{1}{R_H} \int \frac{N}{x^2 a^3} \mathrm{d}\tau \tag{4.47}$$

$$h_k \approx B_1^k + B_2^k \frac{1}{R_H} \int \frac{N}{a^3} \mathrm{d}\tau. \tag{4.48}$$

The integrands of the above equations are plotted in Figs. 4.2 and Figs. 4.3.

Tensor-to-scalar ratio

In the studied sets of parameters, set1 and set2 are the closest to the observational constraints. In particular, they are examples of matter bounces in which the tensor-to-scalar ratio is smaller than 0.1. That estimation had not yet been obtained by single field matter bounces in the literature and the known multiple field models that produce such result do not consider the influence of the bounce phase in the final spectra. This original result is only possible because we are in the domain of quantum cosmology.

During the classical contraction, the long wave-length solution of ζ_k, Eq. (4.47), is essentially dominated by the scale factor contraction, since $x \in (\frac{\sqrt{2}}{2}, 1)$. However, when the quantum potential starts to act, x is no longer restricted to those values and it can contribute significantly to the growth of the scalar mode amplitude.

Indeed, that phenomenon can be observed by comparing Figs. 4.3 and 4.2. For the scalar mode, both set1 and set2 present two peaks around the bounce (Fig. 4.3), which are responsible for the "boost" in the amplitude during the quantum phase. Those peaks are not present for the tensor mode, Fig. 4.2. Actually, for set1 and set2, the integrands for the tensor modes are even "frozen" during the bounce.

It is precisely the peaks generated by the quantum bounce dynamics that boosts the scalar modes and produce a scalar-to-tensor ratio smaller than unit. For set3

and set4 the scalar modes have no significant contribution around the bounce, Fig. 4.3, and r assumes values completely out of the accepted range.

To understand how the model parameters influence r, one has to understand how the quantum phase changes the value of x. From the equations developed in Chapter 3, we obtain the following relation

$$\frac{1}{x} = \frac{\dot{\alpha}}{\dot{\phi}} = \frac{\mathrm{d}\alpha}{\mathrm{d}\phi}.$$

Whenever, $\dot{\phi} \approx 0$, $1/x$ will significantly contribute to the integral in Eq. (4.47). Those are precisely the center solutions for the phase space for the Bohmian trajectories, Fig. 3.5, which happens when

$$\frac{\sigma^2 \alpha}{2d} = \cot d\alpha.$$

For the choices of the parameters d and σ in Tab. 4.1, rough estimates for the α_{center} that satisfies the previous condition are

$$\begin{aligned}
\mathrm{set1}: &\quad \alpha_{\mathrm{center}} \approx 16 \times 10^{-2}, \\
\mathrm{set2}: &\quad \alpha_{\mathrm{center}} \approx 14 \times 10^{-3}, \\
\mathrm{set3}: &\quad \alpha_{\mathrm{center}} \approx 35, \\
\mathrm{set4}: &\quad \alpha_{\mathrm{center}} \approx 35.
\end{aligned}$$

One can notice that the chosen α_{b} for set1 and set2, Tab. 4.1, are very close to the α_{center} for the fixed d and σ, while the chosen values for set3 and set4 are orders of magnitude further. Hence, the Bohmian trajectories that allow smaller values of r are those close to the centers solutions, Fig. 4.4.

Amplitudes

The main contribution to the amplitudes comes from the classical contraction. Since x has the order of unit, the scalar and tensor modes have a similar evolution. During the matter domination, $N/a^3 \approx \tau/a^{3/2}$, while for stiff matter $N/a^3 \approx \tau$, where we are using the definition of N and that $H \propto a^{-3/2}$ in the matter phase and $H \propto a^{-3}$ in the stiff matter phase. Hence, the main contribution to the amplitude growth comes from the matter epoch, whose duration is closely connected with the parameters d and $\mathcal{X}_{\rm b}$, both also controlling the bounce depth[2].

As discussed in Sec. 3.4, bigger values of $\mathcal{X}_{\rm b}$ gives longer matter contractions. However, even though $\mathcal{X}_{\rm b}$ is bigger in set3 and set4 then in set1 and set2, this is not the cause of the difference between the amplitudes. Actually, in those cases, the parameter d was more relevant, since it varied about 3 orders of magnitude, Tab. 4.1. Smaller values of d allows longer matter contractions, and for that reason, the amplitudes of sets 1 and 2 are larger.

In principle, one could choose the parameters in order to make the bounce deeper, hoping to get the right amplitude. Nevertheless, we must take care to not go beyond the scale of validity of these models. One should verify whether the energy scale of the bounce is not dangerously close to the Planck energy scale, where our simple approach would not be appropriate. The curvature scale at the bounce is given by the Ricci scalar,

$$R = 12H^2 + 6\dot{H}, \quad L_R = 1/\sqrt{R}, \tag{4.49}$$

and the Ricci scale L_R should not be smaller than the Planck length in order for the quantum canonical quantization of gravity to be a valid effective description. Figure 4.5 displays the Ricci scale evolution for all parameter sets. This figure shows that the absolute value of d controls the minimum scale L_R attained around

[2]The bounce depth is connected to the energy scale of the bounce, Eq. (4.49).

the bounce. This means that it's not possible to increase the amplitudes of set3 and set4 by increasing $|d|$ without violating the validity of our approach.

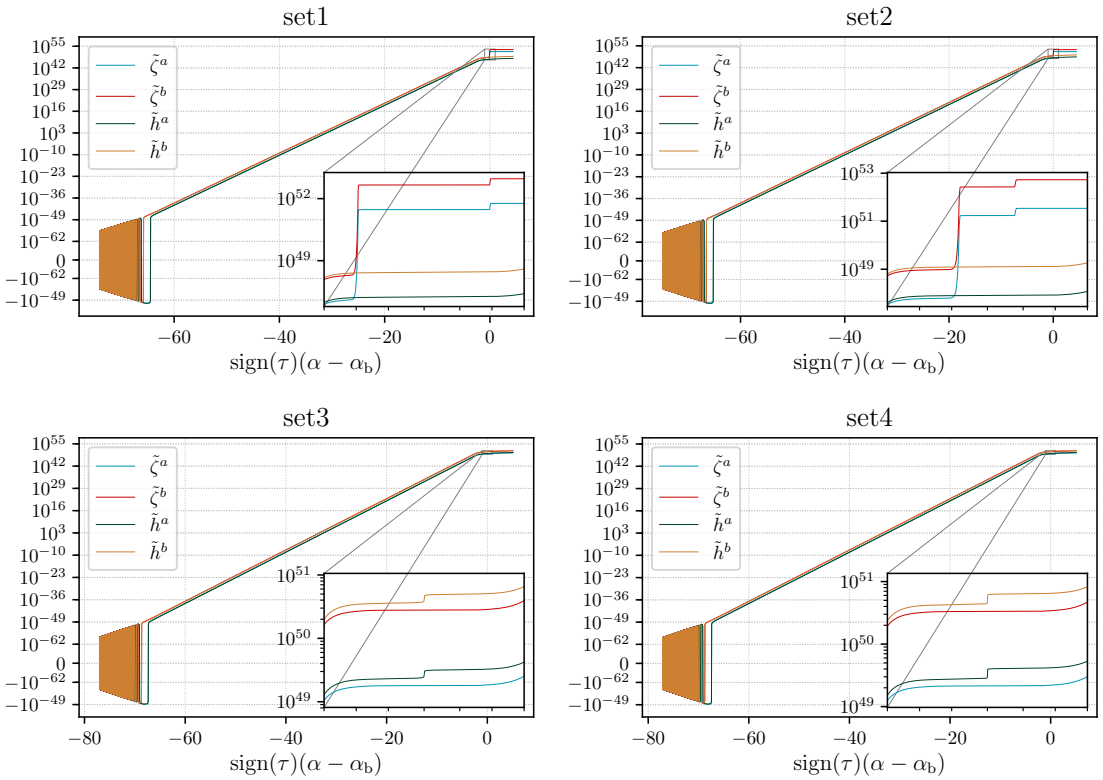

Figure 4.1.: Evolution of the mode functions $\tilde{\zeta}_k$ and $\tilde{h}_k$ for set1, set2, set3 and set4. In the detail, we can see the result of the integration of the two peaks in Fig. 4.3 for the scalar mode in the upper panels and the single peak of Fig. 4.2 integration for the tensor mode. For example, in the upper left figure, the first peak around -0.1 increases the amplitude of $\tilde{\zeta}^a$ and the second peak at $+0.1$ double this value. In contrast, since the tensor perturbations amplitude does not depend directly on the evolution of x, they are not modified by these peaks. Nonetheless, the tensor amplitude is sensible to peaks in the lapse function N. Hence, for set3 and set4 where these peaks are pronounced, we have an increase in the amplitude of tensor perturbations at the bounce, which is otherwise overcome by scalar perturbations in the cases where the $\frac{1}{x^2}$ term become relevant.

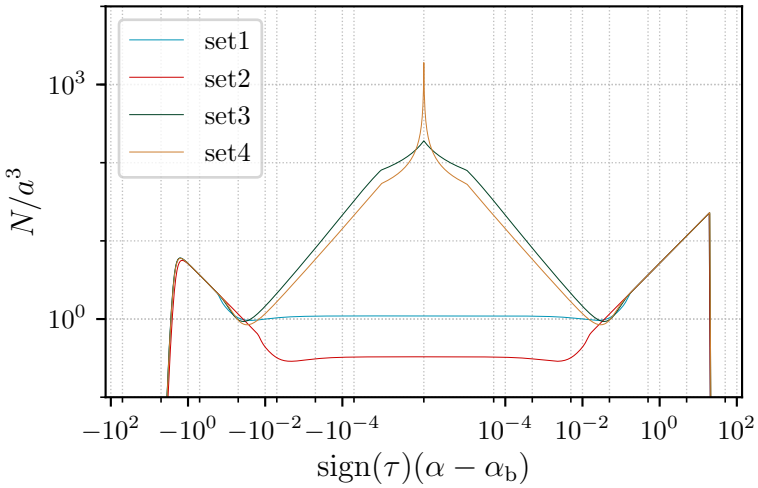

Figure 4.2.: Integrand of the super Hubble approximation for the tensor modes, which are sensitive to the peaks in N.

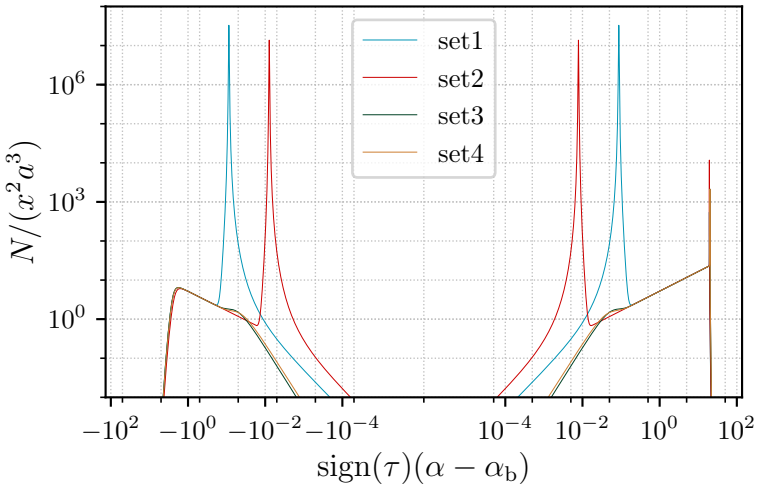

Figure 4.3.: Integrand of the super Hubble approximation for the scalar modes . It is worth noting the presence of the $1/x^2$ term in the scalar mode integrals, which goes through zero during the bounce phase, overcoming any possible additional contribution to the amplitude from the peak in the lapse function $N = \tau/H$.

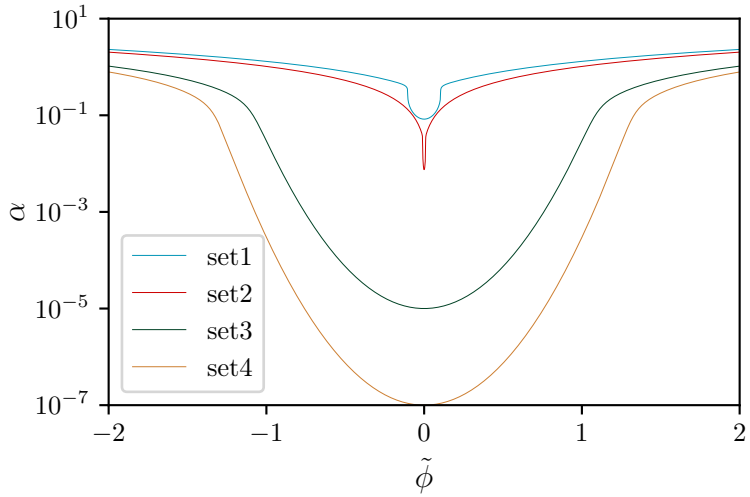

Figure 4.4.: Phase space evolution for the four sets of parameters appearing in Tab. 4.1. Note that the set1 and set2 curves are almost vertical near the bounce. This happens because they pass close to the periodic trajectories (see Fig. 3.5 for a full picture of the phase space trajectories). At these points, $x \propto \mathrm{d}\phi/\mathrm{d}\alpha \approx 0$, which results in the peaks seen in Fig. 4.3. Contrastingly, the set3 and set4 curves pass far from the center points of Fig. 3.5, resulting in a smoother transition through the bounce phase. With all parameters fixed, we can control how close one gets to the cyclic solutions by increasing the value of α_{b}. One can also see in the figure, by comparing set1 with set2, that a larger σ induces a faster bounce.

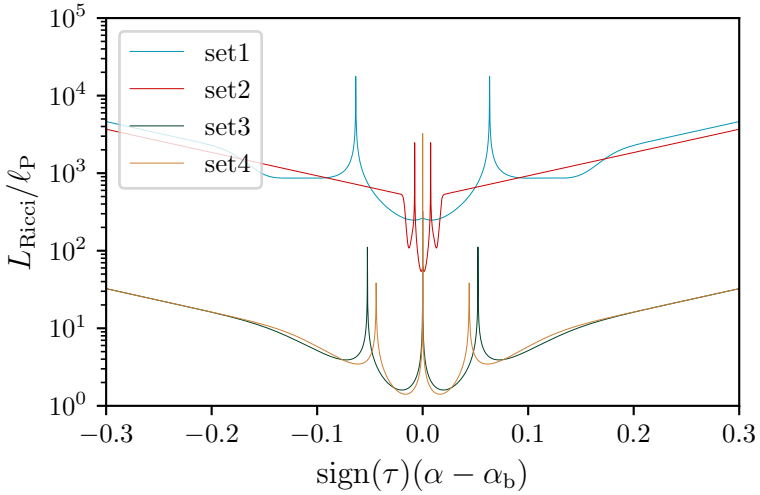

Figure 4.5.: Time evolution of the Ricci scale for all sets appearing in Tab. 4.1. The parameter d controls how close the scale gets to the Planck length, and set3 and set4 are in the limit of validity of the present model. Thus, a large value of $|d|$ would violate this constraint. Note also that faster bounces (for instance, set2) result in stronger oscillations of L_R near the bounce. This means that faster bounces must take place at even higher scales in order to avoid a violation of $L_R/\ell_{\mathrm{Pl}} > 1$ during the oscillations.

5 The anisotropy problem and multiple bounce models

The present chapter is dedicated to the work developed in Ref. [6] in which the anisotropy problem is explored in the context of the so-called "New Ekpyrotic" models, i.e., matter bounce models with an ekpyrotic phase during contraction and a ghost condensate performing the non-singular classical bounce [66, 3, 70, 33].

As showed in Chapter 2, bouncing models may suffer from the BKL instability when approaching the end of the contraction phase. The reason for the "anisotropy problem" that causes the instability is the growth of the initial shear with a^{-6}, implying an effective EoS $w = 1$ that eventually overcomes all the regular matter components, as dust ($w = 0$) and radiation ($w = 1/3$), when the Universe approaches the singularity [3, 33, 6].

In this current version of the new ekpyrotic model, the ghost condensate is obtained via a Galileon term that couples the scalar field with the metric [70]. By means of two different functions of the scalar field, namely a negative potential $V(\phi)$ controlling the ekpyrotic phase, and a non-standard kinetic coupling $g(\phi)$ controlling the ghost condensate, it was then argued that the anisotropy growth is suppressed and the non-singular bounce is achieved even in the presence of small anisotropic deviation [3, 33], since in the ekpyrotic phase the effective EoS of the scalar field is $w > 1$. In such models a curvaton mechanism [126, 127] is then invoked to finally produce scale invariant perturbations in the expansion phase.

Present calculations of the perturbations in anisotropic bounce models have been done assuming an FLRW perturbed metric, under the assumption that the anisotropic stress can be made negligible at the relevant scales. On the other hand, if this assumption is not strictly valid and the background space-time is in fact

Bianchi I, at least in some range of times, then it was shown [116] that the scalar, vector and tensor modes evolve in a coupled way already at first order. Even for an inflationary phase, this is known to yield possible effects in the resulting spectrum [128], and one may expect a similar conclusion to hold in a contracting Universe model. This could drastically modify any prediction for the final perturbation spectrum produced in such a model.

However, due to the high non-linear dynamics presented by the existence of the ekpyrotic and the ghost condensate phases, the cosmological scenario may not reduce to the case previously discussed in the literature [3, 33], and before properly addressing perturbation in those models, the phase space should be well understood. These are the motivations for Ref. [6], which is discussed in this chapter.

The present work aims at exploring the evolution stemming from the theory proposed in [33]; as it happens, it is much richer than previously anticipated preseting scenarios with one, two or even three bounces, which would significantly change the predicted spectra.

In the next section the basic equations of the model described in [33] are reviewed. Section 5.2 is dedicated to the numerical solution for the equations developed in Sec. 5.1 and the main phenomenology behind the different scenarios will be discussed. Section 5.3 contains the numerical solutions of Sec. 5.2, with the analytical discussion of the dynamical equations of Sec. 5.1 and the role of the anisotropy in the multiple bounce scenario is clarified.

To be coherent with Ref. [6], the reduced Planck mass $M_{\rm Pl} = 1/\sqrt{8\pi G}$ may be occasionally invoked. The metric signature is still the same as in the previous model $(+,-,-,-)$ and from here on the scale factor will be normalized by the scale factor in the bounce or in the first bounce for the cases in which there are more then one. Through out this chapter all quantities should be considered only in the context of the present "New Ekpyrotic" scenario. It is worth emphasizing that the findings presented in this chapter enlighten interesting topics concerning

how the current literature on matter bounce is treating the anisotropy problem and bears no resemblance with the latter quantum bounce model, except for an initially contracting matter epoch.

5.1 General equations

The ghost condensate, responsible for performing the bounce, is obtained via a Galileon scalar field ϕ minimally coupled to gravity, i.e.

$$\mathcal{S} = \int \mathrm{d}^4x\sqrt{-g}\left(\frac{1}{2}M_{\rm Pl}^2 R + \mathcal{L}\right), \tag{5.1}$$

where the scalar field Lagrangian is taken to be

$$\mathcal{L}\left[\phi\left(x\right)\right] = K(\phi, X) + G(\phi, X)\Box\phi, \tag{5.2}$$

K and G are functions of the scalar field and its canonical kinetic term

$$X \equiv \frac{1}{2}\partial_\mu\phi\partial^\mu\phi, \tag{5.3}$$

with $\Box\phi \equiv g^{\mu\nu}\nabla_\mu\nabla_\nu\phi$.

The energy momentum tensor is obtained from the variation of the Lagrangian and reads

$$\begin{aligned} T^\phi_{\mu\nu} &= (-K + 2XG_{,\phi} + G_{,X}\nabla_\sigma X\nabla^\sigma\phi)g_{\mu\nu} \\ &\quad +(K_{,X} + G_{,X}\Box\phi - 2G_{,\phi})\nabla_\mu\phi\nabla_\nu\phi \\ &\quad -G_{,X}(\nabla_\mu X\nabla_\nu\phi + \nabla_\nu X\nabla_\mu\phi), \end{aligned} \tag{5.4}$$

where the notations $F_{,\phi}$ and $F_{,X}$ stand for derivatives of with respect to ϕ and X, respectively.

Following Ref. [33], function K is chosen to be

$$K(\phi, X) = M_{\rm Pl}^2 \left[1 - g(\phi)\right] X + \beta X^2 - V(\phi), \tag{5.5}$$

with the positive-definite parameter β ensuring the kinetic term to be bounded from below at high energy scales and the scalar field ϕ dimensionless, hence the Planck mass coefficient on the first term. The arbitrary functions in (5.5) must be such as to render an ekpyrotic contraction phase together with a non singular ghost condensate dominated bounce. As explained in [33], an acceptable choice is provided by

$$g(\phi) = \frac{2g_0}{\mathrm{e}^{-\sqrt{\frac{2}{p}}\phi} + \mathrm{e}^{b_g\sqrt{\frac{2}{p}}\phi}}, \tag{5.6}$$

with $g_0 > 1$, $p > 0$ and b_g dimensionless constants, while the potential can be taken as

$$V(\phi) = -\frac{2V_0}{\mathrm{e}^{-\sqrt{\frac{2}{q}}\phi} + \mathrm{e}^{b_{\rm v}\sqrt{\frac{2}{q}}\phi}}, \tag{5.7}$$

where $V_0 > 0$ is a constant with dimension of $(\mathrm{mass})^4$ and there are two other dimensionless constants q and $b_{\rm v}$. This negative-definite potential reduces to the exponential form of the ekpyrotic scenario [20] for large values of ϕ. Finally, the function $G(\phi, X)$ is of the Galileon type [129], again chosen in agreement with [33] as $G(X) = \gamma X$, where γ is a positive dimensionless constant.

The above described scalar field will evolve in a flat, homogeneous and anisotropic Universe, whose metric is chosen to be Bianchi I, Eq. (2.25), and relations (2.26) to (2.30) hold.

The equation of motion of the scalar field ϕ is derived from the Lagrangian (5.2) and can be cast in the form of a modified Klein-Gordon equation

$$\mathcal{P}\ddot{\phi} + \mathcal{D}\dot{\phi} + V_{,\phi} = 0, \tag{5.8}$$

where the functions $\mathcal{P}$ and $\mathcal{D}$ are, respectively,

$$\mathcal{P} = (1-g)M_{\rm Pl}^2 + 6\gamma H\dot{\phi} + 3\beta\dot{\phi}^2 + \frac{3\gamma^2}{2M_{\rm Pl}^2}\dot{\phi}^4, \tag{5.9}$$

and

$$\begin{aligned}\mathcal{D} =& 3(1-g)M_{\rm Pl}^2 H + \left(9\gamma H^2 - \frac{1}{2}M_{\rm Pl}^2 g_{,\phi}\right)\dot{\phi} + 3\beta H\dot{\phi}^2 \\ &- \frac{3}{2}(1-g)\gamma\dot{\phi}^3 - \frac{9\gamma^2 H\dot{\phi}^4}{2M_{\rm Pl}^2} - \frac{3\beta\gamma\dot{\phi}^5}{2M_{\rm Pl}^2} - \frac{3}{2}\gamma\sum_i \dot{\theta}_i^2\dot{\phi}.\end{aligned} \tag{5.10}$$

The parameters of the model are g_0, V_0, b_g, $b_{\rm v}$, p, q, β, γ, all real, positive and assumed to be non vanishing. Without lack of generality, $M_{\rm Pl} \to 1$ for the rest of this chapter.

In (2.27) and (2.28) the total energy density and pressure are the ones of the scalar field, p_ϕ and ρ_ϕ, respectively, and in the present case they read

$$\rho_\phi = \frac{1}{2}(1-g)\dot{\phi}^2 + \frac{3}{4}\beta\dot{\phi}^4 + 3\gamma H\dot{\phi}^3 + V(\phi), \tag{5.11}$$

$$p_\phi = \frac{1}{2}(1-g)\dot{\phi}^2 + \frac{1}{4}\beta\dot{\phi}^4 - \gamma\dot{\phi}^2\ddot{\phi} - V(\phi). \tag{5.12}$$

Finally, as discussed in Chapter 2, the shear evolves as

$$\sigma^2 = \sigma_{\rm ini}^2\left(\frac{a_{\rm ini}}{a}\right)^6, \tag{5.13}$$

i.e., as a stiff-matter fluid, where the subscript "ini" denotes an arbitrary initial time. For future convenience, the effective pressure and energy density of the shear are

$$\rho_\sigma \equiv \frac{\sigma^2}{2} = p_\sigma. \tag{5.14}$$

5.2 Numerical solutions

The system of first order differential equations to be solved numerically is

$$\dot{\phi} = \varphi, \tag{5.15}$$

$$\dot{\varphi} = -\frac{\mathcal{D}\varphi}{\mathcal{P}} - \frac{V_{,\phi}}{\mathcal{P}}, \tag{5.16}$$

$$\dot{H} = -\frac{\rho_\phi + p_\phi}{2} - \frac{\sigma_{\rm ini}^2}{2}\left(\frac{a_{\rm ini}}{a}\right)^6, \tag{5.17}$$

$$\dot{a} = aH, \tag{5.18}$$

where a new variable φ was introduced to reduce the system order of Eqs. (5.8), (2.28), (5.13), and the definition of the mean Hubble rate H was used. The model parameters are chosen as in ref. [33], in which a single bounce model with a small initial anisotropy has an isotropic expansion. Maintaining the model parameters and changing the initial conditions reveal the rich dynamics of the models and many interesting scenarios. The adopted parameters are

$$V_0 = 10^{-7}M_{\rm Pl}^4, \qquad g_0 = 1.1,$$
$$b_{\rm v} = 5, \qquad b_g = 0.5,$$
$$p = 0.01, \qquad q = 0.1,$$
$$\beta = 5, \qquad \gamma = 10^{-3}.$$

The initial conditions are chosen by the set

$$\theta = (\phi_{\rm ini},\ \varphi_{\rm ini}) \quad \text{and} \quad \sigma_{\rm ini}^2 = 5\times 10^{-12}, \tag{5.19}$$

with $\varphi_{\rm ini}$ chosen in such a way that the kinetic contribution $\propto \varphi_{\rm ini}^2$ be comparable to the shear contribution at the initial time ($a_{\rm ini}$ is fixed, $= 1$), while H is given by the constraint (2.27), namely

$$H_{\rm ini} = -\sqrt{\frac{\rho_{\phi_{\rm ini}}}{3} + \frac{1}{6}\sigma_{\rm ini}^2}, \tag{5.20}$$

where $\rho_{\phi_{\rm ini}}$ is obtained with Eq. (5.11) evaluated at $\phi_{\rm ini}$ and $\varphi_{\rm ini}$. The scale factor was omitted since it enters explicitly only in the expression for the shear in Eq. (5.13) through the combination $\sigma_{\rm ini}a_{\rm ini}^3$: without loss of generality, one can renormalize the initial shear to account for the initial value of the scale factor, which can thus be chosen as $a_{\rm ini} = 1$ for simplicity.

Reference [33] considers the presence of a matter component, $p \ll \rho$, assumed to produce the initial scale-invariant spectrum. Here, the focus is on the bounce itself, or the behavior of the scale factor in general when the Universe is dominated by the scalar field. This means that the analysis begins at a time for which it is assumed that the dust fluid contribution has already turned negligible, having been overcome by the other components when the initial conditions are settled. In other words, for $a < a_{\rm ini}$ (in the contraction and expansion phases), the matter fluid is negligible and will be ignored in the calculations.

In the numerical solutions presented below in Figs. 5.1 through 5.9, the cosmic time t is expressed in units of $10^4 M_{\rm Pl}^{-1}$ and the Hubble rate H in units of $10^{-4}M_{\rm Pl}$. In order to compare the solutions with the same reference point, the initial time is $t_{\rm ini} = 0$ for all scenarios. The estimated absolute error in the calculations shown are of order $\mathcal{O}(10^{-10})$ during the contraction and expansion epochs, and $\mathcal{O}(10^{-7})$ during the bounce phase.

5.2.1 One bounce scenario

The single bounce scenario is the most widely discussed background evolution for bouncing cosmologies. The background evolves dominated by the scalar field during contraction, passes through the ghost condensate phase, makes a single non singular bounce and enters an ever lasting expansion phase afterwards, as exemplified in Fig. 5.1. These numerical solutions were obtained for $\phi_{\rm ini,1} = -2.5$ and $\phi_{\rm ini,2} = -3.0$, with $\varphi_{\rm ini} = 8 \times 10^{-6}$ in both cases. As noted earlier, the initial shear value is close to the kinetic term $\varphi^2 \sim \times 10^{-11}$, and is subsequently diminished (in comparison to ρ) during the ekpyrotic phase, Fig. 5.3.

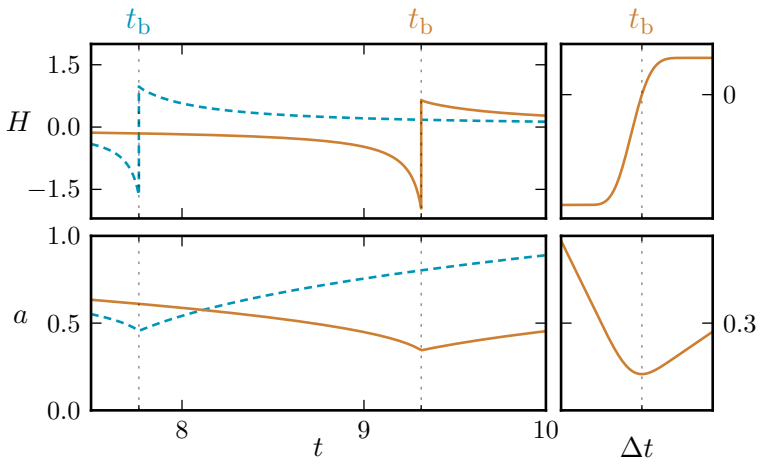

Figure 5.1.: Time evolution of the Hubble constant H (top left) and scale factor a (bottom left) for $\varphi_{\rm ini} = 8 \times 10^{-6}$ and two different values of $\phi_{\rm ini}$: $\phi_{\rm ini} = -3$ (full brown) and $\phi_{\rm ini} = -2.5$ (dashed blue). The bounce times are marked as $t_{\rm b}$. The discontinuity is only apparent and a mere consequence of the fact that the relevant time scale is extremely short for the fast bounce that takes place in this theory: the right panels show the details of this actually smooth transition (shown only for $\phi_{\rm ini} = -3.5$) over the much smaller time interval of $\Delta t = 10^{-4}$ around the bounce time $t_{\rm b}$.

The ghost condensate and ekpyrotic phases are presented in Fig. 5.2 where the time evolution of the kinetic term coefficient g and the potential V are presented. Before the bounce takes place, the scalar field is driven by the potential which becomes very negative throughout the ekpyrotic phase, until g takes over, at which point the bounce occurs. Figure 5.3 shows, for this case and the following (with more than one bounce taking place), the time evolution of the energy contained in the scalar field and in the shear. The top panel is for the case at hand: the difference between ρ_ϕ and ρ_σ is entirely due to $V(\phi)$ in this case, and as expected, the shear contribution decreases with respect to that of the field.

As previously exposed, the ekpyrotic phase is present in order to reduce the shear. Indeed, with the potential (5.7), there exists an attractor solution with EoS for the scalar field w_ϕ

$$w_\phi \approx -2 + \frac{2}{3q}, \tag{5.21}$$

while on the other hand, Eq. (5.13) implies that the EoS of the shear is $w_\sigma = 1$. For small values of q, as the one chosen for the numerical calculations, the shear

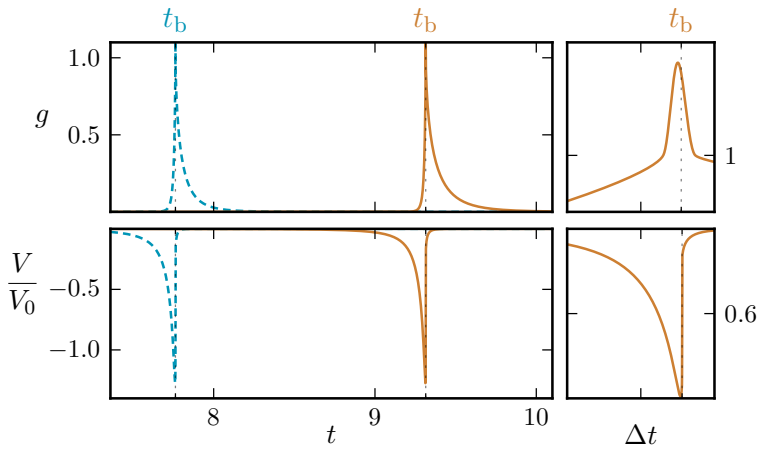

Figure 5.2.: Time development of the kinetic function $g[\phi(t)]$ (top left) and potential $V[\phi(t)]/V_0$ (bottom left), with the same convention as Fig. 5.1. The ghost condensate phase begins as soon as $g(\phi) \geq 1$. The right panel shows how smooth the transition goes when looked at on shorter timescales.

can never dominate during contraction. The more negative ϕ_{ini}, the longer the contraction phase, because the scalar field begins farther away from the ghost condensate state that allows the bounce. There is a degeneracy in the initial condition space, since one could achieve a similar behavior by changing φ_{ini}, an initially small velocity for the field leading to a longer contraction phase as it takes more time to reach the ghost condensate phase.

At first sight, one is tempted to conclude from the previous discussion that ϕ_{ini} or φ_{ini} could be chosen as small as one wishes in order to yield a longer contraction phase and varying the bounce characteristic features. However, this is not the case at all: changing the initial conditions produces drastically different solutions involving more than one bounce.

5.2.2 Two bounce case

The figure 5.4 illustrates what happens if one keeps decreasing ϕ_{ini}, trying to trigger a longer contraction phase: one reaches a region in parameter space in which the Universe instead experiences two bounces. The Universe contracts, bounces, expands again, passes through a maximum, starts contracting again and

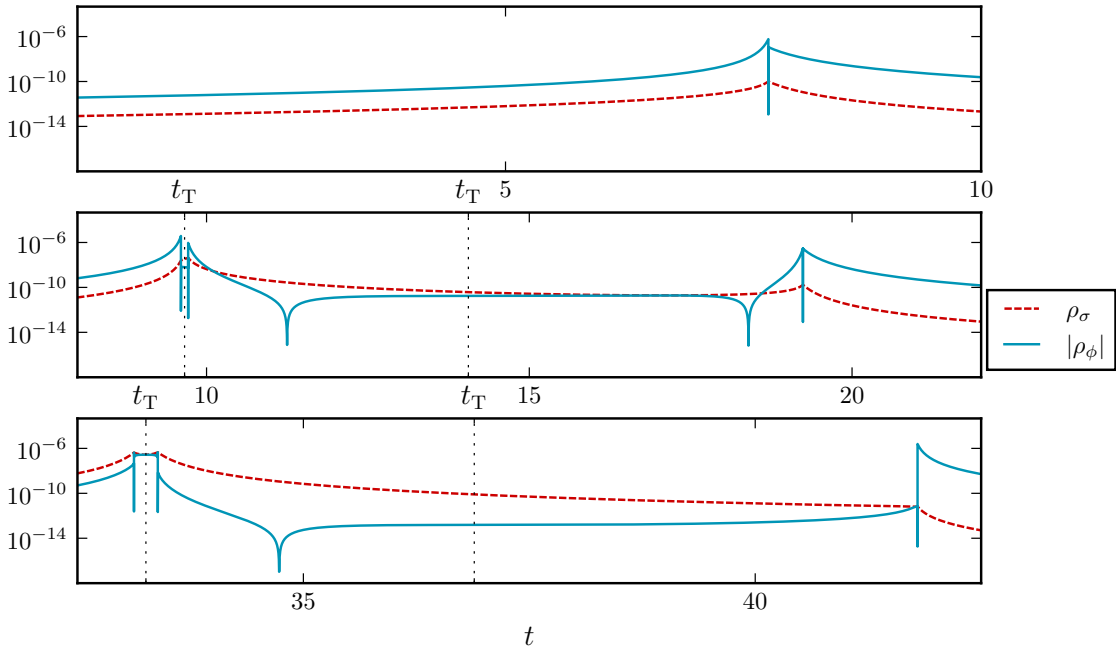

Figure 5.3.: Comparative evolution of the energy densities for the anisotropy, ρ_σ (red dashed) and the scalar field, ρ_ϕ (blue full) for the initial conditions $\{\phi_{\text{ini}} = -2.5,\ \varphi_{\text{ini}} = 8 \times 10^{-6}\}$ (top, single bounce), $\{\phi_{\text{ini}} = -3.5,\ \varphi_{\text{ini}} = 8 \times 10^{-6}\}$ (middle, two bounces) and $\{\phi_{\text{ini}} = 1.9,\ \varphi_{\text{ini}} = -10^{-6}\}$ (bottom, three bounces). The initial anisotropic stress for all the plots is $\sigma^2_{\text{ini}} = 5 \times 10^{-12}$. The indicated t_T are the turning points at which the scalar field goes through the maximum of $g(\phi)$.

moves towards a second bounce, from which it finally expands forever. For that to happen, the scalar field must go twice through the ghost condensate phase, a possibility which was always assumed hard to achieve, whereas in fact, the system goes through this phase three times (Fig. 5.5) even though only two bounces took place.

This evolution is exemplified by $\varphi_{\text{ini}} = 8 \times 10^{-6}$ and the two initial field conditions $\phi_{\text{ini},1} = -3.49$ and $\phi_{\text{ini},2} = -3.50$, whose subsequent time evolution is shown in Figs. 5.4 and 5.5.

The behavior found here is due to the existence of a turning point for ϕ, marked as t_T in Fig. 5.3. At this point, the scalar field passes through the first ghost condensate phase while still contracting. It eventually returns and goes back to pass through the top of the potential $g(\phi)$ again. Then, the Universe bounces.

]

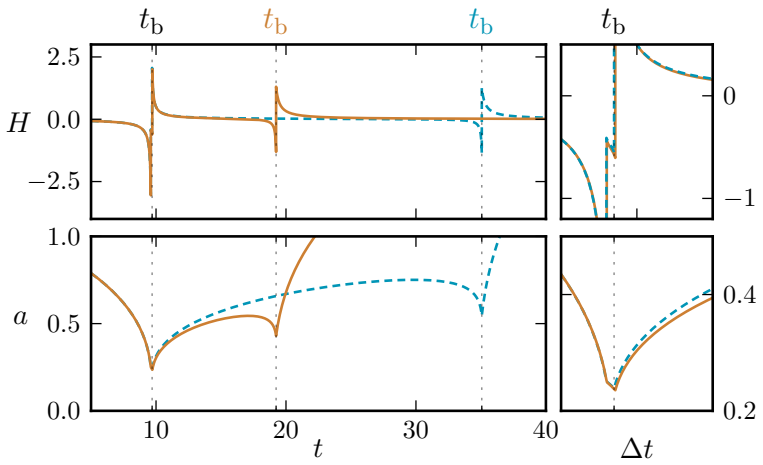

Figure 5.4.: Evolution of the Hubble parameter H (top left) and the scale factor a (bottom left) for the two different initial conditions: $\phi_{\text{ini}} = -3.5$ (full yellow) and $\phi_{\text{ini}} = -3.49$ (blue dashed). The bounces are marked as t_b. The first bounce of the two solutions are indistinguishable on the figure (numerically extremely close), but the solutions then drift away and bifurcate, yielding a second bounce at very different times, first for $\phi_{\text{ini}} = -3.5$, then for $\phi_{\text{ini}} = -3.49$. This indicates an extreme sensibility in the initial conditions that has never been discussed in such a context. The plots on the right detail what happens during the first time the system goes through the ghost condensate phase, with time scales of the plot taken as $\Delta t \approx 3$ around t_b.

In Fig. 5.5, one can notice that after the first bounce took place, the expansion phase is again dominated by the ekpyrotic potential $V(\phi)$. As mentioned before, during the ekpyrotic phase, the effective EoS of the scalar field is built to be larger than that of the anisotropy. This means that, during contraction, the scalar field dominates for small values of a, but conversely also that during expansion, the anisotropy becomes more and more important. This is illustrated in Fig. 5.3 where the shear domination after the first bounce is clearly visible.

With the expansion dominated by the anisotropy, ϕ reaches a second turning point, while H became negative again. This is the beginning of the second contraction phase that will eventually drive ϕ into the ekpyrotic phase again (third peak of Fig. 5.5), thereby reducing the shear contribution again. When the scalar field again reaches the peak of $g(\phi)$, (third ghost condensate phase), this triggers the bounce in an even more isotropic state.

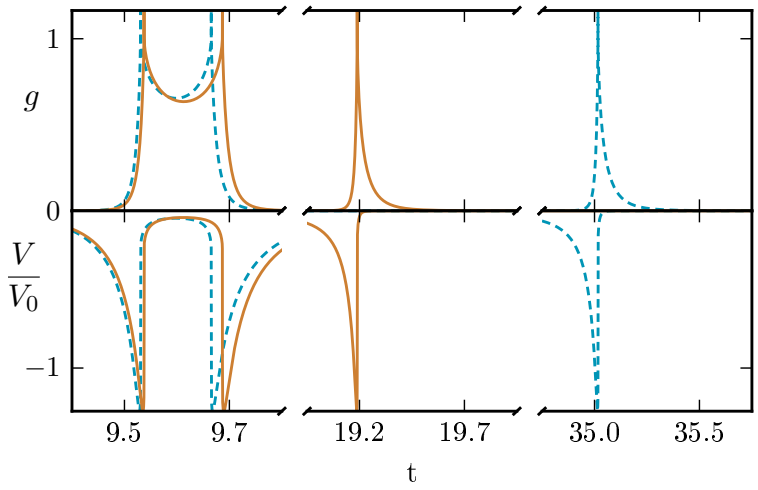

Figure 5.5.: Time developments of $g(\phi)$ (top) and the potential $V(\phi)$ (bottom). The two solutions are for $\phi_{\text{ini}} = -3.5$ (full yellow), $\phi_{\text{ini}} = -3.49$ (blue dashed), both with $\varphi_{\text{ini}} = 8 \times 10^{-6}$. As in Fig. 5.2 the peaks only appear discontinuous but they are actuality smooth.

From that example, one can imagine two possible scenarios. Without the first turning point, the Universe would have gone through a ghost condensate phase without triggering a bounce and a singularity would have been achieved. It is often stated that one of the most dangerous effect that can prevent a bounce from taking place is the uncontrolled growth of anisotropy. The numerical examples shows that the scalar field initial conditions are also important in order to ensure that the bounce can occur. In the next section it is argued that, in fact, it is thanks to the existing anisotropy that the Universe does not plunge straightforwardly into a singularity. The second scenario is when conditions are such as to avoid the second turning point altogether. In that case, the last expansion epoch begins anisotropic: the ekpyrotic contraction, although controlling the relative shear decay, is not sufficient as the multiple bounces subsequently spoil its effect. A phase of ekpyrotic contraction is thus not necessarily enough to guarantee that the resulting Universe, after the bounce, expands isotropically, the scalar field initial conditions playing a crucial role in the overall evolution of the Universe.

5.2.3 Three bounces

The final example is the most counter intuitive. It begins with an anisotropic contraction phase not leading to a BKL instability and resulting into a final expansion phase even more isotropic than the previous cases, Fig. 5.3. To produce this scenario, the value of ϕ_{ini} is chosen positive, keeping the amount of initial anisotropy as before, $\sigma^2_{\text{ini}} = 5 \times 10^{-12}$, and $\varphi_{\text{ini}} = -10^{-6}$, together with the two field values $\phi_{\text{ini},1} = 1.9$ and $\phi_{\text{ini},2} = 1.9001$, noting that since the initial field time derivative is smaller, the anisotropy is initially larger than the kinetic term $\varphi^2 = 10^{-12}$.

The usual ekpyrotic approach consists in beginning with the ekpyrotic phase so as to lower, dissolve really, the relative shear contribution immediately, during the initial contraction, thereby solving the anisotropy problem. The case here is completely different, as the system starts with $\phi_{\text{ini}} > 0$ and $\varphi_{\text{ini}} < 0$ so that the scalar field starts evolving from the right hand side of the potential $V(\phi)$ and of $g(\phi)$. This means that, contrary to the cases discussed above, the evolution of the Universe does not begin in the ekpyrotic phase: this phase only happens after the first ghost condensate peak, as shown in Fig. 5.6.

As in the two bounces case of Sec. 5.2.2, the existence of a turning point is mandatory for the observed behavior. Otherwise, the Universe merely collapses into a singularity.

The presence of three ghost condensate phases, i.e., the peaks of $g(\phi)$ in Fig. 5.6, leads to the three bounces of Fig. 5.7. The first contraction, containing no ekpyrotic phase, is completely dominated by the anisotropy (Fig. 5.3). After the first bounce, the Universe expands ekpyrotically as it reaches the first peak of $V(\phi)$, Fig. 5.6. During this ekpyrotic expansion, ϕ reaches a turning point and H changes sign, initiating the second contraction.

After the second contraction, the Universe once again goes through the ghost condensate phase and another bounce occurs. The ensuing expansion is still anisotropic, until the scalar field reaches another turning point, at which point

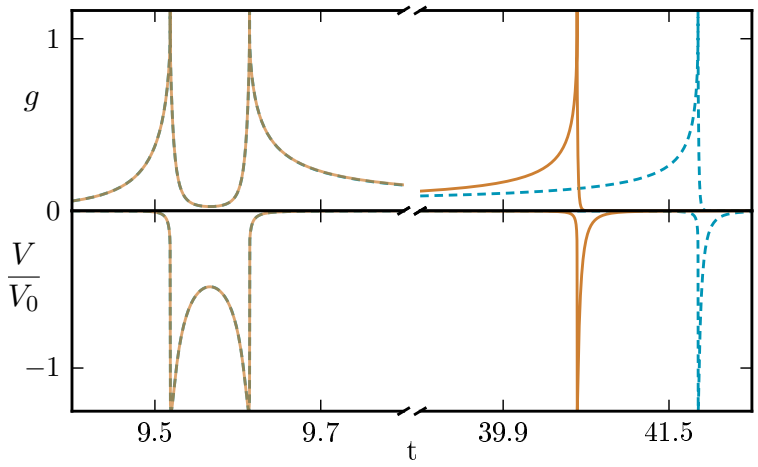

Figure 5.6.: Time developments of $g(\phi)$ (top) and the potential $V(\phi)$ (bottom). The three peaks leads to the three bounces of Fig. 5.7 with initial conditions given by $\phi_{\text{ini}} = 1.9001$ (full yellow), and $\phi_{\text{ini}} = 1.900$ (blue dashed). The fine-tuning required on ϕ_{ini} reflects the fact that it is extremely difficult to obtain a final isotropically expanding state when beginning with a shear dominated contracting Universe. In fact, almost any other initial condition leads to a singularity.

the Universe begins contracting for the third time while ϕ climbs back up in $g(\phi)$. During this third contraction, which is not ekpyrotic-like, the scalar field energy contribution appears to grow faster than the anisotropy, as shown in Fig. 5.3. The scenario ends after ϕ crosses the last peak of $g(\phi)$, and the Universe bounces for the third time.

As can be seen in Fig. 5.7, the third contraction is a very short phase with a minimum Hubble scale of $H_{\text{min}} \approx 10^{-2}$ before the third bounce. Because the contraction was shorter than the expansion, the anisotropy is more diluted. At the same time, ϕ starts to grow faster than the anisotropy. This is a very unexpected behavior. As one can see in Fig. 5.6, there is no ekpyrotic potential contribution before the third bounce to render the effective EoS of the scalar field larger than that of the anisotropy.

The final stage of the process described above is the third bounce itself, at which point the scalar field overcomes the anisotropy, leading the Universe to the required isotropic expansion. Even though the expansion in dominated by the scalar field in

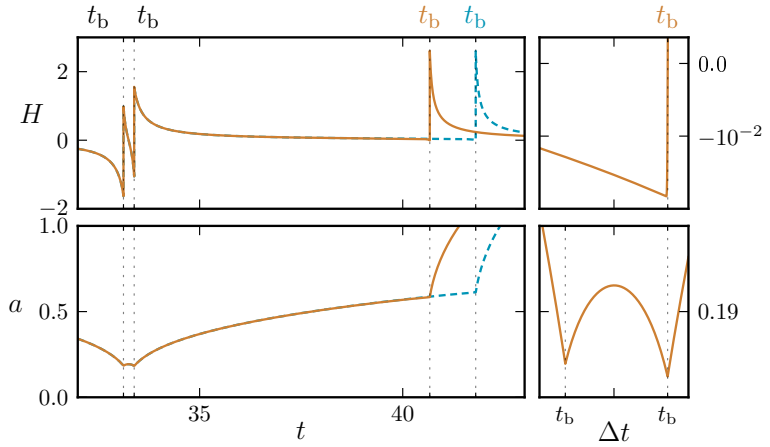

Figure 5.7.: Evolution of the Hubble constant H (top left) and the scale factor a (bottom left) for the same initial conditions as in Fig. 5.6. The other initial conditions for both cases are $\varphi_{\text{ini}} = -10^{-6}$ and $\sigma^2_{\text{ini}} = 5 \times 10^{-12}$. The first two bounces happen at roughly the same time for both initial conditions, and the solutions then drift away as in the previous example before reaching the third bounce. The top right panels emphasizes the smoothness of the evolution of H around the third bounce in the case $\phi_{\text{ini}} = 1.9001$ (the other has a similar shape). It turns out that the Hubble scale becomes slightly negative only, and for a very limited amount of time, indicating a very short contraction phase. The bottom left panel details the first two bounces for the case $\phi_{\text{ini}} = 1.9001$. The time scale of the plots are $\Delta t \approx 10^{-3}$ around the third bounce, t_b (top right panel) and $\Delta t \approx 10^{-1}$ around the first two bounces, indicated by t_b (bottom right). Enlarging more the time scale on this latter plot shows that the bounces are, again, smooth and only appear discontinuous because of the time scales used to represent them.

the ekpyrotic phase (Fig. 5.6), the difference between the energy densities is large enough that the anisotropy does not end up dominating.

5.2.4 Singular solutions

Despite the presence of an ekpyrotic phase and a ghost condensate regime, the existence of a bouncing solution is not guaranteed. In Fig. 5.8, it is shown a sequence of solutions for different values of ϕ_{ini}, assuming in all cases $\varphi_{\text{ini}} = 8 \times 10^{-6}$ and $\sigma^2_{\text{ini}} = 5 \times 10^{-12}$, some solutions being regular and bouncing, other contracting to a singularity, for initial values of the scalar field not too far away from one another. The list of initial conditions used here is $\phi_{\text{ini},1} = -2.5$, $\phi_{\text{ini},1} = -3.5$, $\phi_{\text{ini},1} = -4.0$, and $\phi_{\text{ini},1} = -4.5$.

This last case leads us to conclude that the more negative ϕ_{ini}, the longer the contraction phase and the larger the anisotropy when the system reaches the ghost condensate state. Fig. 5.8 shows the transitions from one bounce, two bounces and no bounce solutions while decreasing ϕ_{ini}. As it turns out, the singular solution is not the limit of a single bounce case, but rather a two-bounce situation in which the second bounce is failed, the Hubble rate suddenly increasing while the scalar field passes through the ghost condensate phase, but not enough to render it positive, so the ghost condensate epoch terminates in a still contracting phase, and the Universe has subsequently no chance to return to expansion.

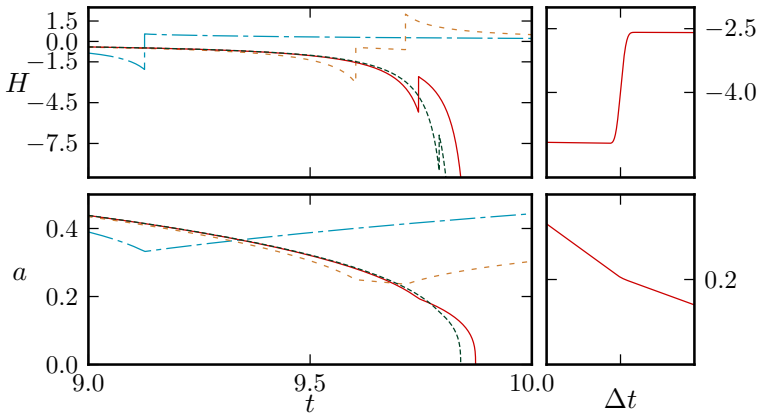

Figure 5.8.: Time evolution of the Hubble constant, H (top left), and the scale factor, a (bottom left), for $\dot{\phi}_{\text{ini}} = -8 \times 10^{-6}$ and $\sigma^2_{\text{ini}} = 5 \times 10^{-12}$, with four different initial conditions on ϕ_{ini} leading respectively to one bounce (blue dot-dashed line, $\phi_{\text{ini}} = -2.5$), two bounces (yellow small dashed line, $\phi_{\text{ini}} = -3.5$) and singular solutions (red full line, $\phi_{\text{ini}} = -4.0$, and green long dashed line, $\phi_{\text{ini}} = -4.5$). The right panel details what happens at the point where the dynamics would lead to a bounce in a regular solution: the system goes through the ghost condensate, but for an insufficient amount of time, and even though H increases (top right), changing the slope of a (bottom right), it remains negative, leading ultimately to an unavoidable singularity. The time scale for the right panel plots is $\Delta t = 10^{-4}$ around $t = 9.7$.

5.3 Turning points and the role of the anisotropy

The main feature that generates the multiple bounce is the existence of one or more turning points, making the scalar field climb the potentials more than one time.

A turning point at a time $t_{\rm T}$, is then characterized by $\varphi(t_{\rm T})=0$ and $\dot{\varphi}(t_{\rm T})<0$, if $\phi(t_{\rm T})$ is a local maximum or $\dot{\varphi}(t_{\rm T})>0$, if $\phi(t_{\rm T})$ is a local minimum. This solution should necessarily satisfy the Friedmann equation, Eq. (2.27). Substituting $\varphi=\dot{\phi}=0$ in Eqs. (5.8) and defining

$$y\equiv \mathrm{e}^{\sqrt{\frac{2}{q}}\phi}, \tag{5.22}$$

the Friedmann constraint reads:

$$y^{-1}+y^{b_V}+\frac{2}{3}\frac{V_0}{H^2-\frac{1}{6}\sigma^2}=0 \tag{5.23}$$

For $y\to 0$, $\phi\to-\infty$, and for $y\to\infty$, $\phi\to\infty$. The existence of a turning point means that there should be at least one root for the above equation.

From basics mathematics, it is known that: for a given continuous function $f(x)$ in the closed interval $[a,b]$, if $f(a)f(b)<0$, then exists a $c\in(a,b)$ for which $f(c)=0$. If f is defined as the polynomial in the left hand side of Eq. (5.23), one can easily check that:

$$\lim_{y\to 0} f(y)=\infty \tag{5.24}$$

and

$$\lim_{y\to\infty} f(y)=\infty \tag{5.25}$$

if there is a $\bar{y}$ for which $f(\bar{y})<0$, then, it is guaranteed the existence of, at least, two roots, $y(\phi_1^*)\in(\bar{y},\infty)$ and $y(\phi_2^*)\in(0,\bar{y})$ in which the turning point could happen. However, $f(\bar{y})<0$ if, and only if,

$$H^2<\frac{1}{6}\sigma^2. \tag{5.26}$$

This is exactly the role of the anisotropy in the existence of the turning point, it allows Eq. (5.23) to possibly have a root. For a very small value of anisotropy, the system goes through one bounce, $H^2>\frac{1}{6}\sigma^2$. An intermediate value of it allows that the system to go to one or two bounces $H^2<\frac{1}{6}\sigma^2$. But if $H^2<<\frac{1}{6}\sigma^2$, the singularity is unavoidable, Fig. 5.8. In Fig. 5.9 there is a comparison of anisotropic

stress energy density in the cases of one and two bounces, previously studied in Sections 5.2.1 and 5.2.2, respectively.

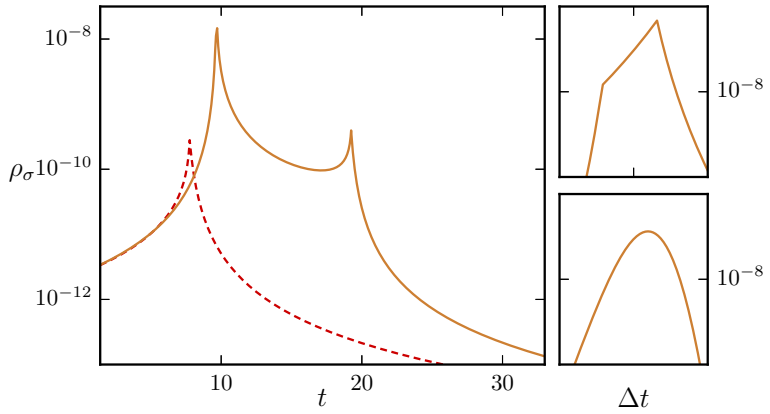

Figure 5.9.: Evolution of the effective energy density for the anisotropic stress, ρ_σ (left) for $\dot{\phi}_{\rm ini} = 8 \times 10^{-6}$ and $\sigma^2_{\rm ini} = 10^{48}$ with $\phi_{\rm ini} = -2.5$ (red dashed line) and $\phi_{\rm ini} = -3.5$ (full yellow line), both cases discussed in Sections 5.2.1 and 5.2.2 respectively. In top right the first peak of the anisotropy energy density for the two bounces case is amplified. One can see the effect of the first turning point and the ekpyrotic expansion in the increase of the anisotropy before the first bounce in the two peaks in the top right plot. In the bottom right the smoothness of one of the peaks is shown. The time scale in the plots are $\Delta t \approx 10^{-1}$ around $t = 9.6$ for top right and $\Delta t \approx 10^{-4}$ around $t = 9.7$.

From the modified Klein-Gordon equation, Eq. (5.8), in the turning point $\dot{\phi}$ satisfies

$$\dot{\phi} = -\frac{V_{,\phi}}{(1-g)} \tag{5.27}$$

Taking the derivative of $V(\phi)$, one can easily show that the sign of $V_{,\phi}$ is minus the sign of v, where

$$v \equiv 1 - b_V e^{(b_V+1)\sqrt{\frac{2}{q}}\phi}. \tag{5.28}$$

and

$$V_{,\phi} = V\sqrt{\frac{2}{q}} \mathrm{e}^{-\sqrt{\frac{2}{q}}\phi} \frac{v}{\mathrm{e}^{-\sqrt{\frac{2}{q}}\phi} + \mathrm{e}^{b_V\sqrt{\frac{2}{q}}\phi}}. \tag{5.29}$$

The straightforward result is:

- $v > 0$, if $\phi < \frac{1}{b_V+1}\sqrt{\frac{q}{2}} \ln\left(\frac{1}{b_V}\right)$, and
- $v < 0$, if $\phi > \frac{1}{b_V+1}\sqrt{\frac{q}{2}} \ln\left(\frac{1}{b_V}\right)$.

From Eq. (5.8), $\mathrm{sign}(\varphi) = \mathrm{sign}(v)$, since outside the ghost condensate phase, $(1-g) > 0$. Defining

$$\phi_{\rm lim} \equiv \frac{1}{b_V+1}\sqrt{\frac{q}{2}}\ln\left(\frac{1}{b_V}\right), \tag{5.30}$$

one has:

- $\varphi_{\rm T} < 0$ if $\phi_{\rm T} > \phi_{lim}$ and
- $\varphi_{\rm T} > 0$, if $\phi_{\rm T} < \phi_{lim}$.

Evaluating Eq.(5.23) in $y_{\rm lim} \equiv y(\phi_{\rm lim})$ reads:

$$f(\phi_{\rm lim}) = b_V^{\frac{1}{b_V+1}} + b_V^{\frac{b_V}{b_V+1}} + \frac{2}{3}\frac{V_0}{H^2 - \frac{1}{6}\sigma^2} \tag{5.31}$$

For the model parameters chosen

$$b_V^{\frac{1}{b_V+1}} + b_V^{\frac{b_V}{b_V+1}} \approx 5.$$

Because $H^2 < \frac{1}{6}\sigma^2$, taking σ^2 as the dominant term around the turning points (signed in Fig. 5.3) one has

$$\frac{2}{3}\frac{V_0}{H^2 - \frac{1}{6}\sigma^2} \approx -\frac{10^{-7}}{10^{-10}} \approx -10^3,$$

and so $f(\phi_{\rm lim}) < 0$, implying what have already been found numerically, that Eq. (5.23) has two roots: $\phi_{\rm T}^1 \in (\phi_{\rm lim}, \infty)$ and $\phi_{\rm T}^2 \in (-\infty, \phi_{\rm lim})$, but only one of them satisfying the necessary condition on the sign in $\varphi_{\rm T}$ to be a maximum or a minimum.

In the present numerical solutions the value of $\phi_{\rm ini}$ were the mostly varied, but the same scenarios could be found by changing $\varphi_{\rm ini}$ and $\sigma^2_{\rm ini}$. Increasing $\sigma^2_{\rm ini}$ for the same choices of the other two will lead to a bigger value of anisotropy when the system reaches the ghost condensate phase, facilitating the existence of turning points and other bounces. By the other hand, the initial speed of the scalar field, φ, has not a very obvious effect. Slowing the scalar field leads to the same contraction

phase, in the sense of the variation of the scale factor, but a slower one, the system takes longer to reach the ghost condensate phase. This does not change specially the amount of anisotropy, but the final value of φ when leaving the potential $g(\phi)$. There seems to be a minimum value of φ after the bounce that separates the solutions with one bounce and two bounces. The present analysis was not able to precise exactly which second order mechanism influences that limit, but the numerical essays made during the development of the present work assure there is no obvious effect when changing $\varphi_{\rm ini}$ as to guarantee the existence of only one bounce.

The other parameters, as the potential parameters, will influence as long as they change the amount of anisotropy. The choices of (5.6) and (5.7) give the same role for the parameters V_0 and g_0, q and p, b_V and b_g. Bigger potentials can be obtained increasing V_0 (g_0) and q (p) and decreasing b_V (b_g). For a bigger ekpyrotic potential, the anisotropy will be smaller when the system reaches the ghost condensate. For a bigger ghost condensate potential, the bounce would happen earlier, meaning a small contraction phase and consequently a smaller amount of anisotropy.

All those scenarios led to isotropic final expansions, which make them indistinguishable from the background point of view if confronted with observations. However, one should expect severe changes in the primordial power spectrum specially in the sense of spoiling out the scale-invariance of long wavelength modes supported in previous approaches.

In order to finally understand the effect of such a rich background dynamics in the primordial perturbation spectrum, a complete analysis considering the coupling in the scalar, tensor and vector modes is necessary. Further developments should consider choices of initial conditions and should describe the perturbation in scenarios of multiple bounces to see the types of signals it would leave.

6 Conclusion

Matter bounces are appealing scenarios in what concerns the production of primordial perturbations, since a past adiabatic vacuum is naturally defined and the modes entering the horizon during the matter domination are scale invariant. However, previous studies on the subject pointed out that single canonical field matter bounces were unable to produce a tensor-to-scalar ratio within the observables limit, $r < 0.1$, if GR is maintained during the bounce. The attempts to introduce a second scalar field were successful in diminishes the value of r, but contributed to the increase of non-Gaussianities in the spectrum. Those previous results suggest a "non-go" theorem for bounce cosmologies and they were the state of the art before the findings presented in the present work [7].

Another important issue that has been receiving attention of researches in the field is the role of the Dark Energy in bounce cosmologies. If DE is present nowadays, were it present in a former contraction phase? In that case, would it influence the primordial power spectra? The answers for those questions are different in different bounce scenarios. For the model studied in chapters 3 and 4, DE exists only in the expansion phase if a former matter bounce took place, and because of that it does not influence the primordial perturbations.

Finally, the problem of anisotropy that plagues some matter bounces were discussed in the context of the most studied mechanism that addressed it: the ekpyrotic contraction. This discussion in chapter 5 involves a matter bounce model completely different from the one presented in chapters 3 and 4, named "New Ekpyrotic" model, in which a matter contraction is followed by a an ekpyrotic phase, ending up in a ghost condensate phase responsible to perform the bounce. The previous envisaged scenarios contained a single bounce, and the suppression of the anisotropy by the ekpyrotic phase. The findings in Ref. [6], which are discussed in chapter 5, reveals unforeseen and interesting outcomes for the background dynam-

ics achieved only by means of changing the initial conditions in the contraction phase. In those new scenarios, the Universe bounces once, twice or even a third time before reaching an ever expanding isotropic phase. Those are key results if one is interested in studying perturbations in the New Ekpyrotic scenario, since it is claimed that even a small amount of anisotropy couples the STV modes, which could be more severe in multiples bounces scenarios.

The aforementioned results will be summarized in the next sessions as well as their future developments.

6.1 Consistent primordial power spectra in matter bounce model with a future DE epoch

In chapter 3 a scalar field with an exponential potential evolving in a flat, homogeneous and isotropic eternal Universe were studied. Its effective EoS assumes values in the interval $(-1, 1)$, which produces matter-like, sitff-matter-like and DE epochs. In Sec. 3.1, the determination of the critical points of the system showed two possible scenarios for the background, refereed all along as cases **A** and **B**.

In case **A**, the past repeller is equivalent to a matter dominated phase, and the contraction has three distinguished epochs: matter epoch, DE epoch and stiff matter epoch. If a new physics is present, the final stiff-matter stage transits to the expansion, which contains only an initial stiff-matter epoch and a final matter epoch, which is an attractor solution for the background.

In case **B**, the opposite happens. The Universe starts with a matter contraction followed by a stiff-matter phase, at which a new physics takes place and drives a bounce. The expansion phase starts in a stiff-matter epoch followed by a DE one and the background finally reaches the final attractor, which is equivalent to a matter dominated phase. Consequently, case **B** is more realistic, as it contains a

DE epoch in the expansion phase, and it is the background in which perturbations should be evolved.

The new physics driving the bounce in both cases can be obtained by the canonical quantization of gravity during the stiff-matter epoch, which the main developments are summarized in Sec. 3.2. The studies developed in Ref. [27] shows that, when adopting the dBB formulation of QM to solve and give meaning to the Wheeler-deWitt equation for Universe's wave-function, a Gaussian superposition of the solutions leads to Bohmian trajectories in which the Universe bounces. Those Gaussian superpositions introduce three parameters that characterize the quantum phase of the Universe: d, σ and $a_{\rm b}$, i.e, the minimum scale factor.

Since the classical backgrounds of cases **A** and **B** are stiff-matter dominated in the end of contraction and in the beginning of the expansion phase, the results in Ref. [27] can be used to prescribe a quantum bounce. The matching between the classical and quantum backgrounds, discussed in Sec. 3.3, is performed during the classical phase of the quantum solutions, when $x = \pm(1-\epsilon)$, with $0 < \epsilon \ll 1$. In order to better constraint the matching and control relevant features of the background, as the depth of the bounce, the duration of matter phase, and the DE energy scale, the new parameters $\mathcal{X}_{\rm b}$, Ω_Λ and Ω_d were introduced.

The final set of model parameters that are used to determine the complete background is: d, σ, $a_{\rm b}$, $\mathcal{X}_{\rm b}$ and Ω_Λ ($\Omega_d = 1$ without loss of generality). The numerical solutions for the background are shown in Sec. 3.4, where the phase space is explored and the role of the model parameters is discussed. Longer matter contractions and deeper bounces are obtained by changing $\mathcal{X}_{\rm b}$ and d in case **B**. However, one should take care not to transpose the validity limit of the canonical quantization procedure adopted. The parameters $a_{\rm b}$ and σ affect the bounce itself, controlling its time and energy scale.

Chapter 4 was dedicated to the primordial perturbations. Using the library NumCosmo [120] to implement the AA variables, the scalar and tensor power spectra were studied for four different sets of model parameters, Tab. 4.1. The choice of

d, σ and $a_{\rm b}$ close to the cyclic solutions provides $\frac{{\rm d}\alpha}{{\rm d}\phi} \to \infty$ in the quantum phase, thereby directly boosting the scalar modes around the bounce. Those are cases for set1 and set2, in which the scalar-to-tensor ratios are found to be within the observational limit.

The duration of the matter contraction, sensible to $\mathcal{X}_{\rm b}$ and d, influences the amplitudes and the spectral index, which is scale invariant for all the sets studied in Sec. 4.2. The configuration named set1 has the right amplitude, spectral index and scalar-to-tensor ratio, hence is one amongst many possible sets in which a single field matter bounce model with a future DE epoch produces scalar and tensor primordial power spectra consistent with the observational limits, a scenario not yet envisaged by the literature [7].

The simplicity of the model can lead to the aforementioned finding only due to the prescription of a quantum bounce, alerting to the need of solving the perturbation all along the Universe's evolution until the expansion phase, which is not always the case in the previous studies on the subject, where matching conditions on the power spectra are adopted to ignore the delicated bounce dynamics.

The fact that both a consistent power spectra and a DE epoch are accomplished by the present bounce model, motivates a more realistic scenario containing other fluid components, as radiation, although it is a more involved calculation due to the entropy perturbations.

Also it is important to constraint the non-Gaussianities in the present scenario. Since GR is modified during the bounce, the previous findings in the literature, for instance Refs. [26, 24], can not be extended to the model in question.

Finally, the presented model provides a scenario, case **A**, which is a laboratory for studying the presence of a transitional DE epoch during the contraction phase in what concerns the primordial fluctuations. This study may lead to very interesting results and perhaps motivate realistic scenarios.

6.2 Anisotropy problem and multiples bounces in the New Ekpyrotic scenario

Classical non singular bouncing models faces many intriguing issues [29] that need be addressed before any realistic model can be constructed and seriously compared with the available data. Among the challenges lies the question of the shear, whose behavior during a contraction phase my lead to the BKL instability, and consequently to the a singularity. The studies in the subject so far points to the need of a long-enough ekpyrotic phase, in which the scalar field has an effective EoS $w > 1$. Chapter 5 is dedicated to study this proposal and based in the previous work developed by Ref. [33] and further developed in Ref. [6].

Assuming the same underlying microscopic parameters as in [33], numerical solutions were found to present four different scenarios depending only on the choice of the initial conditions, see Sec. 5.2. These are: a singular solution, following a long contraction phase which increases the anisotropy despite the presence of an ekpyrotic potential and failing to bounce because of a too fast ghost condensate phase; a single-bounce solution, already encountered in the existing literature, in which the Universes contracts, passes through a minimum scale factor and expands again isotropically; two and three bounce solutions, in which the Universe shows many turning points and consequently passes more than once though the top of the potentials $g(\phi)$ and $V(\phi)$, presenting multiples ghost and ekpyrotic phases.

There are many potentially observable consequences that such a rich background dynamics may lead to, which should be derived and subsequently either confronted with the data or constrained by them. In particular, since the shear is not necessarily negligible at all times, and because there is a long and crucial contraction phase, vector modes can be produced, which should be limited in order not to spoil the bounce and the following isotropic expansion. Besides, couplings between the scalar, vector and tensor modes could trigger new imprints and correlations [116],

whose exact properties and characteristic features should be provided by a more complete and thorough analysis.

As we have seen, the background dynamics seems very sensitive (chaotic?) to the initial conditions on the scalar field, and it may well be that this sensitivity also transfers to the perturbations. The negative side of this fact is that the models are probably not as generic as one would have wanted them to be, but this also means a positive side, namely, that some a priori unwanted consequences may induce very easily identifiable effects, either in the perturbation spectra (e.g., specific correlations between scalars or tensors going beyond the consistency relation), or in higher order functions (non-Gaussianities) [130].

Appendices

A

Main features of the dynamical system analysis

A system of ordinary differential equations (ODEs) can be written in a matricial form as:

$$\frac{\mathrm{d}\mathbf{x}}{\mathrm{d}\epsilon} = \mathbf{F}(\mathbf{x}). \tag{A.1}$$

The matrix $\mathbf{x} = (x_1 x_2 ... x_n)^{\mathrm{T}}$ contains the variables x_i, whose dynamics in terms of the "time" parameter ϵ is to be determined. The matrix $\mathbf{F}(\mathbf{x}) = (F_1(\mathbf{x}) ... F_n(\mathbf{x}))^{\mathrm{T}}$ contains the functions F_i, that couple the variables x_i and are not explicitly dependent of the parameter ϵ. The system represented by eq. (A.1) is linear if all F_i's are linear combinations of the variables and non-linear otherwise.

The critical points of a systems of ODE's are $\mathbf{x}^1, \mathbf{x}^2, ... \mathbf{x}^m$ that satisfies the equation

$$\mathbf{F}(\mathbf{x^i}) = 0. \tag{A.2}$$

The Hartman's theorem states that in the vicinity of a hyperbolic critical point, the phase space of the non-linear system of ODE's is equivalent to the linearized one. Evaluating the Jacobian matrix of the system (A.1) at one of the critical points and calculating the eigenvalues, if they have non-zero real part the critical point is called hyperbolic, otherwise, it is non-hyperbolic and the following depicted procedure no longer works. For a two dimensional system, the Jacobian reads:

$$\mathrm{J}(x_1, x_2) = \begin{bmatrix} \frac{\partial \mathcal{F}_1(x_1,x_2)}{\partial x_1} & \frac{\partial \mathcal{F}_1(x_1,x_2)}{\partial x_2} \\ \frac{\partial \mathcal{F}_2(x_1,x_2)}{\partial x_1} & \frac{\partial \mathcal{F}_2(x_1,x_2)}{\partial x_2} \end{bmatrix}, \tag{A.3}$$

where $\mathcal{F}_i$ is the first order Taylor expansion of the non-linear F_i. The eigenvalues $\gamma_{(1,2)}$ are determined by the characteristic equation

$$\gamma^2 - \mathrm{Tr}(\mathrm{J})\gamma + \det(\mathrm{J}) = 0, \tag{A.4}$$

in which J is evaluated in the critical point we want to study. In the case $\gamma_1\gamma_2 < 0$, the critical point is a *saddle point*:it means that a region of the phase space is attracted to the critical point and another region is repealed. In the case $\gamma_1\gamma_2 > 0$ it means that the eigenvalues have the same sign. If both are positive, the critical point is an unstable point, and all solution diverge from it. If both are negative, the critical point is an attractor, and all solutions converges to it.

B

Action Angle variables

The action angle variables are used to solve high oscillatory differential equations. Physical system that presents this characteristic have a quadratic hamiltonian form:

$$\mathcal{H} = \frac{\Pi^2}{2m} + \tilde{\zeta}^2 \frac{m\nu^2}{2}, \tag{B.1}$$

where m is the associated "mass" of the system and ν the frequency and Π is $\tilde{\zeta}$'s associated momentum. The quantity $\tilde{\zeta}$ is defined in Eq. (4.46), but from here it will be written without the tilde not to charge the notation. The Hamilton-Jacobi equation are

$$\zeta_k' = \frac{\Pi_\zeta}{m} \tag{B.2}$$

$$\Pi_k' = -m\nu^2\zeta. \tag{B.3}$$

Let us introduce action angular variables, based on the adiabatic invariant of an oscillatory system [131, 117, 121]. For the real part (superscript a) of the complex solution ζ reads

$$\zeta^a = \sqrt{\frac{2I}{m\nu}} \sin(\theta) \tag{B.4}$$

$$\Pi^a = \sqrt{2Im\nu} \cos(\theta). \tag{B.5}$$

Differentiating the above equations, the equation of motion in terms of the new variables θ e I can be obtained and read:

$$I' = -I \frac{(m\nu)'}{m\nu} \cos(2\theta) \tag{B.6}$$

$$\theta' = \frac{1}{2} \frac{(m\nu)'}{m\nu} \sin(2\theta) + \nu \tag{B.7}$$

The imaginary term of ζ (superscript b) can be written in a similar manner:

$$\zeta^{\rm im} = \sqrt{\frac{2J}{m\nu}}\sin(\psi) \tag{B.8}$$

$$\Pi_{\zeta}^{\rm im} = \sqrt{2Jm\nu}\cos(\psi) \tag{B.9}$$

and they follow equivalent equations of motion:

$$J' = -J\frac{(m\nu)'}{m\nu}\cos(2\psi), \tag{B.10}$$

$$\psi' = \frac{1}{2}\frac{(m\nu)'}{m\nu}\sin(2\psi) + \nu. \tag{B.11}$$

The complex solution is

$$\zeta = \frac{\zeta^{\rm re} + \zeta^{\rm im}}{2i}$$

with the imaginary and complex parts satisfying the normalization condition imposed by the initial quantum vacuum perturbations:

$$\sqrt{IJ}\sin(\psi - \theta) = 1. \tag{B.12}$$

The above constraint should be maintained through the numerical calculation and the new variables ϵ, $\bar{\theta}$ and $\Delta\theta$ are defined in order to re-write de above equations accounting for the constraint:

$$\sinh(\epsilon) = \cot(\Delta\theta), \tag{B.13}$$

$$\Delta\theta = \psi - \theta, \tag{B.14}$$

$$\bar{\theta} = \frac{\psi + \theta}{2}. \tag{B.15}$$

The following relations can be easily demonstrated:

$$\sqrt{IJ} = \cosh(\epsilon),, \tag{B.16}$$

$$\sin(\Delta\theta) = \frac{1}{\cosh(\epsilon)}, \tag{B.17}$$

$$\cos(\Delta\theta) = \tanh(\epsilon). \tag{B.18}$$

Differentiating Eqs. (B.16) and (B.15), and using the above relations to rewrite ψ and θ in terms of ϵ and $\bar{\theta}$ we find

$$\bar{\theta}' = \nu + \frac{(m\nu)'}{m\nu}\tanh(\epsilon)\sin\left(\bar{\theta}\right)\cos\left(\bar{\theta}\right) \tag{B.19}$$

$$\epsilon' = -\frac{(m\nu)'}{m\nu}\cos\left(2\bar{\theta}\right). \tag{B.20}$$

However, the system is not fully described since we have only the dynamics for a composition of I and J through ϵ. Let's define:

$$\mathrm{e}^{\gamma} = \sqrt{\frac{J}{I}}, \tag{B.21}$$

from which we easily obtain

$$\gamma' = -2\frac{(m\nu)'}{m\nu}\frac{\sin\left(\bar{\theta}\right)\cos\left(\bar{\theta}\right)}{\cosh(\epsilon)}. \tag{B.22}$$

The quantities I and J can be recovered using:

$$I = \mathrm{e}^{\gamma}\cosh(\epsilon), \tag{B.23}$$

$$J = \mathrm{e}^{-\gamma}\cosh(\epsilon), \tag{B.24}$$

where Eq. (B.16) was used. Finally, the complete set of equations that replaces eqs. (B.6), (B.10), (B.7), (B.11) already accounting the constraint (B.12) is:

$$\bar{\theta}' = \nu + \frac{(m\nu)'}{m\nu}\tanh(\epsilon)\sin\left(\bar{\theta}\right)\cos\left(\bar{\theta}\right) \tag{B.25}$$

$$\epsilon' = -\frac{(m\nu)'}{m\nu}\cos\left(2\bar{\theta}\right), \tag{B.26}$$

$$\gamma' = -2\frac{(m\nu)'}{m\nu}\frac{\sin\left(\bar{\theta}\right)\cos\left(\bar{\theta}\right)}{\cosh(\epsilon)}. \tag{B.27}$$

Now we have to rewrite the adiabatic vacuum initial conditions, which are obtained when $\frac{(m\nu)'}{m\nu} \to 0$. Expanding in the leading order in $(m\nu)'/m\nu$ the set of equations provides

$$\epsilon \approx \epsilon_0, \tag{B.28}$$

$$\gamma \approx \gamma_0, \tag{B.29}$$

$$\bar{\theta} \approx \bar{\theta}_0 + k\eta. \tag{B.30}$$

Using the above approximations to calculate the complex ζ_k, we have, as an initial condition, that the following choice recovers the leading order WKB approximation, Eqs. (4.31) and (4.32):

$$\epsilon_0 = \gamma_0 = 0, \tag{B.31}$$

which, naturally, satisfies the Eq. (B.12). The real solutions using this choice are

$$\zeta_k^a = \sqrt{\frac{2}{m\nu}} \sin\left(\bar{\theta} - \frac{\pi}{4}\right),$$
$$\zeta_k^b = \sqrt{\frac{2}{m\nu}} \cos\left(\bar{\theta} - \frac{\pi}{4}\right),$$

then, consequently, the complex solution is

$$\zeta_k = \frac{\mathrm{e}^{-i\left(\bar{\theta} - \pi/4\right)}}{\sqrt{2m\nu}}.$$

Because it is just a phase, we can choose $\bar{\theta}_0 = \pi/4$.

The same treatment follows through in the case of the dimensionless tensor perturbation, with the only difference being the "mass" definition

$$m_h = 4\kappa^2 R_H z_h^2 = \frac{a^3 R_H}{N}, \qquad \nu_h = \frac{Nk}{aR_H}. \tag{B.32}$$

Bibliography

[1] Justin Khoury, Burt a. Ovrut, Paul J. Steinhardt, and Neil Turok. “A Brief Comment on "The Pyrotechnic Universe"”. In: (2001). arXiv: 0105212 [hep-th] (cit. on p. 1).

[2] Patrick Peter and Nelson Pinto-Neto. “Cosmology without inflation”. In: *Physical Review D* 78.6 (Sept. 2008), p. 063506. arXiv: 0809.2022 (cit. on pp. 1, 16).

[3] Yi-Fu Cai, Damien a. Easson, and Robert Brandenberger. “Towards a Nonsingular Bouncing Cosmology”. In: 1 (2012), pp. 1–21. arXiv: 1206.2382 (cit. on pp. 1, 2, 4, 6, 14, 20, 60, 70, 71).

[4] Marc Lilley and Patrick Peter. “Bouncing alternatives to inflation”. In: 2147.01 (2015). arXiv: 1503.06578 (cit. on p. 1).

[5] Planck Collaboration, P. A. R. Ade, N. Aghanim, et al. “Planck 2015 results. XIII. Cosmological parameters”. In: (Feb. 2015). arXiv: 1502.01589 (cit. on p. 1).

[6] Anna Paula Bacalhau, Patrick Peter, and Sandro D. P. Vitenti. “Anisotropic multiple bounce models”. In: *Phys. Rev. D* 96 (2 July 2017), p. 023517 (cit. on pp. 1, 4, 19, 70, 71, 90, 94).

[7] Anna Paula Bacalhau, Nelson Pinto-neto, and Sandro D. P. Vitenti. “Consistent Scalar and Tensor Perturbation Power Spectra in Single Fluid Matter Bounce with Dark Energy Era”. In: (2017), pp. 1–23. arXiv: 1706.08830 (cit. on pp. 1, 2, 17, 20, 32, 90, 93).

[8] Jingfei Zhang, Xin Zhang, and Hongya Liu. “Holographic dark energy in a cyclic universe”. In: *The European Physical Journal C* 52.3 (Sept. 2007), pp. 693–699. arXiv: 0708.3121 (cit. on pp. 2, 17).

[9] Jean-Luc Lehners and Paul J. Steinhardt. “Dark energy and the return of the phoenix universe”. In: *Physical Review D* 79.6 (Mar. 2009), p. 063503. arXiv: 0812.3388 (cit. on pp. 2, 15, 17).

[10] Mubasher Jamil, D. Momeni, and Muneer A. Rashid. “Notes on dark energy interacting with dark matter and unparticle in loop quantum cosmology”. In: *The European Physical Journal C* 71.8 (July 2011), p. 1711. arXiv: 1107.1558 (cit. on p. 2).

[11]Rodrigo Maier, Stella Pereira, Nelson Pinto-Neto, and Beatriz B. Siffert. “Bouncing models with a cosmological constant”. In: *Physical Review D* 85.2 (Nov. 2011), p. 023508. arXiv: 1111.0946 (cit. on pp. 2, 17, 55).

[12]I. Brevik, V. V. Obukhov, and A. V. Timoshkin. “Bounce universe induced by an inhomogeneous dark fluid coupled with dark matter”. In: *Modern Physics Letters A* 29.15 (May 2014), p. 1450078. arXiv: 1404.1887 (cit. on pp. 2, 17).

[13]S.D. Odintsov and V.K. Oikonomou. “Deformed matter bounce with dark energy epoch”. In: *Physical Review D* 94.6 (Sept. 2016), p. 064022. arXiv: 1606.03689 (cit. on pp. 2, 17).

[14]Halliwell; J. J. *Scalar Fields in Cosmology with an Exponential Potential* (cit. on pp. 2, 20).

[15]Bharat Ratra and P. J E Peebles. “Cosmological consequences of a rolling homogeneous scalar field”. In: *Physical Review D* 37.12 (1988), pp. 3406–3427 (cit. on pp. 2, 20).

[16]Christopher Kolda and William Lahneman. “Exponential Quintessence and the End of Acceleration”. In: May (2001), p. 8. arXiv: 0105300 [hep-ph] (cit. on pp. 2, 20, 23).

[17]Edmund J Copeland, Andrew R Liddle, and David Wands. “Exponential potentials and cosmological scaling solutions”. In: 57.8 (1997), p. 6. arXiv: 9711068 [gr-qc] (cit. on pp. 2, 20, 23).

[18]David Wands. “Duality invariance of cosmological perturbation spectra”. In: *Physical Review D* 60.2 (June 1999), p. 023507. arXiv: 9809062 [gr-qc] (cit. on p. 2).

[19]Patrick Peter, Emanuel J. C. Pinho, and Nelson Pinto-Neto. “Noninflationary model with scale invariant cosmological perturbations”. In: *Physical Review D* 75.2 (Jan. 2007), p. 023516. arXiv: 0610205 [hep-th] (cit. on pp. 2, 16, 60).

[20]Fabio Finelli and Robert Brandenberger. “Generation of a scale-invariant spectrum of adiabatic fluctuations in cosmological models with a contracting phase”. In: *Physical Review D* 65.10 (May 2002), p. 103522. arXiv: 0112249 [hep-th] (cit. on pp. 2, 60, 73).

[21]Patrick Peter and Nelson Pinto-Neto. “Cosmology without inflation”. In: (Sept. 2008). arXiv: 0809.2022 (cit. on pp. 2, 13).

[22]Robert H. Brandenberger. “The Matter Bounce Alternative to Inflationary Cosmology”. In: (June 2012), p. 15. arXiv: 1206.4196 (cit. on pp. 2, 6).

[23]Laura E. Allen and David Wands. “Cosmological perturbations through a simple bounce”. In: *Physical Review D* 70.6 (Sept. 2004), p. 063515. arXiv: 0404441 [astro-ph] (cit. on pp. 2, 20, 23, 60).

[24]Yu-Bin Li, Jerome Quintin, Dong-Gang Wang, and Yi-Fu Cai. “Matter bounce cosmology with a generalized single field: non-Gaussianity and an extended no-go theorem”. In: (Dec. 2016). arXiv: 1612.02036 (cit. on pp. 2, 93).

[25]Yu-Bin Li, Jerome Quintin, Dong-Gang Wang, and Yi-Fu Cai. “Matter bounce cosmology with a generalized single field: non-Gaussianity and an extended no-go theorem”. In: (Dec. 2016), p. 23. arXiv: 1612.02036 (cit. on pp. 2, 16, 17, 60).

[26]Jerome Quintin, Zeinab Sherkatghanad, Yi-Fu Cai, and Robert H. Brandenberger. “Evolution of cosmological perturbations and the production of non-Gaussianities through a nonsingular bounce: Indications for a no-go theorem in single field matter bounce cosmologies”. In: *Physical Review D* 92.6 (Sept. 2015), p. 063532. arXiv: 1508.04141 (cit. on pp. 2, 17, 60, 93).

[27]R. Colistete, J. C. Fabris, and N. Pinto-Neto. “Gaussian superpositions in scalar-tensor quantum cosmological models”. In: *Physical Review D* 62.8 (Sept. 2000), p. 083507. arXiv: 0005013 [gr-qc] (cit. on pp. 3, 27–29, 32–34, 92).

[28]V.a. Belinskii, I.M. Khalatnikov, and E.M. Lifshttz. “Oscillatory approach to a singular point in the relativistic cosmology”. In: *Advances in Physics* 19.80 (1970), pp. 525–573 (cit. on pp. 3, 18).

[29]Diana Battefeld and Patrick Peter. “A critical review of classical bouncing cosmologies”. In: *Physics Reports* 571 (Apr. 2015), pp. 1–66. arXiv: 1406.2790 (cit. on pp. 3, 6, 10–14, 94).

[30]Johanna Karouby, Taotao Qiu, and Robert Brandenberger. “Instability of the Lee-Wick bounce”. In: *Physical Review D* 84.4 (Aug. 2011), p. 043505. arXiv: 1104.3193 (cit. on p. 3).

[31]Robert Brandenberger and Patrick Peter. “Bouncing Cosmologies: Progress and Problems”. In: (Mar. 2016), p. 30. arXiv: 1603.05834 (cit. on pp. 3, 6, 12).

[32]Justin Khoury, Burt A. Ovrut, Paul J. Steinhardt, and Neil Turok. “Ekpyrotic universe: Colliding branes and the origin of the hot big bang”. In: *Physical Review D* 64.12 (Nov. 2001), p. 123522. arXiv: 0103239 [hep-th] (cit. on pp. 4, 14).

[33]Yi-Fu Cai, Robert Brandenberger, and Patrick Peter. “Anisotropy in a Nonsingular Bounce”. In: *Class. Quant. Grav.* 30.7 (Jan. 2013), p. 75019. arXiv: 1301.4703 [gr-qc] (cit. on pp. 4, 15, 19, 70, 71, 73, 75, 76, 94).

[34]B. P. Abbott, R. Abbott, T. D. Abbott, et al. “Observation of gravitational waves from a binary black hole merger”. In: *Physical Review Letters* 116.6 (2016), pp. 1–16. arXiv: 1602.03837 (cit. on p. 5).

[35]Adam G. Riess, Alexei V. Filippenko, Peter Challis, et al. “Observational Evidence from Supernovae for an Accelerating Universe and a Cosmological Constant”. In: *The Astronomical Journal* 116.3 (Sept. 1998), pp. 1009–1038. arXiv: 9805201 [astro-ph] (cit. on p. 5).

[36]S. Perlmutter, G. Aldering, G. Goldhaber, et al. “Measurements of Omega and Lambda from 42 High-Redshift Supernovae”. In: (Dec. 1998). arXiv: 9812133 [astro-ph] (cit. on p. 5).

[37]D. J. Eisenstein, I. Zehavi, D. W. Hogg, et al. “Detection of the Baryon Acoustic Peak in the Large-Scale Correlation Function of SDSS Luminous Red Galaxies”. In: (Jan. 2005). arXiv: 0501171 [astro-ph] (cit. on p. 5).

[38]Planck Planck Collaboration, P. A. R. Ade, N. Aghanim, et al. “Planck 2015 results. XIII. Cosmological parameters”. In: (Feb. 2015). arXiv: 1502.01589 (cit. on pp. 5, 13, 16, 59).

[39]Yin-Zhe Ma, Wen Zhao, and Michael L Brown. “Constraints on standard and non-standard early universe models from CMB B -mode polarization”. In: *Journal of Cosmology and Astroparticle Physics* 2010.10 (Oct. 2010), pp. 007–007. arXiv: 1007.2396 (cit. on p. 5).

[40]Marc Postman. “Distribution of Galaxies, Clusters, and Superclusters”. In: *The Encyclopedia of Astronomy and Astrophysics* (2006) (cit. on p. 5).

[41]R.D. Blandford. “Cosmological Applications of Gravitational Lensing”. In: *Annu. Rev. Astron. Astrophys.* 30 (1992), pp. 311–358 (cit. on p. 5).

[42]Alan Heavens. “Cosmology with Gravitational Lensing”. In: (Sept. 2011). arXiv: 1109.1121 (cit. on p. 5).

[43]M. Persic, P. Salucci, and F. Stel. “The Universal Rotation Curve of Spiral Galaxies: I. the Dark Matter Connection”. In: *Monthly Notices of the Royal Astronomical Society* 281.1 (June 1995), pp. 27–47. arXiv: 9506004 [astro-ph] (cit. on p. 5).

[44]Julio F. Navarro, Carlos S. Frenk, and Simon D. M. White. “The Structure of Cold Dark Matter Halos”. In: (Aug. 1995). arXiv: 9508025 [astro-ph] (cit. on p. 5).

[45]M NOVELLO and S BERGLIAFFA. “Bouncing cosmologies”. In: *Physics Reports* 463.4 (July 2008), pp. 127–213. arXiv: 0802.1634 (cit. on p. 6).

[46]Arvind Borde, Alan H. Guth, and Alexander Vilenkin. “Inflationary spacetimes are not past-complete”. In: (Oct. 2001). arXiv: 0110012 [gr-qc] (cit. on pp. 9, 13).

[47]José M. M. Senovilla and David Garfinkle. “The 1965 Penrose singularity theorem”. In: (Oct. 2014). arXiv: 1410.5226 (cit. on p. 9).

[48]Scott Dodelson. *Modern Cosmology*. Academic Press, 2003 (cit. on p. 9).

[49]Steven Weinberg. *Cosmology*. New York: Oxford University Press, 2008 (cit. on pp. 10, 12, 52).

[50]Alan H. Guth. “Inflationary universer: A possible solution to the horizon and flatness problem”. In: *Physical Review D* 23.July (1981), pp. 347–357 (cit. on p. 12).

[51]A. D. Linde. “A new inflationary universe scenario: A possible solution of the horizon, flatness, homogeneity, isotropy and primordial monopole problems”. In: *Physics Letters B* 108.6 (1982), pp. 389–393. arXiv: arXiv:1011.1669v3 (cit. on p. 12).

[52]Vf Mukhanov and Gv Chibisov. *Quantum fluctuations and a nonsingular universe*. 1981 (cit. on p. 13).

[53]Robert H. Brandenberger. “Inflationary Cosmology: Progress and Problems”. In: (Oct. 1999). arXiv: 9910410 [hep-ph] (cit. on p. 13).

[54]Jerome Martin and Robert H. Brandenberger. “The Trans-Planckian Problem of Inflationary Cosmology”. In: (May 2000). arXiv: 0005209 [hep-th] (cit. on p. 13).

[55]Robert Brandenberger, Xinmin Zhang, and General Relativity. “The Trans-Planckian Problem for Inflationary Cosmology Revisited”. In: (Mar. 2009), pp. 1–8. arXiv: arXiv:0903.2065v2 (cit. on p. 13).

[56]Nathalie Deruelle and V. F. Mukhanov. “On matching conditions for cosmological perturbations”. In: (Mar. 1995). arXiv: 9503050 [gr-qc] (cit. on p. 14).

[57]Jerome Martin and Patrick Peter. “Parametric amplification of metric fluctuations through a bouncing phase”. In: (July 2003), p. 17. arXiv: 0307077 [hep-th] (cit. on p. 14).

[58]Felipe T. Falciano, Marc Lilley, and Patrick Peter. “A classical bounce: constraints and consequences”. In: (Feb. 2008). arXiv: 0802.1196 (cit. on p. 14).

[59]Xian Gao, Marc Lilley, and Patrick Peter. “Production of non-gaussianities through a positive spatial curvature bouncing phase”. In: *Jcap* 1407 (Mar. 2014), p. 10. arXiv: 1403.7958 [gr-qc] (cit. on p. 14).

[60]Jaume Haro. “Bouncing cosmologies in geometries with positively curved spatial sections”. In: *Physics Letters, Section B: Nuclear, Elementary Particle and High-Energy Physics* 760 (Nov. 2016), pp. 605–610. arXiv: 1511.05048 (cit. on p. 14).

[61]Chunshan Lin, Robert H Brandenberger, and Laurence Perreault Levasseur. “A matter bounce by means of ghost condensation”. In: *Journal of Cosmology and Astroparticle Physics* 2011.04 (Apr. 2011), pp. 019–019. arXiv: 1007.2654 (cit. on pp. 14, 60).

[62]Lorenzo Battarra, Michael Koehn, Jean-Luc Lehners, and Burt A. Ovrut. “Cosmological perturbations through a non-singular ghost-condensate/Galileon bounce”. In: *Journal of Cosmology and Astroparticle Physics* 2014.07 (July 2014), pp. 007–007. arXiv: 1404.5067 (cit. on p. 14).

[63]Gianluca Calcagni. “Cosmology of the Lifshitz universe”. In: (Apr. 2009). arXiv: 0904.0829 (cit. on p. 14).

[64]Kazuharu Bamba, Andrey N. Makarenko, Alexandr N. Myagky, Shin’ichi Nojiri, and Sergei D. Odintsov. “Bounce cosmology from F (R) gravity and F (R) bigravity”. In: *Journal of Cosmology and Astroparticle Physics* 2014.01 (Sept. 2014), p. 8. arXiv: arXiv:1309.3748v2 (cit. on p. 14).

[65]Ron Y. Donagi, Justin Khoury, Burt A. Ovrut, Paul J. Steinhardt, and Neil Turok. “Visible branes with negative tension in heterotic M-theory”. In: *Journal of High Energy Physics* 2001.11 (May 2001), pp. 041–041. arXiv: 0105199 [hep-th] (cit. on p. 14).

[66] Evgeny I. Buchbinder, Justin Khoury, and Burt A. Ovrut. “New ekpyrotic cosmology”. In: *Physical Review D* 76.12 (Dec. 2007), p. 123503. arXiv: 0702154 [hep-th] (cit. on pp. 15, 70).

[67] Angelika Fertig and Jean-Luc Lehners. “The non-minimal ekpyrotic trispectrum”. In: *Journal of Cosmology and Astroparticle Physics* 2016.01 (Jan. 2016), pp. 026–026. arXiv: 1510.03439 (cit. on p. 15).

[68] Michael Koehn, Jean-Luc Lehners, and Burt Ovrut. “Nonsingular bouncing cosmology: Consistency of the effective description”. In: *Physical Review D* 93.10 (May 2016), p. 103501. arXiv: 1512.03807 (cit. on p. 15).

[69] Angelika Fertig, Jean-Luc Lehners, Enno Mallwitz, and Edward Wilson-Ewing. “Converting entropy to curvature perturbations after a cosmic bounce”. In: *Journal of Cosmology and Astroparticle Physics* 2016.10 (Oct. 2016), pp. 005–005. arXiv: 1607.05663 (cit. on p. 15).

[70] Taotao Qiu, Xian Gao, and Emmanuel N. Saridakis. “Towards anisotropy-free and nonsingular bounce cosmology with scale-invariant perturbations”. In: *Physical Review D* 88.4 (Aug. 2013), p. 043525. arXiv: 1303.2372 (cit. on pp. 15, 70).

[71] a. Notari and a. Riotto. “Isocurvature perturbations in the Ekpyrotic universe”. In: m.May 2002 (2002). arXiv: 0205019 [hep-th] (cit. on p. 15).

[72] Ruth Durrer. “Clarifying perturbations in the ekpyrotic universe”. In: (2001), p. 3. arXiv: 0112026 [hep-th] (cit. on p. 15).

[73] Ben Craps, Thomas Hertog, and Neil Turok. “On the Quantum Resolution of Cosmological Singularities using AdS/CFT”. In: (Dec. 2007). arXiv: 0712.4180 (cit. on p. 15).

[74] Lee Smolin. “An invitation to loop quantum gravity”. In: *Arxiv preprint hepth0408048* (Aug. 2004), p. 50. arXiv: 0408048 [hep-th] (cit. on p. 15).

[75] J. Acácio de Barros and N. Pinto-Neto. “The causal interpretation of quantum mechanics and the singularity problem in quantum cosmology”. In: *Nuclear Physics B - Proceedings Supplements* 57.1-3 (Aug. 1997), pp. 247–250. arXiv: 9611028 [gr-qc] (cit. on p. 15).

[76] Yi-Fu Cai, Antonino Marciano, Dong-Gang Wang, and Edward Wilson-Ewing. “Bouncing cosmologies with dark matter and dark energy”. In: (Oct. 2016), p. 14. arXiv: 1610.00938 (cit. on p. 17).

[77] Imogen P C Heard and David Wands. “Cosmology with positive and negative exponential potentials”. In: *Classical and Quantum Gravity* 19.21 (Nov. 2002), pp. 5435–5447. arXiv: 0206085 [gr-qc] (cit. on pp. 20, 23).

[78] Mónica Forte. “Kinematic equivalence between models driven by DBI field with constant γ and exotic holographic quintessence cosmological models”. In: (Oct. 2016), p. 3. arXiv: 1610.07441 (cit. on p. 20).

[79]V. K. Oikonomou. “Aspects of late-time evolution in mimetic F (R) gravity”. In: *Modern Physics Letters A* 31.33 (Oct. 2016), p. 1650191. arXiv: 1609.03156 (cit. on p. 20).

[80]Hui-Yiing Chang and Robert J. Scherrer. “Reviving Quintessence with an Exponential Potential”. In: (Aug. 2016), p. 5. arXiv: 1608.03291 (cit. on p. 20).

[81]Tiberiu Harko, Francisco S. N. Lobo, Emmanuel N. Saridakis, and Minas Tsoukalas. “Cosmological models in modified gravity theories with extended nonminimal derivative couplings”. In: (Sept. 2016), p. 16. arXiv: 1609.01503 (cit. on p. 20).

[82]L.N. Granda and E. Loaiza. “Phase space analysis for a scalar-tensor model with kinetic and Gauss-Bonnet couplings”. In: *Physical Review D* 94.6 (Sept. 2016), p. 063528. arXiv: 1609.06544 (cit. on p. 20).

[83]Bogdan Danila, Tiberiu Harko, Man Kwong Mak, Praiboon Pantaragphong, and Sorin V. Sabau. “Jacobi Stability Analysis of Scalar Field Models with Minimal Coupling to Gravity in a Cosmological Background”. In: *Advances in High Energy Physics* 2016 (Sept. 2016), pp. 1–26. arXiv: 1609.05636 (cit. on p. 20).

[84]Hua Chen, Naoki Sasakura, and Yuki Sato. “Equation of motion of canonical tensor model and Hamilton-Jacobi equation of general relativity”. In: (Sept. 2016), p. 34. arXiv: 1609.01946 (cit. on p. 20).

[85]John Wainwright and George Francis Rayner Ellis. *Dynamical System of Cosmology*. Cambridge University Press, 1997 (cit. on pp. 21, 23).

[86]A. A. Coley. “Dynamical Systems in Cosmology”. In: (Oct. 1999), p. 38. arXiv: 9910074 [gr-qc] (cit. on p. 23).

[87]Christian G. Boehmer and Nyein Chan. “Dynamical systems in cosmology”. In: (Sept. 2014), p. 29. arXiv: 1409.5585 (cit. on p. 23).

[88]Gianluca Calcagni. “Observational effects from quantum cosmology”. In: *Annalen der Physik* 525.5 (May 2013), pp. 323–338. arXiv: 1209.0473 (cit. on p. 28).

[89]Patrick Peter, Emanuel Pinho, and Nelson Pinto-Neto. “Tensor perturbations in quantum cosmological backgrounds”. In: *Journal of Cosmology and Astroparticle Physics* 2005.07 (2005), pp. 014–014 (cit. on p. 28).

[90]Jérôme Martin, Vincent Vennin, and Patrick Peter. “Cosmological inflation and the quantum measurement problem”. In: *Physical Review D* 86.10 (Nov. 2012), p. 103524. arXiv: 1207.2086 (cit. on p. 28).

[91]Nicolas G. Underwood and Antony Valentini. “Anomalous spectral lines and relic quantum nonequilibrium”. In: (Sept. 2016), p. 15. arXiv: 1609.04576 (cit. on p. 28).

[92]Micol Benetti, Susana J. Landau, and Jailson S. Alcaniz. “Constraining quantum collapse inflationary models with CMB data”. In: (Oct. 2016). arXiv: 1610.03091 (cit. on p. 28).

[93]Assaf Shomer. “A pedagogical explanation for the non-renormalizability of gravity”. In: (Sept. 2007), p. 10. arXiv: 0709.3555 (cit. on p. 28).

[94]Robert B. Griffiths. “Consistent histories and the interpretation of quantum mechanics”. In: *Journal of Statistical Physics* 36.1-2 (1984), pp. 219–272 (cit. on p. 28).

[95]C.R. Bom, N. Pinto-Neto, and G.B. Santos. “Consistent probabilities in perfect fluid quantum universes”. In: *Physical Review D* 89.2 (Jan. 2014), p. 023514. arXiv: 1308.5210 (cit. on p. 28).

[96]Philip Pearle. “Reduction of the state vector by a nonlinear Schrodinger equation”. In: *Physical Review D* 13.4 (1976), pp. 857 –868 (cit. on p. 28).

[97]Hugh Everett. “"Relative state" formulation of quantum mechanics”. In: *Reviews of Modern Physics* 29.3 (1957), pp. 454–462 (cit. on p. 28).

[98]Don N. Page. “Can quantum cosmology give observational consequences of many-worlds quantum theory?” In: *Eighth Canadian conference on general relativity and relativistic astrophysics*. ASCE, Dec. 1999, pp. 225–232. arXiv: 0001001 [gr-qc] (cit. on p. 28).

[99]N Pinto-Neto and J C Fabris. “Quantum cosmology from the de Broglie–Bohm perspective”. In: *Classical and Quantum Gravity* 30.14 (July 2013), p. 143001. arXiv: 1306.0820 (cit. on pp. 28, 31, 32).

[100]Nelson Pinto-Neto. *TEORIAS E INTERPRETAÇÕES DA MECÂNICA QUÂNTICA*. Ed. by Editora Livraria da Física. 1ª. São Paulo, 2010, p. 160 (cit. on pp. 28, 32).

[101]Nelson Pinto-Neto. “The Bohm Interpretation of Quantum Cosmology”. In: (Oct. 2004). arXiv: 0410117 [gr-qc] (cit. on p. 28).

[102]Richard Arnowitt, Stanley Deser, and Charles W. Misner. “Republication of: The dynamics of general relativity”. In: *General Relativity and Gravitation* 40.9 (Aug. 2008), pp. 1997–2027. arXiv: 0405109 [gr-qc] (cit. on p. 29).

[103]Kurt Sundermeyer. *Constrained Dynamics - with applications to Yang-Mills Theory, General Relativity, Classical Spin, Dual String Model*. Springer, 1982, p. 321 (cit. on p. 30).

[104]Edward Anderson. “The Problem of Time and Quantum Cosmology in the Relational Particle Mechanics Arena”. In: (Nov. 2011), p. 77. arXiv: 1111.1472 (cit. on pp. 31, 32).

[105]Karel V. Kuchar and Michael P. Ryan. “Is minisuperspace quantization valid?: Taub in mixmaster”. In: *Physical Review D* 40.12 (1989), pp. 3982–3996 (cit. on p. 32).

[106]Vitorio A. De Lorenci, Jerome Martin, Nelson Pinto-Neto, and Ivano Damiao Soares. “Topology Change in Canonical Quantum Cosmology”. In: (Jan. 1997). arXiv: 9701024 [gr-qc] (cit. on p. 32).

[107]Nelson Pinto-Neto. “The Bohm Interpretation of Quantum Cosmology”. In: *Foundations of Physics* 35.4 (Apr. 2005), pp. 577–603. arXiv: 0410117 [gr-qc] (cit. on p. 32).

[108]Samuel Colin and Nelson Pinto-Neto. “From dust we came and to dust we shall return”. In: (June 2017). arXiv: 1706.03037 (cit. on p. 35).

[109]James Bardeen. “Gauge-Invariant cosmological perturbations”. In: 8 (1980) (cit. on p. 52).

[110]Patrick Peter and Jean-Philippe Uzan. *Primoridal Cosmology*. New York: Oxford University Press, 2009 (cit. on pp. 52, 53, 56).

[111]Viatcheslav Mukhanov. *Physical Foundations of Cosmology*. New York: Cambridge University Press, 2005 (cit. on pp. 52, 54, 56).

[112]V Mukhanov. “Theory of cosmological perturbations”. In: *Physics Reports* 215.5-6 (June 1992), pp. 203–333. arXiv: 9307016 [astro-ph] (cit. on pp. 52, 54, 56).

[113]N. Pinto-Neto, G. B. Santos, and W. Struyve. “Quantum-to-classical transition of primordial cosmological perturbations in de Broglie-Bohm quantum theory: the bouncing scenario”. In: (Sept. 2013). arXiv: 1309.2670 (cit. on p. 55).

[114]Jerome Martin and Dominik J. Schwarz. “WKB approximation for inflationary cosmological perturbations”. In: *arXiv* 0210090 (2002), p. 11. arXiv: 0210090 [astro-ph] (cit. on p. 57).

[115]N. Pinto-Neto and S. D. P. Vitenti. “Comments on "Growth of Covariant Perturbations in the Contracting Phase of a Bouncing Universe" by A. Kumar”. In: (Dec. 2013). arXiv: 1312.7790 (cit. on p. 57).

[116]Thiago S Pereira, Cyril Pitrou, and Jean-Philippe Uzan. “Theory of cosmological perturbations in an anisotropic universe”. In: *Journal of Cosmology and Astroparticle Physics* 2007.09 (July 2007), pp. 006–006. arXiv: 0707.0736 (cit. on pp. 57, 71, 94).

[117]Diogo C. F. Celani, Nelson Pinto-Neto, and Sandro D. P. Vitenti. “Particle Creation in Bouncing Cosmologies”. In: (Oct. 2016), p. 18. arXiv: 1610.04933 (cit. on pp. 60, 99).

[118]Sandro D. P. Vitenti. “Unitary evolution, canonical variables and vacuum choice for general quadratic Hamiltonians in spatially homogeneous and isotropic space-times”. In: (May 2015). arXiv: 1505.01541 (cit. on p. 60).

[119]Patrick Peter, N. Pinto-Neto, and Sandro D. P. Vitenti. “Quantum cosmological perturbations of multiple fluids”. In: *Physical Review D* 93.2 (Jan. 2016), p. 023520. arXiv: 1510.06628 (cit. on p. 60).

[120]S. D. P. Vitenti and Mariana Penna-Lima. “Numerical cosmology”. In: (2017) (cit. on pp. 60, 92).

[121]S. D. P. Vitenti. *In preparation* (cit. on pp. 60, 99).

[122] Edward Wilson-Ewing. “The matter bounce scenario in loop quantum cosmology”. In: *Journal of Cosmology and Astroparticle Physics* 2013.03 (Mar. 2013), pp. 026–026. arXiv: 1211.6269 (cit. on p. 60).

[123] Jaume de Haro and Yi-Fu Cai. “An extended matter bounce scenario: current status and challenges”. In: *General Relativity and Gravitation* 47.8 (Aug. 2015), p. 95. arXiv: 1502.03230 (cit. on p. 60).

[124] Patrick Peter and Nelson Pinto-Neto. “Primordial perturbations in a nonsingular bouncing universe model”. In: *Physical Review D* 66.6 (Sept. 2002), p. 063509. arXiv: 0203013 [hep-th] (cit. on p. 60).

[125] Xian Gao, Marc Lilley, and Patrick Peter. “Non-Gaussianity excess problem in classical bouncing cosmologies”. In: *Physical Review D* 91.2 (Jan. 2015), p. 023516. arXiv: 1406.4119 (cit. on p. 60).

[126] David H. Lyth and David Wands. “Generating the curvature perturbation without an inflaton”. In: (Sept. 2001). arXiv: 0110002 [hep-ph] (cit. on p. 70).

[127] Takeo Moroi and Tomo Takahashi. “Effects of Cosmological Moduli Fields on Cosmic Microwave Background”. In: (Oct. 2001). arXiv: 0110096 [hep-ph] (cit. on p. 70).

[128] Cyril Pitrou, Thiago S. Pereira, and Jean-Philippe Uzan. “Predictions from an anisotropic inflationary era”. In: (Jan. 2008). arXiv: 0801.3596 (cit. on p. 71).

[129] C. Deffayet, G. Esposito-Farese, and A. Vikman. “Covariant Galileon”. In: (Jan. 2009). arXiv: 0901.1314 (cit. on p. 73).

[130] Mindaugas Karciauskas, Konstantinos Dimopoulos, and David H. Lyth. “Anisotropic non-Gaussianity from vector field perturbations”. In: (Dec. 2008). arXiv: 0812.0264 (cit. on p. 95).

[131] Sandro D. P. Vitenti. “Unitary evolution, canonical variables and vacuum choice for general quadratic Hamiltonians in spatially homogeneous and isotropic space-times”. In: (May 2015). arXiv: 1505.01541 (cit. on p. 99).

List of Figures

List of Tables